PROPERTIES OF γ-AMINOBUTYRIC ACID ACTIVATED CHLORIDE CHANNELS IN MAMMALIAN NEURONES

by

Claire Fiona Newland

A Thesis submitted for the degree of Doctor of Philosophy at the University of London.

Department of Pharmacology
University College London

Supervisors: Dr. S. G. Cull-Candy & Prof. D. Colquhoun, FRS.

1990

ProQuest LLC.
789 East Eisenhower Parkway
P.O. Box 1346
Ann Arbor, MI 48106 – 1346

ABSTRACT

$GABA_A$ receptor-channels in dissociated rat sympathetic ganglion neurones have been studied by conventional patch clamp techniques, with both whole-cell and outside-out patch configurations.

These $GABA_A$ receptor-channels are shown to be pharmacologically similar to those of mammalian central neurones, being inhibited by bicuculline, picrotoxin, picrotoxinin and penicillin, and potentiated by pentobarbitone. Furthermore, peripheral $GABA_A$-channels resemble central ones in their current-voltage relationship (whole-cell and single-channel) and in the voltage-dependence of their kinetic properties (noise analysis).

The mechanism of action of the well established $GABA_A$ antagonist, picrotoxin, has been further investigated in these neurones. The effects of picrotoxin on GABA noise, on the GABA current-voltage relationship, and on single-channel currents have been considered. Also the rate of onset of block by picrotoxin was found to be 'use-dependent'. Based on these results and previous reports, the mechanism of action of picrotoxin appears to be a complex channel block rather than an open channel block, as originally proposed.

The analysis of $GABA_A$ single-channel currents evoked by high concentrations of GABA has provided basic information about the kinetic behaviour of this receptor-channel in rat superior cervical ganglion neurones. Analysis of the 'probability of being open' of these channels has revealed kinetic heterogeneity, which was not apparent from previously reported single-channel analysis employing low agonist concentrations. Randomization testing of observed and simulated single-channel activity (simulated activity of identical and independent channels) verify that this kinetic heterogeneity was a real phenomenon.

The most frequently observed conductance level of the $GABA_A$ receptor-channels in these neurones (measured from single-channel currents) was approximately 30pS (at room temperature). Conductance levels of 15-18pS and 22-23pS were also common, while conductance levels of 33-36pS and 7-9pS were occasionally, but reliably observed. Increasing the temperature or reducing the pH, increased the amplitude of the most frequently occurring conductance level.

TABLE OF CONTENTS

LIST OF TABLES

Page number

LIST OF FIGURES

ACKNOWLEDGEMENTS

Many people have contributed a lot to my endeavours over the past three years, some of whom I would like to acknowledge here. Firstly I would like to acknowledge significant input from my supervisors, David Colquhoun and Stuart Cull-Candy; I feel I have learned a great deal from them both.

I dare not think where I would be without the rest of 'C-floor'. I am especially grateful to Alistair Mathie for, among other things, help and encouragement with initial experiments. I am also in debt to Nancy Mulrine, Alasdair Gibb, Maria Usowicz and Jim Howe for problem-solving, ideas, encouragement, support, and above all, a friendly ambience.

Thank-you also to Chris Magnus, Cathy Brown, Corinne Symonds and Jackie Carr for consistently excellent tissue culture (they have saved me a lot of work). I would like also to thank Ted Dyett for a helpful introduction to basic electronics.

I would also like to thank Lesley (my twin) for listening to me, sometimes. Finally, I must thank Simon , a bright spark.

This thesis is dedicated to Mrs D.J. Newland,
and Mr. & Mrs V. Woodbridge.

1. INTRODUCTION

GABA functions as an inhibitory transmitter in vertebrates and invertebrates (reviewed by Gerschenfeld, 1973; Curtis & Johnston, 1974; De Feudis, 1977). The presence of $GABA_A$ receptor-channels in mammalian (rat) sympathetic ganglion neurones has been demonstrated both from binding studies (Iversen & Kelly, 1975; Bowery *et al.*, 1978; Balcar *et al.*, 1986) and from electrophysiological studies (De Groat, 1970; Bowery & Brown, 1974; Adams & Brown, 1975; Cull-Candy & Mathie, 1986). A few reports suggest that these receptors have some physiological function. GABA-containing interneurones have been detected in adult rat superior cervical ganglion (SCG) neurones by means of immunohistochemistry (Wolff *et al.*, 1986). Also a fast depolarizing potential, sensitive to bicuculline and picrotoxin, can be evoked in SCG neurones by stimulation of the preganglionic nerve fibres (Eugène, 1987; Eugène & Taxi, 1988). Also, Farkas *et al.* (1986) observed that activation of $GABA_A$ (and $GABA_B$) receptors on rat SCG neurones inhibited (nerve-evoked) release of acetylcholine.

Binding studies also suggest the presence of $GABA_B$ (baclofen sensitive) receptors in mammalian SCG neurones (Balcar *et al.*, 1986), as does the study by Farkas *et al.* (1986; see above). $GABA_B$ receptors are pharmacologically distinct from $GABA_A$ receptors and are coupled via GTP binding proteins (Andrade, Malenka & Nicoll, 1986; Holz, Rane & Dunlap, 1986) either to K^+ channels (Newberry & Nicoll, 1984; Gähwiler & Brown, 1985) or to voltage-gated Ca^{2+} channels (Dunlap & Fischbach, 1981; Deisz & Lux, 1985; Robertson & Taylor, 1986).

The thesis describes some physical and pharmacological properties of the $GABA_A$ receptor-chloride channels present on rat sympathetic neurones. The thesis is divided into three 'results' sections (Chapters 3, 4 and 5) each of which contains a *summary, introduction, results* and *discussion* of a particular topic. The first of these results sections (Chapter 3) investigates further the mechanism of action of picrotoxin in sympathetic ganglion neurones. Chapter 4 describes properties of $GABA_A$ receptor-channels revealed by analysis of single-channel currents activated by high concentrations of GABA. The final results section (Chapter 5) describes the action of several $GABA_A$ receptor-channel antagonists and modulatory drugs, on the receptors in this preparation and investigates the effect of temperature and pH on single-channel conductance. There is an additional overall discussion (Chapter 6) which brings together many of the electrophysiological studies on $GABA_A$ receptor-channel gating and the effects of voltage on this channel.

2. METHODS

2.1 *Preparation of dissociated cells*

Sympathetic ganglion neurones were dissociated from 17-day old female Sprague-Dawley rats as previously described (Cull-Candy *et al*, 1986; Cull-Candy & Mathie, 1986) with some modifications. Briefly, sympathetic ganglia were removed from rats killed by chloroform anaesthesia; ganglia were cleaned of fat, and each ganglion cut into two or three pieces. The pieces were incubated and agitated for 15 min at 37°C in 10ml HEPES buffered MEM (Minimum Essential Medium, Eagle Modified; Flow), containing 266U/ml collagenase (Worthington Biochemical Corporation). Following centrifugation at 200g for 1min, the ganglia were incubated for a further 30 min at 37°C in 10ml MEM containing 6mg/ml bovine serum albumin (Sigma); 11,000U/ml trypsin (Sigma, type X11-S); 3μg/ml deoxyribonuclease I (Sigma, type IV), and continually agitated. The enzyme reaction was stopped by addition of medium containing rat serum (2% by volume), and the ganglion pieces were mechanically dissociated by repeated passage through a flamed down pasteur pipette. The resulting cell suspension was spun through horse serum (at 200g for 5 min) to produce a pellet that was resuspended in a medium containing foetal calf serum (2% complement inactivated; Sigma), rat serum (2%), $NaHCO_3$ (0.131% by weight), D-glucose (1.05% by weight), NGF-7*s* (0.025 μg/ml; Sigma), L-glutamate (2mM, Sigma), penicillin (50U/ml; Sigma), streptomycine (50U/ml; Sigma), insulin transferrin sodium selenite (1μg/ml; Sigma), 199 low bicarbonate Earles Modified salts (10% by volume; Flow). The cells were filtered through a 50μM mesh onto air dried collagen coated coverslips in multiwell plates (Nunc) at a density of 1.5 ganglia per well. These were then incubated at 37°C in a water-saturated atomsphere of 95% air and 5% CO_2.

2.2 *Electrophysiological recording*

For electrophysiological experiments cells were usually used within 5-6 hrs of plating, although in some experiments they were used up to 8hr after dissociation. Single channel currents were recorded from outside-out patches obtained from the cell soma, by means of conventional patch-clamp methods (Hamill, Marty, Neher, Sakmann, and Sigworth, 1981). The cells were viewed with phase contrast optics using a water immersion objective (total magnification x640). The cells and patches were bathed in an extracellular solution containing (mM): NaCl, 150; KCl, 2.8; $CaCl_2$, 1.0; HEPES, 10; $MgCl_2$, 2; pH 7.2. The extracellular

solution (also containing GABA and/or GABA-modulating drugs such as picrotoxin, where indicated) was applied to the patch or whole-cell via a two-way Hamilton tap connected to a catheter positioned under the water immersion lens. Total exchange of solution in the bath (judging from the 10-90% rise-time of changes in pipette tip potential when the bath solution was changed from one containing 70mM NaCl to one containing 150mM NaCl) usually took approximately 1-4s. When a cell was directly in the path of the outlet tube, the solution change around the cell took 300-400ms (judging from the speed of development of whole-cell currents).

Patch-pipettes were filled with an internal solution which contained (mM); CsCl, 140; $CaCl_2$, 1.0; K-HEPES, 10; K-EGTA, 10; pH 7.2. Where indicated 4mM Mg-ATP or 3mM $MgCl_2$ plus 1mM GTP was also added to the pipette solution. The Mg-ATP and GTP were kept as frozen stock solutions. Patch-pipettes were pulled from thick-walled or from thin-walled, borosilicate glass containing glass fibres (O.D. 1.5mm & I.D. 1.17mm for thin-walled glass; O.D. 1.5mm & I.D. 0.86mm for thick-walled glass, Clark Electromedical). Thin-walled glass was used only for whole-cell recording for noise analysis, since this required a low pipette series resistance. In order to reduce stray capacitance, the shanks of pipettes were coated with Sylgard resin, and the level of external solution in the recording chamber (I.D. 10mm) was maintained at a low level. The tips of pipettes were heat polished, and when filled with the internal solution used for the recording, had resistances of 5-15MΩ. Seal resistances of at least 100GΩ were routinely obtained. Single channel currents were recorded with an Axopatch 1B amplifier (Axon Instruments Inc; internal filter set at 10kHz), onto F.M. tape (Racal Store 4; 5kHz -3dB). Whole-cell currents were recorded with an EPC-7 amplifier (List electronics) or an Axopatch 1B amplifier (Axon Instruments Inc; internal filter set at 10kHz), onto F.M. tape (Racal store 4; 2.5kHz - 3dB). All experiments were performed at room temperature (21-23°C). Sympathetic ganglion neurones were used for the investigation of the mechanism of action of picrotoxin, while superior cervical ganglion neurones alone were used for all other experiments.

2.3 *Ionophoretic application of GABA*

In some experiments GABA was applied onto individual cells ionophoretically, rather than in the bathing medium, to obtain consistent duration GABA applications. The ionophoretic pipette (approximate resistance 150MΩ) contained 0.1M GABA at pH 4.0 and was placed a few

μm from the cell. High resistance fibre filled ionophoretic pipettes were used to reduce the leakage of GABA between pulses (Peper & McMahan, 1972). GABA was ejected as the anion and a positive retaining current was used to further ensure that leakage of GABA between pulses was minimized. Cells were continuously perfused with external solution to prevent accumulation of GABA. During individual experiments the amplitude and duration of ionophoretic pulses was kept constant and any movement of the ionophoretic pipette was kept to a minimum. Results were used only if complete recovery of GABA responses was obtained after washout of the GABA modulating drug (for example picrotoxin).

2.4 *Analysis of whole-cell current noise*

Analysis of whole-cell current noise (Katz & Miledi, 1972; Anderson & Stevens, 1973) was basically as described elsewhere (Colquhoun, Dreyer and Sheridan, 1979) . Signals from magnetic tape were band pass filtered at 0.1 - 250Hz, 0.1 - 500Hz, or 0.1 - 1000Hz (-3dB, eight pole Butterworth-type filter, Barr and Stroud, normal mode). The records were low-pass filtered at 0.5 times the sampling frequency to avoid aliasing. Sampling frequencies of 512Hz, 1024Hz, or 2048Hz were used to obtain spectra that extended up to 256, 512Hz or 1024Hz. The separation of individual points in the spectrum (the resolution) was chosen as 0.5 or 1.0Hz. Sampled signals were edited manually and divided into sections of length $1/f_{res}$. For each section a power spectrum was calculated by means of a fast fourier transform. A 'net' spectrum for the drug-induced noise was computed by averaging the spectral densities from each section in the presence of drug, and subtracting from this the similarly obtained mean spectrum in the absence of drug. The resulting drug-induced one sided net spectrum was fitted by the sum of two Lorentzians, using the method of weighted least-squares (Colquhoun *et al.*, 1979). The conductance (γ) of the underlying single channels was estimated, on the assumption that a negligibly small fraction of channels were open, from the area under the fitted spectrum, according to:

$$\gamma = \frac{\pi\,[G_1(0)f_{c1} + G_2(0)f_{c2}]}{2\mu_i\,(V_m - V_{eq})} \qquad (1)$$

where μ_i is the mean membrane current, V_m and V_{eq} are the holding

potential and the GABA equilibrium potential respectively, $G(0)$ is the zero frequency asymptote and f_c is the half-power frequency of each Lorentzian. The time constants, τ, underlying the current fluctuations were calculated from the half-power frequencies of the two Lorentzians according to, $\tau = (2\pi f_c)^{-1}$.

2.5 *Analysis of single-channel currents*

Replayed single channel currents were filtered at 1.5-2.5kHz (-3dB Barr & Stroud, eight-pole Bessel type) and digitized continuously at 15-25kHz (ten times the filter cut-off frequency). Single channel transitions were detected by a 50% threshold crossing program; a resolution of 1.5 x the filter rise-time was subsequently imposed on the results (Colquhoun and Sigworth, 1983), giving resolutions of 200-300μs. The threshold-crossing method was considered adequate because it was not necessary, for the purposes of defining bursts of openings, to have a very high resolution. Furthermore, the exceptionally large amount of open-channel noise made the use of time-course fitting impractical.

2.5.1 *Shut* time, *open time* and burst length *distributions* Analysis was restricted to those runs of single channel currents during which the channel opened mostly to the approximately 30pS conductance level. Any openings to other conductance levels were excluded, as were the shut periods before and after the opening. On the rare occasions when there were two or more channels open simultaneously the whole event was disregarded, as were the closed intervals either side of it. Distributions of shut times were fitted from 250μs with probability density functions using the method of maximum likelihood (Colquhoun & Sigworth, 1983). Bursts were defined as a series of openings separated by closed intervals shorter than some critical value, t_c. The values of t_c were determined from shut-time distributions using the method of equal percentage of misclassified bursts (Colquhoun & Sakmann, 1985), the two shortest shut-time components being defined as intraburst closed times. Distributions of burst lengths were also fitted with probability density functions by the method of maximum likelihood. For display purposes, all histograms show the distribution of log interval, with the ordinate on a square root scale (McManus *et al.*, 1987; Sigworth & Sine, 1987). Therefore each exponential appears as a peaked function, the maximum of which corresponds to the time constant of the exponential.

2.5.2 *Probability of being open* Bursts within clusters were defined as a series of openings separated by closed intervals shorter than some critical value, t_c. The probability of being open, p_o, for bursts was calculated by numerical integration of the digitized record, according to

$$p_o = \frac{\text{integral}}{\text{burst length x mean amplitude}}$$

where the mean amplitude for each cluster was determined from point amplitude histograms (see below). This allowed for any small changes in single-channel current with temperature (or other factors), that may have occurred during the experiment. This method of calculating p_o is less dependent on the resolution of the system than calculation of p_o from open and shut times, because any linear filter will not change the area under the observed current trace.

2.5.3 *Amplitude distributions* The exceptionally large open channel noise (compared to the shut channel noise) of the GABA-evoked channels in these cells made fitting of channel amplitudes with cursors rather dubious. Therefore, in most cases, the amplitude levels of single channel currents were obtained from distributions of the amplitudes of individual data points (with subtraction of the mean shut-channel level). These are referred to as 'point amplitude histograms'. In most cases points for the histogram were selected from the record during periods when the channel was shut, or from periods while it was 'open' (i.e. without resolved shut periods) so that most of the points representing transitions between open and shut levels were excluded. Histograms were fitted with a single Gaussian, or with the sum of several Gaussians, by the method of maximum likelihood (Colquhoun & Sigworth, 1983); reasonable looking fits were usually obtained despite the fact that one would not, in principle, expect the distributions (for open points at least) to be exactly Gaussian. Single channel currents were filtered at 2kHz or 2.5kHz (-3dB) and sampled at ten times the filter cut-off frequency.

The possible presence of *discrete* sublevels was further investigated by inspection of the distribution of the mean amplitudes of short stretches of data that had low variance, and which therefore represented sojourns at a fairly constant amplitude level (using the 'sublevel detection' method of Patlak, 1988). The variance and mean amplitude were calculated for section of 10 points (0.5ms), successive sections being taken by advancing along the digitized record by one

point each time. All those sections for which the standard deviation was greater than some specified multiple (usually 1.0) of the baseline r.m.s. noise were eliminated, and the histograms were constructed from the mean amplitudes of sections not so eliminated. These will be referred to as 'mean low-variance amplitude histograms'.

Single channel current amplitudes are mostly quoted as chord conductances, assuming a linear current-voltage relationship and a reversal potential of 0mV. The reversal potential estimated from whole-cell and single-channel current-voltage relationships ranged from 0 to 3mV, (the theoretical value, estimated from the chloride concentrations, rather than chloride activities, is -2.8mV). Point amplitude and low-variance amplitude histograms gave some idea of whether or not there were significant contributions from levels other than the approximately 30pS level during a cluster.

2.5.4 *Randomization test* Bursts within the same cluster and from different clusters, were compared by a randomization test (Patlak, Ortiz & Horn, 1986) in order to determine whether the open times and shut times ocurring during different bursts all came from the same distribution of open and shut intervals. This test was used to compare the values of p_o, mean open time and mean shut time for bursts of at least 200ms duration (more than 40 openings) and at the same agonist concentration. Briefly, the observed scatter (observed S) for the bursts was calculated according to

$$S = \sum_{i=1}^{N} n_i \ (\bar{y}i - \bar{y})^2 \qquad (2)$$

where N is the number of bursts compared, n_i is the number of openings in the ith burst, $\bar{y}_i$ is the mean open time (or p_o, or mean shut time) for the i^{th} burst, and $\bar{y}$ is the overall mean open time (or overall p_o, or overall mean shut time). Histograms of randomized scatter ('randomized S') were obtained under the null hypothesis that bursts are homogeneous, by generating 1000 or more sets of N bursts, by the use of randomization. Sets of artificial bursts, containing n_1, n_2 , ... , n_N openings, were generated by a random selection of open and shut times from the total population of observed intervals. Each artificial burst consisted of the same number of openings as the observed bursts. A value of randomized S was calculated by equation (2) for each set of N bursts generated in this way. If the randomized S values exceed the observed S value only rarely (in a proportion P, say, of cases), this

implies that the open time (or p_o or shut time) genuinely differ between bursts.

3. MECHANISM OF ACTION OF PICROTOXIN AT $GABA_A$ RECEPTOR-CHANNELS IN DISSOCIATED SYMPATHETIC NEURONES OF THE RAT

3.1 SUMMARY

1. The mechanism of action of picrotoxin on $GABA_A$ receptor channels has been investigated in rat sympathetic neurones with whole-cell voltage clamp. In addition, the action of picrotoxin, on single GABA-channels, has been examined in outside-out membrane patches from these cells.

2. Picrotoxin, at concentrations which dramatically reduced the amplitude of whole-cell GABA currents, did not alter the spectral time constants or single channel conductance estimated by the analysis of GABA activated current noise. This was observed at potentials both negative and positive to the GABA reversal potential (i.e. for both inward and outward GABA-currents). It therefore seems unlikely that picrotoxin acts by a simple voltage-dependent (or voltage-independent) channel blocking mechanism. In the absence of picrotoxin and at -60mV the slow and fast time constants from the noise were 43 ± 17ms and 2.3 ± 1.4ms, while the estimated single channel conductance was 11.8 ± 2.4 pS.

3. Picrotoxin, at concentrations which markedly reduced the amplitude of whole-cell GABA currents, did not alter the shape of the whole-cell GABA current-voltage relationship, indicating that the block by picrotoxin was not voltage-dependent.

4. Closed time distribution of GABA activated chloride channels were obtained from all shut times during the application of low concentrations of GABA to single outside-out patches. These distributions were fitted with four exponential components. Distributions of total burst durations were also obtained from the same records, and these were fitted with three or four exponential components. Picrotoxin had no consistent effect on the time constants of either the shut time distributions or the total burst length distributions, although the latter time constants were not well separated. Picrotoxin also did not alter the apparent amplitude of the main conductance state. However, picrotoxin did reduce the frequency of channel openings.

5. The application of brief ionophoretic pulses of GABA, to cells under whole-cell voltage-clamp, revealed that the rate of onset of block by picrotoxin was accelerated in the presence of GABA. In the absence of agonist, picrotoxin produced only a slowly equilibrating block.

6. Our data are consistent with a mechanism whereby picrotoxin binds preferentially to an agonist bound form of the receptor and stabilizes an agonist bound shut state. This could, for example, mean that picrotoxin enhances the occurrence of a desensitized state or an

allosterically blocked state.

3.2 INTRODUCTION

The inhibitory action of picrotoxin on GABA receptors in both vertebrates and invertebrates is well established. The block of GABAergic synapses by picrotoxin was originally described for insect and crustacean muscle (Robbins & Van der Kloot, 1958; Grundfest *et al.*, 1959; Van der Kloot & Robbins, 1959; Usherwood & Grundfest, 1965; Takeuchi & Takeuchi, 1969). Galindo (1969) was first to describe the blocking effect of picrotoxin on GABA responses in mammalian neurones (from the cuneate nucleus) and similar effects have subsequently been described at various sites in the vertebrate central nervous system (for reviews see Krnjević, 1974; Kelly & Beart, 1975; Nistri & Constanti, 1979). Despite a number of studies showing the inhibition of GABA responses by picrotoxin, the precise mechanism(s) of action of this antagonist is still unclear.

Electrophysiological studies of vertebrate neurones have generally suggested that picrotoxin is not competitive, as judged by displacement of GABA or muscimol dose-response curves (Constanti & Nistri, 1976; Gallagher *et al*, 1978; Simmonds, 1978; 1980; 1982; Nicoll & Wojtowicz, 1980; Lebeda *et al*, 1982; Akaike & Oomura, 1984; Akaike *et al*, 1985; Kaneko & Tachibana, 1986). In contrast, similar electrophysiological studies in crustacean muscle suggest the mechanism of action of picrotoxin to be competitive (Grundfest *et al*, 1959; Shank *et al*, 1974), non-competitive (Takeuchi & Takeuchi, 1969; Constanti & Quilliam, 1974; Earl & Large, 1974) or mixed competitive plus non/uncompetitive (Constanti, 1978; Adams *et al*, 1981b; Smart & Constanti, 1986). Data from ligand binding studies is contradictory; the interaction between GABA and picrotoxin binding apparently depends to some extent on the conditions of the experiment (for a review see Olsen, 1982). For example, several groups have demonstrated that, under low temperature conditions (0-4°C) picrotoxin (or dihydropicrotoxinin, a ligand thought to act at the same site as picrotoxin; Jarboe *et. al.*, 1968; Ticku *et. al.*, 1978) and GABA do not compete for the same binding site on mammalian neurones (Enna *et al*, 1977; Greenlee *et al*, 1978; Olsen *et al*, 1978b; Ticku *et al*, 1978; Willow & Johnston, 1980), or on crustacean muscle (Olsen *et al.*, 1978a; Krogsgaard-Larsen *et al*, 1979; Leeb-Lundberg & Olsen, 1980; Willow, 1981). In contrast to these reports, Quast & Brenner (1983) and Supavilai *et al* (1982) have shown that at 37°C and with 150mM chloride, picrotoxin can reduce specific binding of GABA to mammalian neuronal membranes, although this is probably an allosteric,

rather than a direct, effect of picrotoxin on the GABA binding site. Taken together, these results suggest that picrotoxin binds to a site distinct from the GABA receptor site (*i.e.* that it is not a true competitive antagonist).

Several mechanisms of action could result in inhibition which is not competitive. The purpose of the present study was to investigate further the mechanism of action of picrotoxin on mammalian neuronal $GABA_A$ receptors. In particular the present study examines the possibility that picrotoxin acts by an open channel blocking mechanism, as originally suggested for GABA-channels in crayfish muscle (Takeuchi & Takeuchi 1969; Klunk *et al*, 1983) and more recently in bullfrog dorsal root ganglion neurones (Akaike *et al*, 1985). Also the possibility of a less direct effect of picrotoxin on the GABA-channel (Constanti, 1978; Barker *et al*, 1983; Segal & Barker, 1984) has been investigated. A preliminary report of some of these results has appeared (Cull-Candy, Mathie & Newland, 1987).

3.3 *Influence of picrotoxin on GABA current noise*

It was clear from whole-cell current recordings that in sympathetic neurones responses to GABA were inhibited in the presence of picrotoxin. This reduction in GABA current occurred at holding potentials both negative and positive to the GABA reversal potential (the reversal potential was between zero and +3mV under the conditions of these experiments). Fig. 3.1A shows a typical whole-cell response to 10μM GABA in a sympathetic neurone held at -70mV. GABA produced a large inward current response accompanied by an increase in membrane current noise. In the presence of 2μM picrotoxin (see for example Fig. 3.1B) the steady state GABA current amplitude was reduced to 25% of the control level in the same cell. The initial peak observed when picrotoxin was simultaneously applied with GABA might be expected for any slowly dissociating antagonist. In this experiment the initial peak of the response in the presence of picrotoxin was larger than that of the control. This was not always observed; in other cases the peak was smaller in the presence of picrotoxin (Fig. 3.2). This variability probably reflects differences in the rates of perfusion of drugs. The potentiation of the peak is difficult to explain. For example, binding studies suggest that either picrotoxin has no effect on the binding of GABA, or decreases GABA binding, rather than enhancing the binding. However, such results are difficult to relate to electrophysiological experiments since it is unknown what state of the receptor-channel the drugs are binding to.

As can be seen from the typical example in Fig. 3.2A picrotoxin also inhibited GABA responses at positive membrane potentials, at which the response was an outward current. In this example, at a holding potential of +20mV, the steady-state current amplitude (produced by 10μM GABA) was reduced to 65% of the control level, by the addition of 2μM picrotoxin (Fig. 3.2B). It therefore appears that the block produced by picrotoxin is independent of the direction of current flow.

Noise analysis of current fluctuations, produced by GABA in the absence and presence of picrotoxin, was used to determine whether picrotoxin caused any detectable changes in the kinetics or conductance of the $GABA_A$ receptor-channel. All spectral density functions of GABA current noise, whether produced in the absence or presence of picrotoxin, were best fitted by the sum of two Lorentzians. A representative spectrum of current noise, produced by 10μM GABA in a

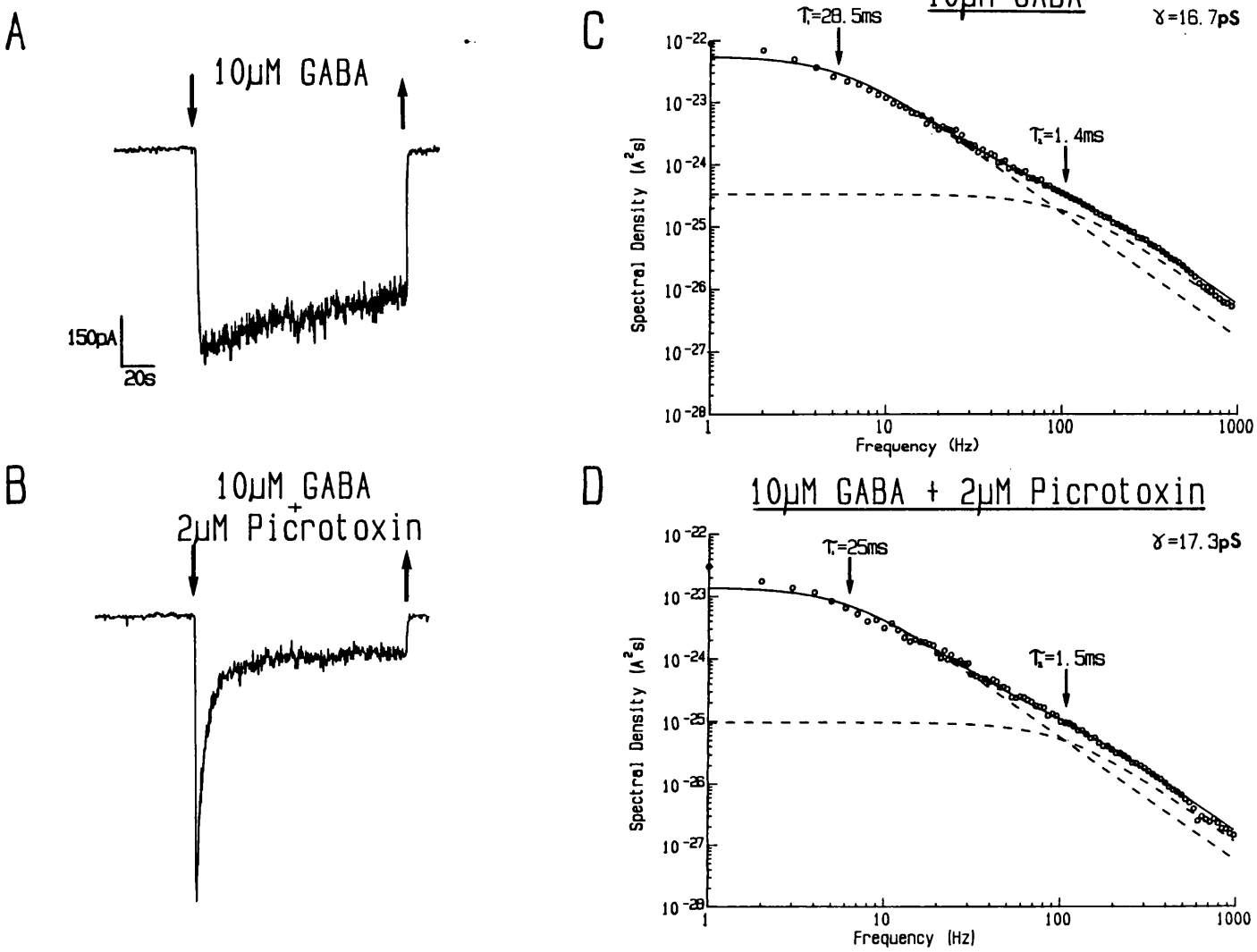
A
10μM GABA
150pA
20s
B
10μM GABA
+
2μM Picrotoxin
C
10μM GABA
τ1=28.5ms
γ=16.7pS
τ2=1.4ms
Spectral Density (A²s)
Frequency (Hz)
D
10μM GABA + 2μM Picrotoxin
τ1=25ms
γ=17.3pS
τ2=1.5ms
Spectral Density (A²s)
Frequency (Hz)

Fig. 3.1 Comparison of whole-cell GABA-currents and noise spectra recorded in a sympathetic neurone in control medium and in the presence of 2μM picrotoxin. A, whole-cell current response to 10μM GABA (V_m=-70mV). GABA application is indicated by arrows; inward current is downwards. Note the increase in noise during GABA application. B, whole-cell response (same cell as A) to the application of 2μM picrotoxin with 10μM GABA, (application indicated by arrows). Note the initial peak which decays rapidly. Calibration, 150pA and 20s. C, spectral density function of GABA current noise in A (band pass filtered 0.1 - 1000Hz, -3dB). Points in the spectrum between 2-400Hz were fitted with the sum of two Lorentzians (continuous curve). Time constants calculated from the half power frequencies of the individual Lorentzians (dashed curves) were 1.4ms and 28.5ms (indicated by arrows). The estimated single channel conductance (γ) was 16.7pS. For the plot, points above 20Hz were averaged, to give an approximately constant frequency spacing of the points above 20Hz. D, spectral density function of GABA current noise in the presence of picrotoxin, during the steady state part of the response in B (band pass filtered 0.1 - 1000Hz, -3dB). The distribution was fitted with the sum of two Lorentzians; 2-400Hz (continuous curve). Time constants of individual Lorentzians were 1.5ms and 25ms, (indicated by arrows), estimated single channel conductance for GABA-noise in the presence of picrotoxin was 17.3pS.

cell held at -70mV, is illustrated in Fig. 3.1C. The background noise spectrum has been subtracted and the continuous line through the points is the sum of two Lorentzians fitted to the data (the whole-cell current was band-pass filtered at D.C. to 1000Hz, -3dB). In this example the time constants calculated from the half power frequencies of the two Lorentzians were 1.4ms and 28.5ms, and the estimated single channel conductance was 16.7pS. Figure 3.1D shows a spectrum of GABA noise obtained from the same cell in the presence of 2μM picrotoxin. The spectral time constants (1.5ms and 25ms in the presence of picrotoxin) were virtually unaltered, and the estimated single channel conductance was very similar to the control value; in this cell it was 17.3pS in the presence of picrotoxin. Similarly, at potentials positive to the GABA reversal potential, picrotoxin had no obvious effect on the time constants underlying GABA noise, or on the estimated single channel conductance (Fig. 3.2C,D), although the time constant of the slow component was itself voltage-dependent (both in control conditions and in picrotoxin). The time constants of GABA noise in Fig. 3.2C, with the cell held at +20mV were 1.5ms and 39ms, while in the same cell in the presence of picrotoxin the GABA-noise time constants were 1.6ms and 49ms (Fig. 3.2D). For this cell the single channel conductance was estimated to be 9.8pS in control conditions, and 12pS in the presence of picrotoxin.

At any given holding potential the time constants and single channel conductance estimated from GABA current noise varied somewhat from cell to cell. For example, for GABA noise in the absence of picrotoxin (recorded from seven cells held at -60mV) the time constants were 43 ± 17ms and 2.3 ± 1.4ms (mean ± S.D.), while the estimated single channel conductance was 11.8 ± 2.4 pS (mean ± S.D.); note that the standard deviations are large, compared with the means, for these values. However, the time constants and conductance estimated in any given cell at a particular potential, remained much the same irrespective of the presence or absence of picrotoxin.

The effect of picrotoxin (2-6μM) on the time constants and single-channel conductance estimated from GABA noise (evoked by 10-30μM) was assessed in a total of nine cells, held at potentials between +30 and -70mV. For each cell GABA noise was obtained both in the absence and in the presence of picrotoxin, at a particular potential. Neither the fast or slow time constants, or the estimated single-channel conductance were altered by picrotoxin (for all parameters: $P > 0.05$, Wilcoxon test, 9 cells).

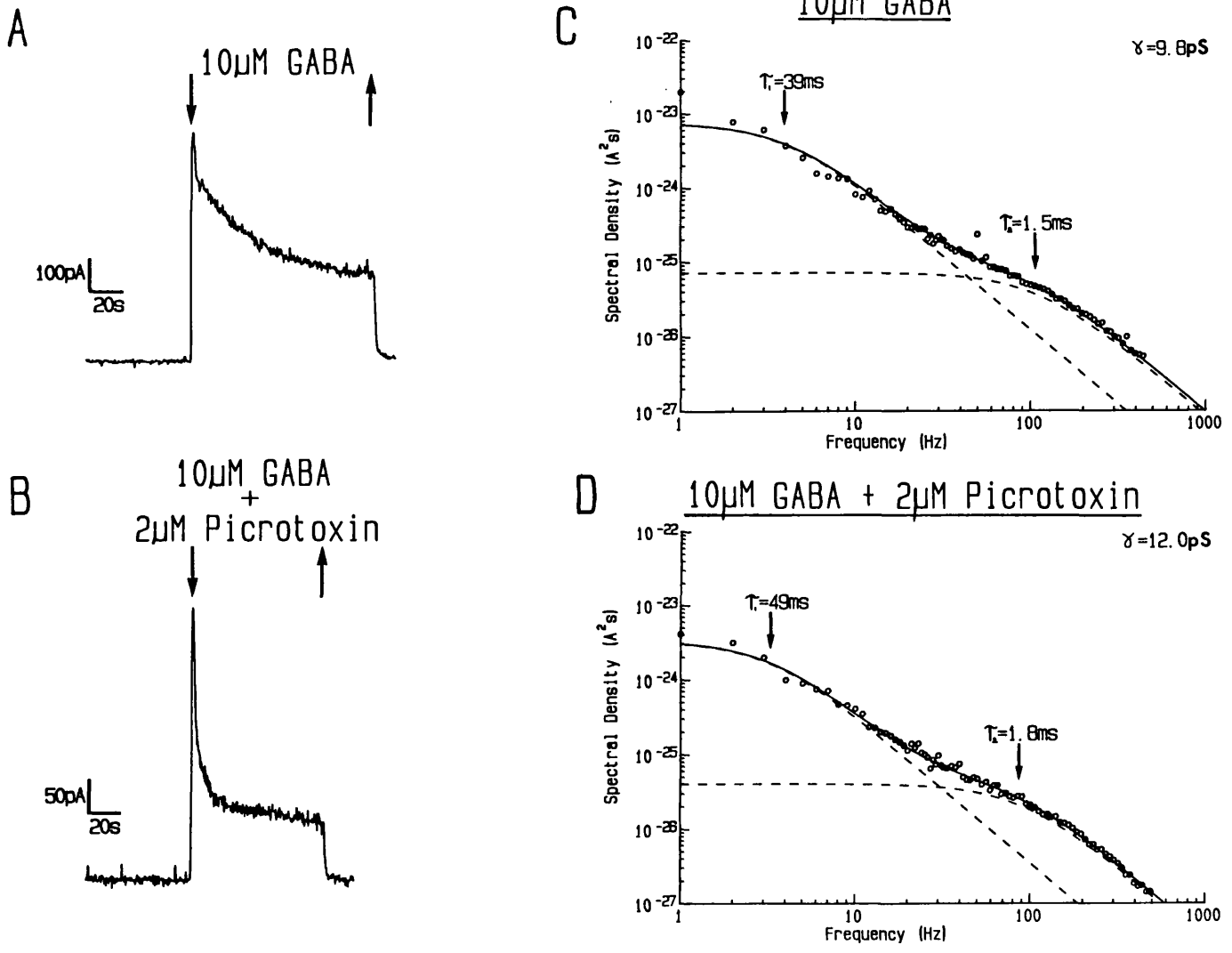
A
10μM GABA
100pA
20s
B
10μM GABA
+
2μM Picrotoxin
50pA
20s
C
10μM GABA
γ=9.8pS
τ=39ms
τ=1.5ms
Spectral Density (A²s)
Frequency (Hz)
D
10μM GABA + 2μM Picrotoxin
γ=12.0pS
τ=49ms
τ=1.8ms
Spectral Density (A²s)
Frequency (Hz)

Fig. 3.2 A, whole-cell current response to 10μM GABA (application indicated by arrows) in a cell held at +20mV. Calibration 100pA and 20s. B, whole-cell response (same cell as A) to the application of 2μM picrotoxin with 10μM GABA (indicated by arrows). Note the presence of an initial peak which decays rapidly at positive, as well as negative potentials (Fig. 3.1B). Calibration 50pA and 20s. C, spectrum of the GABA current noise shown in A (band pass filtered 0.1-500Hz, -3dB). Distribution fitted with the sum of two Lorentzians; 2-400Hz (continuous curve). Time constants derived from the half power frequencies of the individual Lorentzians (dashed curves) were 1.5ms and 39ms (indicated by arrows). Estimated single channel conductance, γ = 9.8pS. Points above 20Hz were averaged, such that above 20Hz the frequency spacing of the points remained approximately constant. D, spectrum of GABA current noise in the presence of picrotoxin, during the steady state part of response B; band pass filtered 0.1 - 500Hz, -3dB). The distribution was fitted (2 to 300Hz) with the sum of two Lorentzians; time constants were 1.8ms and 49ms; estimated single channel conductance, γ = 12.0pS.

3.4 *Picrotoxin on whole-cell current-voltage relationship*

From previously reported studies it is unclear whether the block by picrotoxinin is voltage-dependent (Akaike & Oomura, 1984; Akaike *et al.*, 1985; Akaike *et al.*, 1986). A voltage-dependent channel blocker would change the shape of the current-voltage plot since the degree of block depends on the potential (as a consequence of the charge associated with the blocking molecule).

GABA whole-cell current-voltage relationships were constructed from the peak amplitudes of responses evoked by ionophoretic pulses of GABA. Although picrotoxin reduced the size of the GABA-current in all cells examined, there was no dramatic effect of picrotoxin on the shape of the GABA current-voltage relationship over the voltage range 50mV to -150mV (5/5 cells). An example is illustrated in Fig. 3.3. The two GABA current voltage relationships shown in Fig. 3.3A were obtained from a single cell, continuously perfused either with control bathing medium, or medium containing 1μM picrotoxin. Each point is the amplitude of a GABA response at the end of a 2.2s duration ionophoretic pulse of GABA. Examples of GABA responses obtained in control medium at potentials between +30 and -120mV are shown in Fig. 3.3B, while Fig. 3.3C shows GABA responses recorded under identical conditions, except for the additional presence of 1μM picrotoxin (applied in the bathing medium). It is clear from Fig. 3.3 that 1μM picrotoxin reduced the amplitude of the GABA responses with very little alteration of the shape of the current-voltage relationship. Normalizing the data indicates that the relationships were superimposable (not shown).

The effect of picrotoxin on the GABA current-voltage relationship was examined with brief (e.g. 10ms) as well as with long (e.g. 2.2s) GABA pulses, and gave the same results. Also, when GABA-pulse amplitude was increased in the presence of picrotoxin, to give responses of the same size as in control, then the current-voltage plots were superimposable (1 cell). The current-voltage plots suggest that the block by picrotoxin is not voltage-dependent.

3.5 *Single-channel burst-length and opening frequency*

3.5.1 *Distributions of shut times*

The effect of picrotoxin (1 or 2μM) on currents evoked by GABA (2, 3 or 5μM) was assessed in three outside-out patches. A larger number of patches were examined but the low frequency of openings in the presence of picrotoxin meant that it was difficult to obtain enough

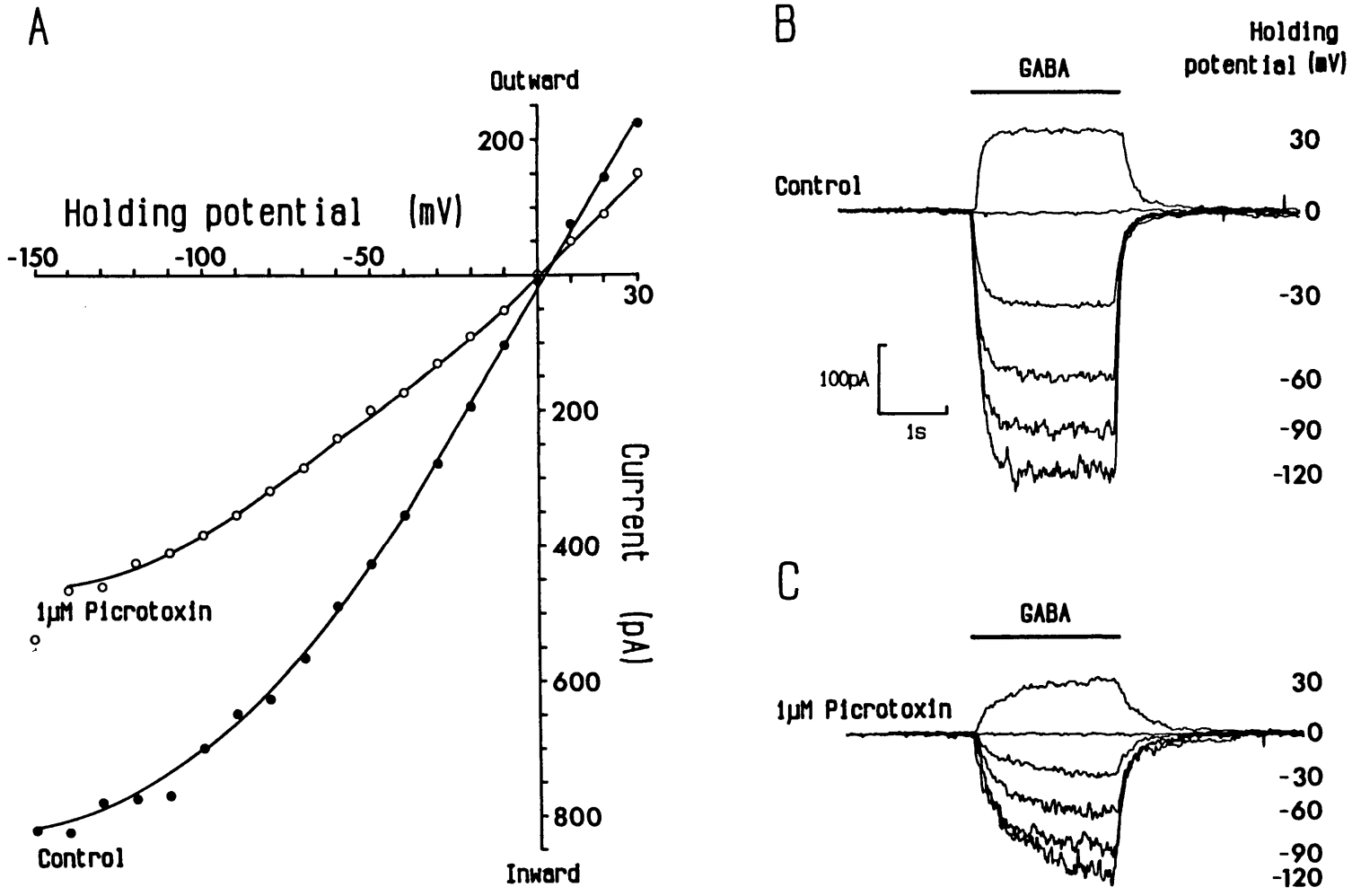
A
Outward
200
Holding potential (mV)
-150
-100
-50
30
200
400
600
800
Current (pA)
1μM Picrotoxin
Control
Inward
B
GABA
Holding potential (mV)
Control
30
0
-30
-60
-90
-120
100pA
1s
C
GABA
1μM Picrotoxin
30
0
-30
-60
-90
-120

Fig. 3.3 $GABA_A$ whole-cell current-voltage relationships recorded from a single cell in the absence(•) and presence (o) of 1μM picrotoxin. The cell was continuously perfused with control medium or medium containing 1μM picrotoxin, and currents were evoked by 2.2s duration ionophoretic pulses of GABA applied every 5.6s. Each point is the current amplitude at the end of a single pulse (or the average of two responses). B, example GABA responses obtained at the holding potentials indicated to the right of the traces. GABA was applied ionophoretically onto the cell for the period indicated by the horizontal bar. Calibrations (also refer to C) 100pA, 1s. C, example GABA responses obtained in the presence of 1μM picrotoxin at the potentials indicated; GABA was ionophoretically applied onto the cell for the period indicated by the horizontal bar.

data for accurate histograms of shut times or burst lengths. For each of the three patches, single-channel currents evoked by GABA were recorded in the absence and in the presence of picrotoxin. These concentrations of GABA produced a fairly high opening frequency, though two channels only rarely opened simultaneously. The concentrations of picrotoxin chosen were ones which significantly reduced the whole-cell responses produced by 2-5μM GABA.

Figure 3.4 and Table 3.1 give detailed analyses of single channel recordings from a representative patch, held at -90mV. The patch was initially exposed to 5μM GABA, followed by 5μM GABA plus 1μM picrotoxin; it was then returned to 5μM GABA. Fig 3.4A, C, show histograms of the distributions of the logarithms of all shut times longer than 200μs that were measured from the record of $GABA_A$ single-channel currents in the absence (Fig. 3.4A) and presence (Fig. 3.4C) of 1μM picrotoxin. Each exponential component appears as a peaked function, the maximum of which correspond to the time constant of the exponential (see McManus *et al*, 1987; Sigworth & Sine, 1987). Both of the untransformed distributions were fitted with four exponential components, between 250μs and 1s. In the presence of 5μM GABA the time constants for the shut times were 0.24, 2.0, 41 and 287ms, and the relative areas under the fitted curves, of the four components, were 62%, 26%, 11% and 0.7% respectively. In the presence of 5μM GABA plus 1μM picrotoxin the two shortest time constants (τ_1 and τ_2 in Table 3.1) were not detectibly changed, being 0.24 and 2.0ms, and the longer time constants (τ_3 and τ_4 in Table 3.1) were only slightly altered, to 38 and 209ms respectively. The relative areas under the fitted curve, of the three shortest exponential components, were slightly less than in the presence of 5μM GABA alone, being (for τ_1 , τ_2 and τ_3) 56%, 23%, and 6% respectively, while the area of the longest component (τ_4) was noticeably greater, being 15%. This may simply reflect a reduced opening frequency in the presence of picrotoxin. The time constants, together with their relative areas, measured from GABA activated single-channel currents following washout of picrotoxin, are also given in Table 3.1.

Shut time distributions (containing all shut times longer than 200μs) were obtained from two other patches; in each case a separate distribution was obtained for $GABA_A$ single-channel currents in the absence, and in the presence of picrotoxin. All of the shut time distributions were well fitted with the sum of four exponential functions. Picrotoxin had no consistent effect on any of the time constants; the mean of the four time constants (τ_1, τ_2, τ_3 and τ_4) measured from the

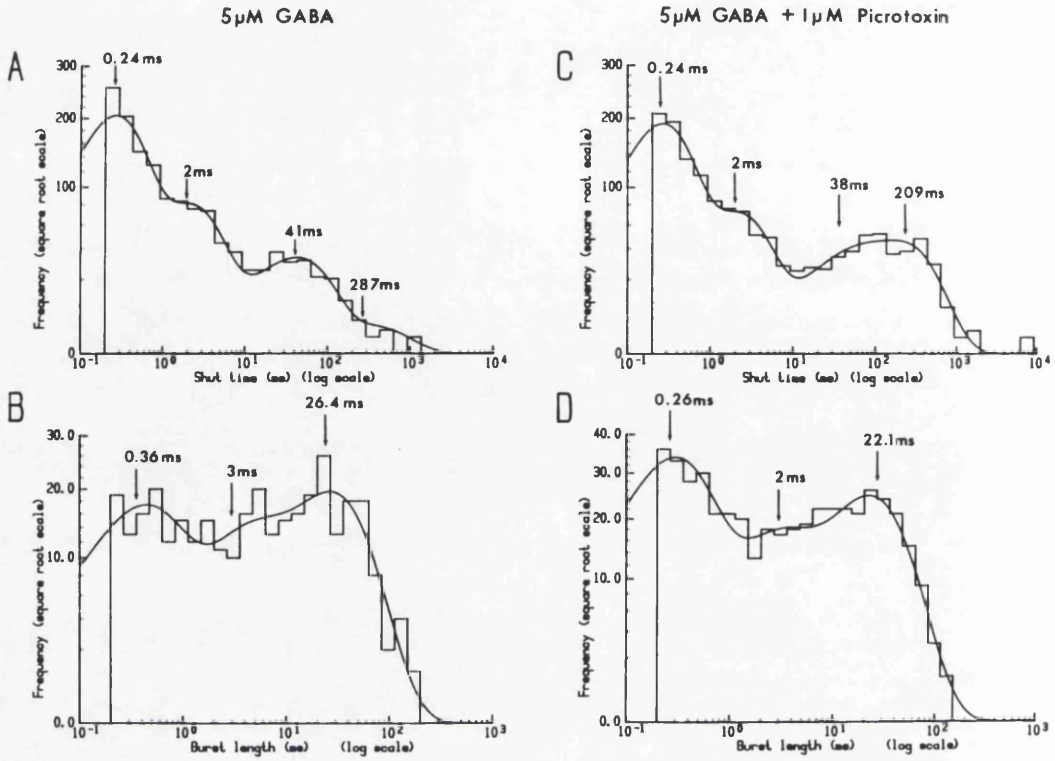
5μM GABA
5μM GABA + 1μM Picrotoxin
A
0.24 ms
2ms
41ms
287ms
Frequency (square root scale)
Shut time (ms) (log scale)
C
0.24 ms
2ms
38ms
209ms
Frequency (square root scale)
Shut time (ms) (log scale)
B
26.4 ms
0.36 ms
3ms
Frequency (square root scale)
Burst length (ms) (log scale)
D
0.26ms
22.1ms
2ms
Frequency (square root scale)
Burst length (ms) (log scale)

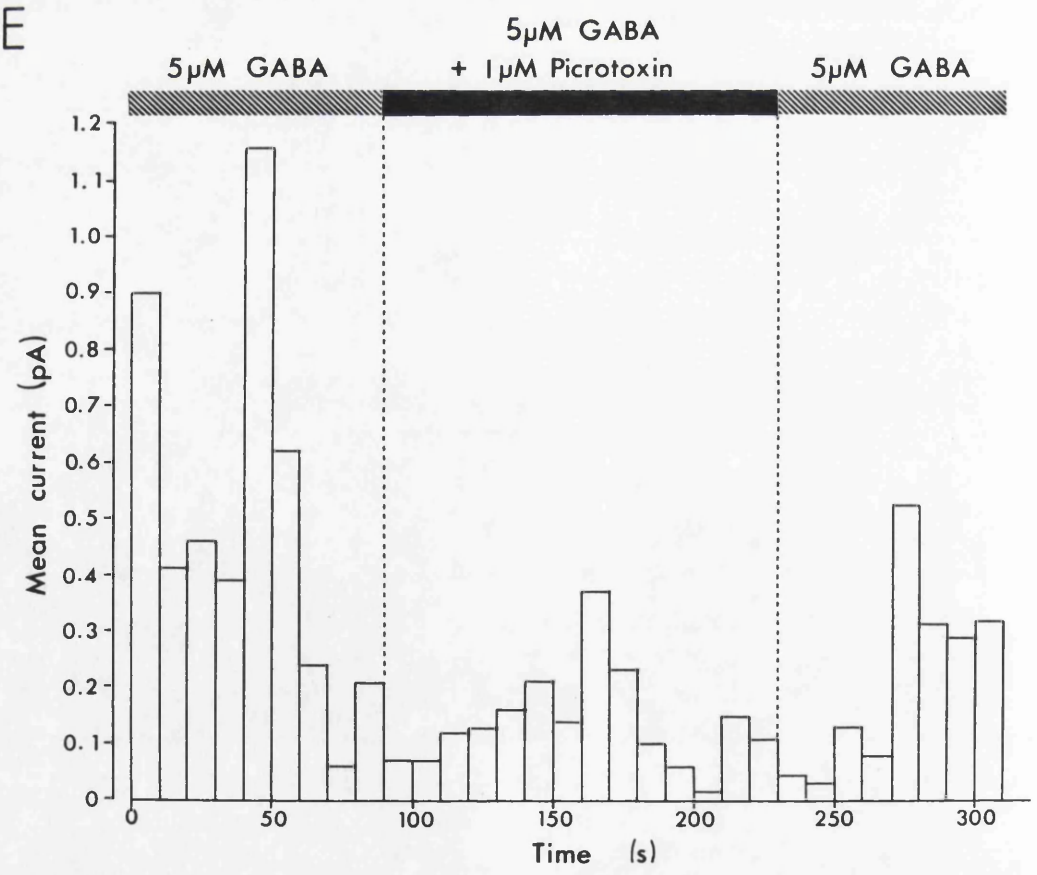
E
5μM GABA
5μM GABA
+ 1μM Picrotoxin
5μM GABA
Mean current (pA)
Time (s)

Fig. 3.4 A, distribution of all shut times measured from an outside-out patch exposed to 5μM GABA (V_m= -90mV). Distribution fitted (over the range 250μs to 1s) with four exponential components (continuous curve); time constants were: 0.24 (relative area, 62%), 2.0 (26%), 41 (11%) and 287ms (0.7%). B, burst length frequency distribution (for the same data as A); critical gap length to define the bursts =5.1ms. Distribution fitted (over the range 0.2 to 900ms) with three exponentials (continuous curve). Time constants were 0.36 (relative area, 34%), 3.0 (19%), and 26.4ms (47%). C, distribution of all shut times measured from an outside-out patch (same as for A and B) exposed to 5μM GABA plus 1μM picrotoxin (V_m= -90mV). Distribution fitted from 0.25 to 4000ms with four exponentials (curve); time constants were 0.24 (relative area, 56%), 2.0 (23%), 38 (6%) and 209ms (15%). D, frequency distribution of burst lengths (for the same data as C); critical gap length = 7.4ms. Distribution fitted by three exponentials (curve); time constants were 0.26 (relative area, 45%), 2.0 (17%) and 22.1ms (39%). For A–D single channel records were low pass filtered 2.5KHz (-3dB), and a resolution of 200μs was imposed on the data; note the absence of brief events in the histograms due to resolution limitation. For display purposes, distributions are of the logarithms of the intervals, such that each exponential component appears as a peaked function whose maximum corresponds to the time constant of the exponential. E, change in mean current with time for the continuous recording analysed in A–D; patch perfused with 5μM GABA followed by 5μM GABA plus 1μM picrotoxin, and then returned to 5μM GABA (as indicated by horizontal bars). The mean current in each bin was calculated from the integral of consecutive 10s sections of data.

TABLE 3.1: Effect of picrotoxin on shut times of GABA channels, measured from a single outside-out patch.

	Time constants(ms),and relative areas of each component							
	τ_1,	$Area_1$	τ_2,	$Area_2$	τ_3,	$Area_3$	τ_4,	$Area_4$
Control: GABA (5μM)	0.24	0.62	2.0	0.26	41	0.11	287	0.007
*GABA (5μM) plus Picrotoxin (1μM)	0.24	0.56	2.0	0.23	38.0	0.06	209	0.15
+Wash: GABA (5μM)	0.26	0.6	3.0	0.26	76	0.11	233	0.03

The data is from a single outside-out patch (also represented in Fig. 3.4). GABA activated single channel currents were recorded before (control data), during (second row *),and after (third row +), the application of 1μM picrotoxin. Closed time distributions were constructed from single-channel currents recorded under each condition. Each closed time distribution was fitted with four exponential components. The four corresponding time constants (τ_1, τ_2, τ_3, τ_4) are given with their relative area under the fitted curve ($Area_1$, $Area_2$, $Area_3$, $Area_4$).

three patches in the absence of picrotoxin were τ_1 = 0.25 ± 0.05ms, τ_2 = 1.63 ± 0.19ms, τ_3 = 17.5 ± 9.6ms and τ_4 = 207 ± 61ms, while in the presence of picrotoxin these mean time constants were 0.24 ± 0.02ms, 1.55 ± 0.20ms, 16.8 ± 8.7ms and 231 ± 35ms respectively (mean ± S.E.M., *n* = 3).

The two shortest time constants in the shut time distributions (0.24 and 2.0ms for the patch in Fig. 3.4) were interpreted as closures during a single receptor activation (i.e. the openings occurred in bursts), by analogy with the kinetics of other receptor-channels. Intraburst shut times of very similar duration have previously been determined for $GABA_A$ receptor-channels in cultured mouse spinal and chick cerebral neurones (Mathers, 1985; Weiss, 1988; Macdonald *et al*, 1989a; Weiss & Magleby, 1989), as well as in bovine chromaffin cells (Bormann & Clapham, 1985) and in cultured rat brain astrocytes (Bormann & Kettenmann, 1988). The two longer time constants were considered to represent closures between receptor activations. The two fastest time constants (τ_1 and τ_2) were very similar for each of the three patchs analysed, whereas the two longer time constants (τ_3 and τ_4) varied somewhat from patch to patch. This would be expected if the two shortest time constants in the shut time distribution represented closures during a single receptor activation , and if the two longer time constants represented closures between receptor activations. The two longer time constants would therefore depend not only on the kinetics of individual channels, but also on the number of channels, which is likely to vary from patch to patch. With this interpretation, the second and third time constants (τ_2 and τ_3) of each shut time distribution (with their relative areas) were used to calculate critical gap lengths (t_C), to define bursts of openings in the same stretch of data. The method of equal percentage of misclassified shut times was used to calculate t_C (Colquhoun & Sakmann, 1985).

3.5.2 *Distributions of burst lengths*

Figure 3.4B,D show distributions of burst lengths measured from $GABA_A$ single channel currents recorded in a patch held at -90mV (same patch as Fig. 3.4A,C). The distributions contain all burst lengths longer than 200μs measured in the absence (Fig. 3.4B; t_C = 5.1ms) or presence (Fig. 3.4D; t_C = 7.4ms) of picrotoxin. For display purposes only, the distributions are of the log intervals. Distributions of the untransformed intervals were fitted, over the range 0.2 to 900ms, with three exponentials. In the presence of 5μM GABA the time constants of the

burst length distribution were, 0.36, 3.0 and 26.4ms, and the relative areas of these exponential components were 34%, 19% and 47% respectively. In the presence of 5μM GABA plus 1μM picrotoxin, the time constants were apparently slightly shorter, being 0.26, 2.0 and 22.1ms. Furthermore the relative area of the shortest exponential component appeared to be greater with 5μM GABA plus 1μM picrotoxin; the relative areas of the 3 exponentials (from briefest to longest) were 45%, 17% and 39% respectively. However the time constants were not very well separated in the distributions (see Fig. 3.4B, D for an example) and in one of the other patches the sum of four exponentials provided a better fit to the distribution than the sum of three exponentials. There is too little data at present to be sure of the effect (if any) of picrotoxin on the length of bursts of openings of $GABA_A$ receptor-channels. However, taken together with the noise experiments (where τ_{fast} from the noise gives a reasonable estimate of burst length, see for example Howe, Colquhoun & Cull-Candy, 1988), there is no evidence for a marked effect of picrotoxin on burst length.

3.5.3 *Integrated open-time*

It was apparent from cursory examination of single channel current records, that picrotoxin reduced the frequency of channel openings. This effect is described more quantitatively in Fig. 3.4E which shows the effect of 1μM picrotoxin on the mean current evoked by 5μM GABA in an outside out patch held at -90mV (same patch as Fig. 3.4A-D). The mean current was measured by integrating successive 10s section of the continuous current record (total duration 310s). 5μM GABA was present throughout the entire record, whereas 1μM picrotoxin was applied only for 140s, during the period 90s to 230s after the start of the recording. It is apparent from Fig. 3.4E that 1μM picrotoxin reduced the mean current evoked by 5μM GABA; the overall mean current was reduced from 0.49pA to 0.17pA by 1μM picrotoxin. It is also apparent from Fig. 3.4E that the single channel activity did not recover to control levels within 80s after the washout of 1μM picrotoxin, at which time recording was stopped. The reason for this is unclear, but may result from a slow washout of picrotoxin, as suggested by the results presented in the next section, or may represent a 'run down' of GABA receptor-channel activity (Gyenes *et al.*, 1988;Stelzer *et al.*, 1988).

Although these results suggest that picrotoxin reduces the opening frequency, there was a lack of consistency in the effect of picrotoxin on the shut time distributions since the time constants of

these distributions were not well separated.

3.6 *Rate of onset of block by picrotoxin*

The rate of onset of block by picrotoxin was slow enough to be followed using brief (8-20ms) applications of GABA at frequencies of 0.5 to 2.5Hz. In all experiments the ionophoretic pipette was positioned close to the cell so that the whole-cell currents reached a peak within less than 200ms. The background level of GABA was kept to a minimum by using high resistance ionophoretic pipettes (>150MΩ), with a braking current, and by washing the cell continuously with control medium.

In all of the cells examined (6 cells) it was clear that the rate of onset of block by picrotoxin was accelerated by GABA. An example of this is shown in Fig. 3.5. The cell was held at -70mV and perfused at a constant rate with bathing medium. The upper trace of Fig. 3.5A shows a continuous whole-cell current record (except for a 50s period indicated by the dashed line). 10ms ionophoretic pulses of GABA were applied every 400ms, including during the 50s period not shown. These pulses of GABA evoked brief, rapidly rising inward current responses (downward deflections in the record), which had a constant amplitude in the control medium. 10μM picrotoxin was applied to the bathing medium 2s after the start of the record, and was applied for 4.8s. Under the conditions of this experiment, 10μM picrotoxin produced a maximum amount of inhibition within approximately 5s. It is apparent from Fig. 3.5A that when GABA pulses were applied continuously the picrotoxin block was completely reversed within 56s following wash-out of picrotoxin.

Fig 3.5B illustrates the rate of onset of block by 10μM picrotoxin in the same cell, in the absence of GABA pulses. Fig. 3.5B shows a continuous whole-cell current record interrupted by a brief gap (dashed line) during picrotoxin application, and a 50s gap (dashed line) during recovery from picrotoxin. The responses to GABA in the absence of picrotoxin were of relatively constant peak amplitude. The GABA pulses were switched off 1.2s before and for 33s during, the application of 10μM picrotoxin in the bathing medium. It is apparent from Fig. 3.5B that when GABA pulses were applied every 400ms, the removal of GABA between the pulses was not complete, since the current responses returned to the baseline only when the pulses were turned off completely. Picrotoxin was applied only when the current trace had returned to the baseline level to ensure that no GABA was present during the initial application of picrotoxin. The GABA pulses were

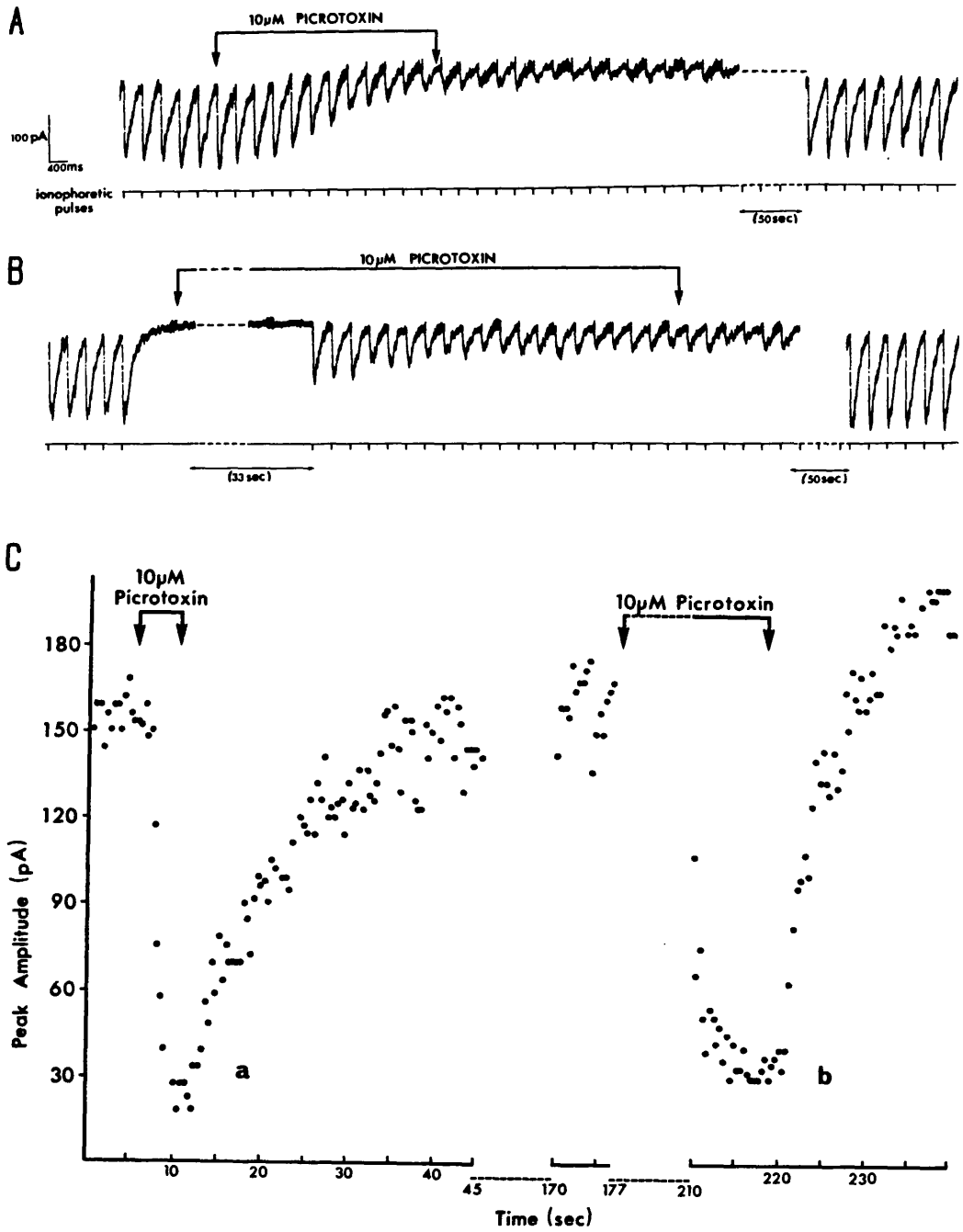
A
10μM PICROTOXIN
100 pA
400ms
ionophoretic pulses
(50sec)
B
10μM PICROTOXIN
(33 sec)
(50sec)
C
10μM Picrotoxin
10μM Picrotoxin
180
150
120
90
60
30
Peak Amplitude (pA)
a
b
10
20
30
40
45
170
177
210
220
230
Time (sec)

Fig. 3.5 Experiment illustrating that block by picrotoxin occurs more rapidly in the presence of GABA. A, upper trace: continuous whole-cell current record (except for a 50s interval, indicated by dashed line); V_m = -70mV. Downward deflections are inward current responses to 10ms ionophoretic pulses of GABA applied every 400ms, (monitored on lower trace). 10μM picrotoxin was bath applied during a period of 4.8s indicated by the horizontal bar above the record; maximum block had occurred within less than 5s of picrotoxin application. B, upper trace: continuous whole-cell current record (same cell as A) interrupted by a brief gap (dashed line) during picrotoxin application, and a 50s gap (dashed line) during recovery from picrotoxin. The pulses of GABA were turned off before, and during the initial 33s of 10μM picrotoxin application (the period indicated by horizontal bar and arrows). The block had reached only 35% of the maximum after 33s of picrotoxin application, in the absence of GABA pulses. Calibration 100pA and 400ms. C, plot of the peak amplitude of consecutive GABA responses evoked during continuous recording from the cell depicted in A and B (denoted as a and b respectively). Each point is the peak amplitude of a single response and is plotted against the time at which it occurred in relation to the start of the record (time zero). 10μM picrotoxin was applied to the cell twice, a, between the period 5.5 to 10.3s and b, 177 to 218s from the start of the record. The time axis is not continuous; a 125s gap (dashed line) during recovery from the first application of picrotoxin, and a 33s gap (dashed line) during the second application of picrotoxin, when the GABA pulses were turned off. Complete recovery from picrotoxin occurred within 28s of the washout of the first application of picrotoxin (part a). Note the responses during the recovery from picrotoxin depicted in part b were larger than the control responses.

reapplied 33s after the start of the application of picrotoxin. The peak amplitude of the response evoked by the first GABA pulse in the presence of picrotoxin was inhibited by only 35% of the maximum inhibition. This contrasts with the experiment depicted in Fig. 3.5A, in which 10μM picrotoxin produced maximal block within 5s of application (which includes time for picrotoxin to reach the cell). The only difference between Fig 3.5A and B is the presence or absence of GABA during the initial application of picrotoxin.

Fig. 3.5C is a more quantitative representation of the results depicted in Fig. 3.5A,B illustrating in particular the recovery from picrotoxin. The plot is of the peak amplitude of consecutive GABA responses evoked during a continuous recording from the cell. Each point is the peak amplitude of a single response, and is plotted against the time at which it occurred in relation to the start of the record (time zero). It is apparent from part a (Fig. 3.5C) that with GABA pulses present the rate of recovery from picrotoxin was far slower than the rate of onset of block, when picrotoxin was applied for 4.8s. Maximum block occurred within 5s of the application of 10μM picrotoxin, whereas complete recovery required 28s. In all cells where the amplitude of GABA responses recovered to approximately 100% of control and where GABA pulses were applied during the entire experiment, the rate of recovery from picrotoxin was slower than the rate of onset of block. However, this observation was not investigated further. In the experiment depicted in part b of Fig. 3.5C, the amplitude of GABA responses that followed recovery from picrotoxin were larger than control GABA responses, probably as a result of a change in the relative position of the ionophoretic pipette and the cell.

It was apparent that although picrotoxin could produce the same degree of block in the absence of GABA, as in its presence, the block occurred more slowly. Figure 3.6 shows a comparison, obtained with a single cell, of the rates of onset of block by picrotoxin in the absence of GABA, and when 18ms GABA pulses were applied every 2s. Fig. 3.6A depicts an experiment during which the GABA pulses were applied during the entire application of picrotoxin. It is apparent from the continuous whole-cell current trace that application of 10μM picrotoxin to the bathing medium produced a rapid reduction in the size of the GABA currents; peak response amplitude was reduced to 20% of control (maximum inhibition under these conditions) within 20s of picrotoxin application. Fig. 3.6B depicts an experiment during which the GABA pulses were turned off 2s before, and for the initial 120s of application

of 10μM picrotoxin. In this case, the peak amplitude of the first response elicited in the presence of picrotoxin (120s from the start of the application) was only reduced to 65% of control, indicating that the onset of block by picrotoxin occurred far more slowly in the absence, than in the presence, of GABA. Fourteen experiments of the type illustrated in Fig. 3.6B were performed; control responses were obtained in each and complete recovery occurred after removal of picrotoxin. The only parameter to be varied between these experiments was the period of time during the initial application of picrotoxin for which the GABA pulses were turned off (varied between 11 and 300s). The solid symbols in Fig. 3.6C (plot b) show results from these experiments. Each point is the peak amplitude of the first response to a GABA pulse in the presence of picrotoxin (expressed as a % of control) plotted against the period of time during which picrotoxin had been applied in the absence of GABA pulses. This graph therefore shows the rate of onset of block by 10μM picrotoxin in the absence of GABA. For comparison the open symbols (plot a) represent the peak amplitude (as a % of the control) of successive single responses from the experiment depicted in Fig. 3.6A, plotted against its time of occurrence in relation to the start of picrotoxin application (at time zero). This plot therefore shows the rate of onset of block by 10μM picrotoxin in the same cell, in the presence of GABA (applied for 18ms every 2s). It is apparent that the onset of block by picrotoxin in the absence of GABA is slow relative to the block in the presence of GABA. Responses were reduced to 25% of control in approximately 290s in the absence of GABA, compared to an equivalent degree of block being obtained within 18s in the presence of GABA. In summary, picrotoxin produced only a slowly equilibrating block in the absence of GABA.

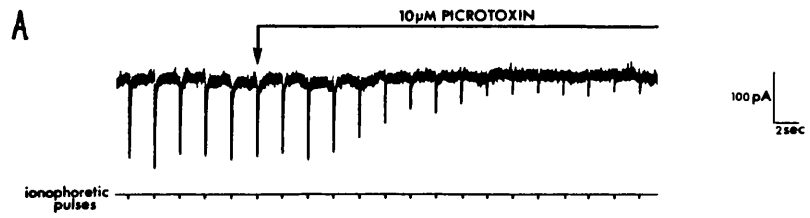
A
10μM PICROTOXIN
100 pA
2sec
ionophoretic pulses

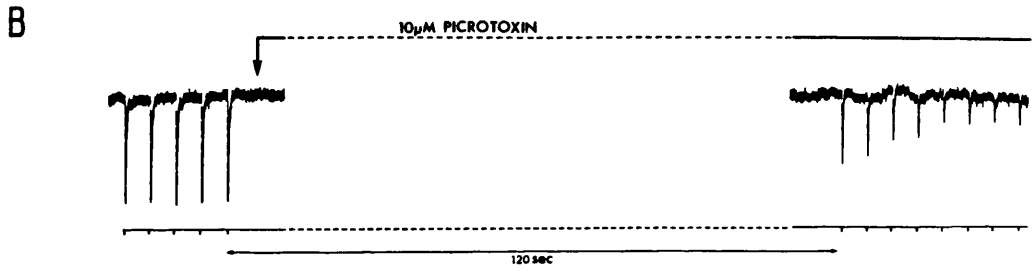
B
10μM PICROTOXIN
120 sec

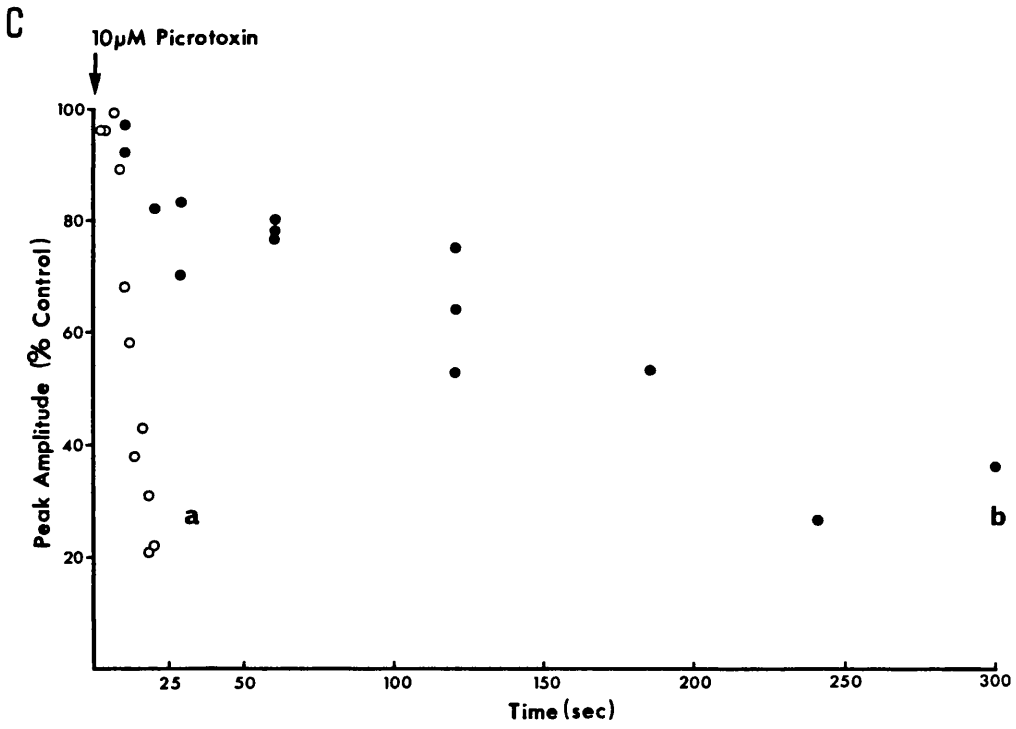
C
10μM Picrotoxin
Peak Amplitude (% Control)
100
80
60
40
20
a
b
25
50
100
150
200
250
300
Time (sec)

Fig. 3.6 Experiment illustrating the slow onset of block by picrotoxin in the absence of GABA. A, upper record: continuous whole-cell current trace; V_m = -70mV. Downward deflections are inward current responses to ionophoretic pulses of GABA (18ms) applied every 2s (ionophoretic current monitored on lower trace). 10μM picrotoxin, applied to the bathing medium during the time indicated by the horizontal bar, produced a rapid reduction in the size of the GABA-currents. Maximum block had occurred within less than 20s of picrotoxin application; response amplitude during maximum block was 20% of control. B, whole-cell current record (same cell as A) interrupted by a long gap (dashed line) during picrotoxin application. The 18ms pulses of GABA were applied every 2s except for 2s before, and 120s during, the initial application of 10μM picrotoxin (applied during the period indicated by the horizontal bar and arrows). The first response in the presence of picrotoxin was 65% of control. C, plot of the peak amplitude of individual GABA responses *vs* time after the initial application of 10μM picrotoxin. Each point of graph a (open circles) is the peak amplitude of a single response from A, plotted against its time of occurrence in relation to the start of picrotoxin application (at time zero). Response amplitude was reduced to 25% of control within 18s of 10μM picrotoxin application. Each point of plot b (closed circles) represents a single experiment of the type depicted in B; total of 14 experiments from one cell. Each point is the peak amplitude of the first GABA response elicited in the presence of 10μM picrotoxin; picrotoxin applied up to this response for the period indicated on the time axis. Responses were reduced to 25% of control in approximately 290s.

It is generally considered, on the basis of dose-response data, that at least part of the action of picrotoxin in both vertebrates and invertebrates is not competitive. Although is is difficult to interpret results from binding studies in terms of mechanisms of action (because the state of the receptor-channel complex to which the drugs are binding is unknown), binding studies generally suggest that picrotoxin binds to a site distinct from the GABA receptor site, but that there is allosteric interaction between the agonist and antagonist binding sites. Several mechanisms of action could result in inhibition of macroscopic (whole-cell) GABA currents that is not competitive, including simple open channel block, complex channel block, enhancement of desensitization, or a combination of these. These possibilities will now be considered in the light of the results presented here, and of previous studies.

It should be noted that picrotoxin, rather than picrotoxinin, was used throughout this study. Picrotoxin is an equimolar mixture of picrotin and picrotoxinin, and several studies suggest that picrotoxinin is the sole active component (Jarboe *et al.*, 1968; Ticku *et al.*, 1978; Simmonds, 1982).

3.7 *General properties of $GABA_A$ receptor channels*

Before discussing the effect of picrotoxin on $GABA_A$ currents it is worth considering briefly the general properties of $GABA_A$ receptor-channels in rat sympathetic neurones. In this study the spectra of GABA current noise were described by the sum of two Lorentzians. The corresponding time constants were somewhat variable from cell to cell, being in the ranges 1-4.7ms and 35-69ms (at -60mV). These values are similar to those previously reported, in which GABA spectra were fitted with the sum of two Lorentzian components, in rat sympathetic neurones(Cull-Candy & Mathie, 1986; Cull-Candy, Mathie & Newland, 1987), bovine chromaffin and glandular cells (Inenagah & Mason, 1987; Cull-Candy, Mathie & Powis, 1988), rat and mouse central neurones (Sakmann, Hamill, Bormann, 1983; Cull-Candy & Ogden 1985; Cull-Candy & Usowicz, 1989a), and crustacean muscle (Dudel, Finger & Stetmeier, 1980). The distributions of bursts lengths, measured directly from $GABA_A$ single channel currents, recorded from rat sympathetic neurones were fitted with three or four exponentials. In the case of three exponentials, the time constants were in the ranges 0.3 - 0.4ms, 1.0 - 3.5ms and 17 - 45ms. Distributions of burst lengths, or of apparent open times, measured directly from $GABA_A$ single channel currents

recorded from various vertebrate neurones have also been fitted with at least two exponential functions (Jackson *et al.*, 1982b; Miledi, *et al.*, 1983; Sakmann *et al.*, 1983; Bormann & Clapham, 1985; Mathers, 1985; Allan & Albuquerque, 1987; Bormann & Kettenmann, 1988; ffrench-Mullen *et al.*, 1988; Mathers & Wang, 1988; Weiss, 1988; Macdonald *et al.*, 1989a; Weiss & Magleby, 1989). The time constants of burst length distributions obtained in the present study were within the range of the values for burst lengths reported for mammalian chromaffin cells and astrocytes (Miledi *et al.*, 1983; Jackson *et al.*, 1982b; Bormann & Clapham, 1985; Bormann & Kettenmann, 1988), but most closely agree with those reported by Macdonald *et al.*, (1989a) for openings to the main conductance state observed in cultured mouse spinal neurones (which were 1.0ms, 5.5ms, and 29.8ms). It has usually been found for other agonist activated channels, that the time constants derived from noise represents the burst of channel openings produced by a single receptor activation (*i.e.* the 'burst-length'). There is some agreement between the time constants estimated from GABA noise and the longer time constants of the distributions of burst lengths, though there is a lot of variability in these estimates between preparations (and between reported values).

The amplitude of the most frequently observed conductance level in single-channel recordings under control conditions in rat sympathetic neurones was about 30pS. Also levels of about 22-23pS and 15-18pS were often observed, while levels of 7-9pS could also be seen with reasonable reliability (see Chapter 4). It is therefore not surprising that the conductance estimated from GABA noise in these cells was smaller than the main state conductance level measured directly from single channel records (mean conductance estimated from noise was 11.8 ± 2.4pS; mean ± S.D., n = 7, -60mV). $GABA_A$ receptor channels in other vertebrate cells apparently open to several discrete conductance levels with amplitudes between 10 and 45pS (Hamill *et al*, 1983; Miledi *et al*, 1983; Cottrell *et al*, 1985; Bormann *et al*, 1987; Huck & Lux, 1987; 1987; Bormann & Kettenmann, 1988; McBurney *et al*, 1985; Weiss *et al*, 1988; Macdonald *et al*, 1989a; Yang & Zorumski, 1989).

A complication in the interpretation of the effects of picrotoxin, is the suggestion that, in frog sensory neurones, there are three functionally different subtypes (in terms of single-channel conductance and GABA concentration dependence) of the $GABA_A$ receptor-channel complex, and that these subtypes also differ in their sensitivity to picrotoxin (Yasui *et al*, 1985). The possibility of more than one type of

$GABA_A$ receptor-channel in rat sympathetic neurones is discussed further in Chapter 4.

3.8 Possible mechanisms of action of picrotoxin on $GABA_A$ receptor channels

3.8.1 *Simple open channel block*

The simplest mechanism of action of picrotoxin that would result in block of $GABA_A$ currents that is not competitive, is simple sequential open channel block, as originally proposed by Armstrong (1971) and extended by Adams (1976):

$$A + R \underset{k_{-1}}{\overset{2k_1}{\rightleftharpoons}} AR \underset{2k_{-1}}{\overset{k_1}{\rightleftharpoons}} A_2R \underset{\alpha}{\overset{\beta}{\rightleftharpoons}} A_2R^* \underset{k_{-B}}{\overset{k_{+B}}{\rightleftharpoons}} A_2R^*B \qquad (1)$$

where A represents the agonist molecule, R the closed receptor channel, R^* the open receptor channel, B the blocker molecule, and β, α, k_1 , k_{-1} , k_{+B} and k_{-B} are the forward and backward microscopic rate constants for transitions between states. A consequence of this sequential mechanism of block is that the blocked channel must re-open in order for the blocking molecule to dissociate and the channel to shut. The effect of open channel blockers on single channel currents depends on the relative rate of dissociation of the blocker from the channel, and these effects can be predicted from scheme (1). Furthermore, in the simplest case where agonist spectra can be fitted by a single Lorentzian, with a time constant that reflects the burst length of the underlying single channel currents, the effect of a simple open channel blocker on the spectra can also be predicted. Although the gating of $GABA_A$ receptor channels appears far more complex than that depicted in scheme (1), it is still possible to assess whether picrotoxin acts as a simple open channel blocker from its effects on GABA spectra, and single-channel currents.

When considering single channel currents, an open channel blocker would be expected to reduce the duration of individual openings (from $1/\alpha$ to $1/(\alpha+[B]k_{+B})$, in scheme (1), where [B] is the concentration of blocker) and increase the total burst duration (due to the introduction of several blockage gaps, between individual openings, during a single activation). However, the total open time per burst is expected to be independent of the antagonist concentration, since the blocked channel has to re-open in order for the blocker molecule to dissociate and the channel to shut, and because the channel is 'memoryless' (Neher & Steinbach, 1978; Colquhoun & Hawkes, 1982; 1983). The extent of the

changes in open time and burst length would of course depend on the dissociation rate of the open channel blocker (assuming similar association rate constants).

Open channel blockers would also be expected (depending on the dissociation rate) to change a single Lorentzian spectrum to a double-Lorentzian, with one time constant faster, and the other slower, than the time constant of the control spectrum; the faster time constant representing (very roughly) the individual openings, and the slower time constant reflecting the bursts. The fast time constant should get briefer, and the slow time constant longer, as the antagonist concentration is increased (Adams, 1976; Neher & Steinbach, 1978). Furthermore, there should be a linear relationship between the antagonist concentration and the sum of the reciprocal of the fast and slow time constants, minus the reciprocal of the control time constant, that is, $\tau_f^{-1} + \tau_s^{-1} - \tau_c^{-1}$ (Colquhoun & Sheridan, 1981; Ogden, Siegelbaum & Colquhoun, 1981).

In the case of the nicotinic acetylcholine receptor, there are numerous drugs whose blocking action can be described, at least to a first approximation, by a simple open channel block mechanism. These drugs produce the predicted changes in the open time, burst length and noise spectra of nicotinic acetylcholine receptor channels. Included in this category are tubocurarine (Manalis, 1977; Ascher, Marty & Neild, 1978; Katz & Miledi, 1978; Colquhoun, Dreyer & Sheridan, 1979; Ascher, Large & Rang, 1979; Rang, 1982), gallamine (Katz & Miledi, 1978; Colquhoun & Sheridan, 1981), some barbiturate local anaesthetics (Adams, 1976; 1977), and low concentrations of QX222, a lignocaine derivative (Ruff, 1977; 1982; Neher & Steinbach, 1978). Drugs which appear to act, at least in part, as open channel blockers of another agonist-gated ion channel, the *N*-methyl-D-aspartic acid-activated channel (NMDA channel) include magnesium, nickle, cobalt, and manganese ions (Ault *et al*, 1980, Mayer *et al*, 1984; Nowak *et al*, 1984; Mayer & Westbrook, 1985; 1987; Ascher & Nowak, 1988; Mayer *et al*, 1988), MK-801 (Huettner & Bean, 1988), desipramine (Sernagor, Kuhn, Vyklicky & Mayer, 1989) and phencyclidine (Bertolino, Vicini & Costa, 1978).

An open channel blocking mechanism may account for part of the action of penicillin at $GABA_A$ receptor channels. There are a limited number of quantitative studies of the effect of penicillin on $GABA_A$ channel kinetics. However Chow & Mathers (1986) observed that penicillin reduced the fast time constant of channel open time distributions for GABA currents from mouse spinal neurones, while

Barker *et al* (1983) reported that penicillin caused complex changes in the power spectra of GABA currents from mouse spinal neurones. Furthermore, Smart (1983) suggested that penicillin binds preferentially to the open bound, A_2R^* species, based on quantitative analysis of GABA dose-response data (measured in crustacean muscle).

Intermediate dissociation rate Changes in open times and burst lengths of $GABA_A$ receptor-channels, and changes in the GABA noise spectrum would be more obvious with an intermediate dissociation rate blocker than with either fast or slow dissociation rate blockers. We could not detect any effect of picrotoxin on the time constants of GABA spectra in rat sympathetic neurones, where the spectra were fitted with the sum of two Lorentzian components in control conditions and in the presence of picrotoxin. A lack of effect of picrotoxin on GABA spectra has been previously observed, in mouse spinal neurones and hippocampal neurones (Barker, McBurney & Mathers, 1983; Segal & Barker, 1984) although in contrast to the present work, spectra were fitted with a single Lorentzian, and a narrower frequency range was investigated (0.1 to 100Hz or 0.2 to 200Hz respectively). However, Barker *et al* (1983) observed 'excess' noise at the high frequency end of many of their fitted spectra.

In the present study the effect of picrotoxin on $GABA_A$ single-channel currents was measured directly, with the minimum resolvable interval set at 200μs (1.5 times the filter rise time). For the three patches analysed no consistent effect of picrotoxin on burst lengths was observed. Akaike & Oomura (1984) and Akaike *et al* (1985) have previously observed that picrotoxin did not produce the 'flickery' block of GABA single channel currents (in bullfrog sympathetic neurones) expected of an intermediate dissociation rate open channel blocker. However no measure of the effect of picrotoxin on channel open times or burst lengths was made. Taken together, our noise and single channel data suggest that picrotoxin does *not* act as an intermediate dissociation rate open channel blocker.

Rapid dissociation rate The present observation that picrotoxin did not reduce the apparent conductance of $GABA_A$ receptor channels, measured directly from single channel recordings or estimated from GABA spectra, is inconsistent with a very rapidly dissociating open channel blocking mechanism. A very rapidly dissociating open channel blocker (which would be likely to have low potency; equilibrium constant for open channel block, K_B say, in the order of 1-100mM) would be expected to produce an *apparent* reduction in single channel

conductance, because openings would be very short and the transitions of the channel between the fully open state and the blocked state would be too rapid to be fully resolved. Such a rapid open channel block is seen for a variety of channel types and blockers, including block of nicotinic acetylcholine channels by carbamylcholine or acetylcholine itself (Sine & Steinbach, 1984b; Ogden & Colquhoun, 1985), block of ATP sensitive potassium channels in frog skeletal muscle by Cs^+ and Ba^+ (Quayle, Standen, Stanfield, 1986), and block of Ca^{2+}-activated K^+ channels of bovine chromaffin cells by internal Na^+ (Yellen, 1984), to mention but a few. Although we did not investigate the possibility that picrotoxin caused a shift in the relative frequency of occurrence of the various conductance levels to ones of lower amplitude, a significant change would have been expected to reduce the channel conductance estimated from noise.

Slow dissociation rate On the basis of our single channel data and noise analysis, and the noise analysis of Barker *et al* (1983) and Segal & Barker (1984), a slowly dissociating open channel block mechanism for picrotoxin cannot easily be ruled out. A slowly dissociating open channel blocker (K_B in the nM range) may produce only a slight change in apparent burst length, because with a typical association rate (K_{+B} in scheme 1) of the order of $5 \times 10^7 M^{-1}s^{-1}$, multiplied by a concentration of say 20nM, would contribute only $1s^{-1}$ to the reciprocal mean open time ($1/(\alpha+[B]k_{+B})$ in scheme 1). Furthermore, the expected blockage gaps ($1/k_{-B}$ in scheme 1; of the order of seconds) would be so long as to be difficult to distinguish from other sorts of long silent periods such as gaps between activations, or gaps that result from desensitization. Indeed the three outside-out patches analysed contained long gaps-between-bursts, with mean values in the range of 20-300ms.

A further prediction that can be made from the sequential blocking scheme (1) is that a slowly dissociating open channel blocker may exhibit 'use-dependence', that is, the blocker becomes more effective as more channels are opened, and since the blocking molecule dissociates relatively slowly from the channel, the blocker accumulates. Such use-dependence has been widely described for the action of various open-channel blockers, including local anaesthetic block of voltage-gated sodium channels in nerve (Strichartz, 1973; Courtney, 1975; Khodorov, 1976; Cahalan, 1978) and in muscle (Schwartz *et al*, 1977) and for ganglionic blocking drugs acting on nicotinic receptors at muscle end plates (Magazanik & Vyskocil, 1976; Burgermeister *et al*, 1977; Maleque *et*

al, 1982), and for block of NMDA receptor-channels by ketamine (Macdonald *et al*, 1987; Mayer *et al*, 1988). Although the use-dependent effect of picrotoxin observed in the present study may reflect an underlying slowly dissociating open channel blocking mechanism, this is not a unique interpretation. A complex channel blocking mechanism may also result in use-dependence (see below).

Akaike *et al* (1985) suggested that the site of action of picrotoxin is in the channel, since picrotoxin inhibited GABA responses in bullfrog sensory neurones, when the antagonist was applied intracellularly. However, we have not been able to block or reduce significantly the whole-cell GABA currents in rat sympathetic neurones by including picrotoxin (up to 40μM) inside the patch pipettes (results not shown). An alternative interpretation of the results of Akaike *et al* (1985)is that picrotoxin can reach its site of action through the membrane rather than via the open channel.

There is some evidence, however to suggest that picrotoxin does not act as a slowly dissociating open channel blocker. The concentration of picrotoxin required to reduce GABA currents by 50% (IC_{50} value) in vertebrate neurones, has been estimated to be in the range 0.6μM (Sigel & Baur, 1988) to 37μM (Bowery & Brown, 1974). In contrast a slowly dissociating channel blocker would be expected to have a K_B in the nM range, though IC_{50} could be considerably greater than the true K_B if measurements were made under conditions where a small proportion of channels were open. Thus, for scheme (1), the ratio of the proportion of channels in the open (A_2R^*) state at equilibrium in the absence ($P_1(O)$ say), to in the presence ($P_1(B)$ say) of blocker, is $1+(x_B P_1(O)/K_B)$ where K_B is the equilibrium dissociation constant, and x_B is the concentration of blocker. Under conditions where the concentration of blocker produces 50% inhibition (*i.e.* $x_B = IC_{50}$) then $P_1(O)/P_1(B) = 2$. Thus $1/P_1(O) = IC_{50}/K_B$. Consequently K_B will be equal to IC_{50} only when all channels were open at equilibrium in the absence of blocker (*i.e.* when $p_1(O)=1$), otherwise IC_{50} will be greater than K_B. The measurement of K_B values from binding studies is difficult to relate to actual potency since it is not known to which conformation of the receptor-channel the drug is binding (for example picrotoxin could have highest affinity for the receptor channel complex in the desensitized state).

The slowly developing block by picrotoxin in the absence of GABA observed for rat sympathetic neurones in the present study, suggests that there is no absolute requirement that the channel be open before

picrotoxin block can occur. In agreement with this observation, Yakushiji *et al.* (1987) and Kudo *et al.* (1984) observed that pretreatment with picrotoxin enhanced the degree of block of GABA responses in frog spinal cord neurones and frog sympathetic ganglion neurones. Of course this may still mean that picrotoxin is an open channel blocker, but that it can gain access to the channel via, say the membrane lipid. It is interesting to note that the onset of block of GABA currents by t-butylbicyclophosphorothionate (TBPS), a compound thought to act at the same site as picrotoxin and picrotoxinin on the $GABA_A$ receptor-channel (Squires *et al*, 1983) also occurs slowly in the absence of GABA (Van Renterghem *et al*, 1987). Furthermore, both the binding and the dissociation rates of TBPS binding can be measured in the absence of agonist (Maksay & Ticku, 1985; Squires *et al*, 1983). It should be noted that TBPS binding, rather than picrotoxin binding, has generally been used to investigate the interaction between the picrotoxin site and the GABA binding site since TBPS binds to the same site as ^{3}H-dihydropicrotoxinin, but has the advantages of higher affinity and lower levels of non-specific binding (Squires *et al*, 1983).

Stabilization of a transmitter operated ion channel in an open but blocked state should result in the receptor having a higher affinity for the agonist in the presence of blocker (Neher & Steinbach, 1978). However binding studies suggest that picrotoxin reduces, rather than increases, the affinity of GABA and muscimol for the $GABA_A$ receptor (Fujimoto & Okabayashi, 1981; Supavilai *et al*, 1982; Matsumo & Fukuda, 1982; Quast & Brenner, 1983).

The present observation that the block of GABA responses in rat sympathetic neurones by picrotoxin is voltage-independent cannot be taken as evidence against an open channel blocking mechanism since the two components of picrotoxin (picrotin and picrotoxinin) are neutral molecules (Porter, 1967). In agreement with these results, Adams *et al*, (1981b) observed that picrotoxin did not alter the voltage-dependence of the decay of GABAergic inhibitory post synaptic currents in crayfish stretch receptors. Furthermore Yakushiji *et al* (1987) and Akaike *et al* (1986) observed that picrotoxin did not alter the current-voltage relationship of whole-cell GABA currents from bullfrog sensory neurones. However, the observation by Akaike & Oomura (1984) and Akaike *et al* (1985) that picrotoxin eliminated the non-linearity (outward rectification) of whole-cell GABA current voltage relationships (for bullfrog dorsal root ganglion neurones) is incompatible with the present results.

3.8.2 *Complex channel block*

Complex channel block mechanisms are still expected to shorten individual openings (e.g. Ogden & Colquhoun, 1985) and may involve either the introduction of additional (possibly long-lived) blocked states into the simple sequential mechanism described above, or cyclical schemes whereby the channel can shut without returning to the open state and with the blocking molecule still bound. It is also possible either that the antagonist binds to more than one site (perhaps with different affinities) to produce two or more blocked states, or that the antagonist acts at a site (or sites) away from the ion channel, but blocks the channel allosterically, or both.

Such complex blocking mechanisms can result in 'use-dependence', say if the antagonist binds with higher affinity to the agonist bound receptor-channel and stabilizes an agonist bound shut state. Therefore the use-dependent block by picrotoxin of GABA currents in rat sympathetic neurones may be due to a complex channel block mechanism. Use-dependence has been observed for the complex block of other agonist gated ion channels including block of nicotinic acetylcholine receptors in rat submandibular ganglia by hexamethonium, which appears to get trapped within a shut channel and can therefore dissociate only slowly from the receptor-channel (Gurney & Rang, 1984), and for the block of NMDA receptor-channels by ketamine (Macdonald, Miljkovic, Pennefather, 1987; Mayer *et al* 1988). More relevant to the present study, Van Renterghem *et. al.* (1987) observed that the onset of block of $GABA_A$ currents by TBPS was use-dependent (measured from *Xenopus* oocytes which had been injected with chick brain mRNA). The observation by Van Renterghem *et al* (1987), that the offset of TBPS block was also use-dependent, is consistent with conclusions from binding studies in which the dissociation rate of TBPS binding from rat brain membranes was increased in the presence of GABA or muscimol (Maksay & Ticku, 1985; Trifiltti *et al*, 1984). In view of the use-dependent onset of block, it therefore seems likely that the association rate of picrotoxin binding to the $GABA_A$ receptor would also be increased in the presence of GABA. The use-dependent block by picrotoxin may explain the observation by Constanti (1978) that picrotoxin caused "fading" of the first GABA test pulse in the presence of picrotoxin, which was not seen in subsequent GABA responses (in lobster muscle). Use-dependence may also explain the 'peak in residual current' reported for the effect of picrotoxin on frog sensory neurones at low GABA concentrations (Yashui, Ishizuk & Akaike, 1985). Similarly,

use-dependence could explain our observation (see Figs. 3.1 and 3.2) (and that of Kudo *et al*, 1984) that, when picrotoxin was applied simultaneously with the first GABA application, the initial part of the GABA response decayed very rapidly, compared with that observed in the absence of picrotoxin.

A range of compounds, when examined in detail (electrophysiologically) appear to act, at least in part, as complex blockers of agonist-gated ion channels. Complex blockers of the nicotinic acetylcholine receptor-channel (some of which were originally thought to act as simple open channel blockers) include procaine (Katz & Miledi, 1975; Adams, 1977), trifluoperazine (Clapham & Neher, 1984b), benzocaine (Ogden *et al* 1981), pentobarbitone (Gage & Mckinnon, 1985), substance P (Clapham & Neher 1984a; Role, 1984), and clonidine (Cull-Candy, Mathie & Powis, 1988). Although many of these compounds produce obvious, though complex, changes in the spectra and single-channel currents of the relevant agonist-gated ion-channels, it is feasible that the blocking and unblocking rates for picrotoxin are such that the changes in these parameters are too small to be detected in the present study.

A mechanism difficult to distinguish from complex channel block is enhancement of desensitization, not least because the physical mechanism of desensitization is not understood. For example, Clapham & Neher (1984a) suggested that the inhibition of nicotinic acetylcholine-induced currents in isolated bovine chromaffin cells by substance P, could equally well be due to enhancement of the rate of desensitization or complex channel block (with a slow dissociation rate) in which there was an additional pathway from blocked to desensitized states. Either way, substance P caused a decrease in the duration of bursts, a decrease in the number of openings per burst, a reduction in the mean open time and an increase in interburst interval within clusters. Enhancement of desensitization has also been suggested as the mechanism of inhibition of $GABA_A$ currents of chick spinal cord neurones by trifluoperazine (Yang & Zorumski, 1989). However, unlike Clapham & Neher (1984a), Yang & Zormuski (1989) observed that trifluoperazine did not alter the open times of $GABA_A$ single channel currents (or alter the corner frequency of the single Lorentzian spectra). Akaike *et al* (1987) observed that picrotoxin speeded the rate of inactivation of whole-cell $GABA_A$ currents of bull frog dorsal root ganglion cells, and suggested that this was consistent with a channel-blocking mechanism.

3.8.3 *Combination of mechanisms*

An extension of the complex blocking mechanism is the suggestion that picrotoxin exhibits two or more mechanisms of action. This possibility cannot be excluded in the case of the present results. Indeed extensive quantitative studies of GABA dose-response data from crustacean muscle have led Constanti (1978) and Smart & Constanti (1986) to suggest that picrotoxinin is a 'mixed antagonist' producing an 'apparent' competitive block (binding at a site other than the GABA binding site) plus a block that is not competitive. Smart & Constanti (1986) proposed the following cyclical scheme for $GABA_A$ receptor-channel inhibition by picrotoxinin (see also Colquhoun, 1980, for the inhibition of end-plate acetylcholine receptors by tubocurarine)

$$\begin{array}{ccccc} R & \rightleftharpoons & AR & \rightleftharpoons & A_2R & \rightleftharpoons & A_2R^* \\ \Big\uparrow\downarrow K_{B1} & & \Big\uparrow\downarrow K_{B2} & & \Big\uparrow\downarrow K_{B3} & & \Big\uparrow\downarrow K_{B3}{}^* \\ BR & \rightleftharpoons & BAR & \rightleftharpoons & BA_2R & \rightleftharpoons & BA_2R^* \end{array} \qquad (2)$$

where R is the receptor, with two binding sites for the agonist (A), B is the antagonist, A_2R^* is the only open state, and K_{B1} to $K_{B3}{}^*$ are the equilibrium dissociation constants for the binding of antagonist to the various states of the receptor-channel. In this scheme the antagonist can combine with the receptor-channel (at a site or sites other than the agonist binding site) when the channel is shut as well as when it is open.

Apparent competitive inhibition would occur if the antagonist had preferential affinity for the unliganded (R) or monoliganded (AR) states, while uncompetitive block (such as allosteric block of the open channel) occurs when the antagonist binds preferentially, or only, to the A_2R species. Obviously if the affinity of picrotoxin for the four proposed states of the GABA receptor-channel are different (as suggested by Constanti, 1978 and Smart & Constanti, 1986), then the apparent mechanism of action of picrotoxin will vary according to the conditions of the experiment. This may explain any apparent differences in the effect of picrotoxin(in) on GABA dose-response curves observed by various investigators. Van Renterghem *et al* (1987) have provided further support for unequal binding of picrotoxin-like antagonists to the closed and open states of the $GABA_A$ receptor, since it was observed that the relative equilibrium block by TBPS was reduced when the GABA concentration was increased (e.g. TBPS has lower affinity for A_2R and A_2R^* species than for A or AR species). This would tie in with the

observation that GABA agonists reduce the amount of [^{35}S]-TBPS bound in the steady state, at least when non saturating concentrations of TBPS were used (Squires *et al.*, 1983; Ramanjaneyln & Ticku, 1984; Supavilai & Korobath, 1984; Trifillet *et. al.*, 1984). Based on scheme (2), Smart & Constanti (1986) proposed that picrotoxin stabilizes the closed form of the receptor-channel, perturbs the allosteric or conformational equilibrium constant between the open and closed receptor states, and affects the agonist binding affinity (and vica versa). The concentration ranges of picrotoxin (and of GABA) examined in the present study were far too limited to determine whether picrotoxin exhibited such a 'mixed antagonism' of $GABA_A$ receptor-channels in rat sympathetic neurones. However all of the present results are consistent with such a mechanism.

4. $GABA_A$ RECEPTOR-CHANNELS IN RAT SUPERIOR CERVICAL GANGLION NEURONES ACTIVATED BY HIGH CONCENTRATIONS OF GABA

4.1 SUMMARY

1. Single channel currents evoked by high concentrations of GABA (10-2000μM) have been analysed to investigate the characteristics of $GABA_A$ receptor-channels. Currents were recorded from outside-out patches from rat superior cervical ganglion neurones. When high concentrations of GABA were applied to a patch, channel openings occurred in prolonged clusters (3.8 ± 3.7seconds, mean ± S.D. n = 19, at 50μM GABA) consisting, on average, of 350 apparent openings per cluster (mean of 4 clusters, 50μM GABA), and individual clusters were separated by long silent intervals.

2. Channel openings were to many (often ill-defined) conductance states (range 7-35pS), but the most frequently observed conductance level was approximately 30pS, (29.6 ± 0.34pS; mean ± S.E.M., n=42). Only those clusters during which the channel was open to this main state conductance for at least 95% of the cluster open time were used in the analysis of probability of being open. Other frequently observed conductance levels were 15-18pS and 22-23pS, while levels of 33-36pS and 7-9pS were occasionally, but reliably observed.

3. Bursts within clusters were defined as a series of openings separated by closed intervals shorter than some critical value, t_c. At 50μM GABA the mean burst length was 439 ± 434ms (mean ± S.D., n = 40, t_c = 50ms). The probability of being open, p_o, during bursts within clusters has been analysed as a function of GABA concentration.

4. As expected, increasing the concentration of GABA resulted in an overall increase in p_o. However, for a given agonist concentration there was a wide spread in p_o, far greater than that predicted for a population of identical and independent receptor-channels (demonstrated by comparison with simulated channel activity).

5. The wide range of p_o values at a particular concentration of GABA was not due to inappropriate selection of t_c. At 50μM GABA the range of p_o values was similar for t_c of 20-1000ms, although the overall mean p_o became lower (0.71 rather than 0.81).

6. It is unlikely that variability in p_o arose from overlapping activity of two or more channels. There was no detectable tendency for p_o to be higher in the middle of clusters than at their ends, and at most of the observed p_o values even a brief overlap should give rise to double openings, which were not in fact observed.

7. The values for p_o, mean open time, and mean shut time for bursts within the same cluster, and between different clusters, were compared by a randomization test. The aim of this test was to determine

whether the wide variability in p_o could plausibly occur if all the open and closed intervals came from the same population. Values of p_o were found to differ not only between one channel and another (i.e. between clusters), but also for the same channel at different times (i.e. between bursts within a cluster).

8. The inclusion of 1mM GTP inside the patch pipette did not reduce the variability in p_o values obtained at 50μM GABA. Similarly there was no reduction in the variability in p_o values when 4mM Mg-ATP was included in the pipette solution and the external surface of the membrane patch was perfused with 10μM pentobarbitone.

9. The heterogeneity of $GABA_A$ receptor channel properties may result either from several structurally distinct populations of $GABA_A$ receptor-channels, or one population of $GABA_A$ receptor-channels that changes its activity with time, or both.

4.2 INTRODUCTION

Studies on the kinetics of $GABA_A$ receptor-channels in various vertebrate neurones (by the use of patch-clamp techniques) have employed only low concentrations of agonist. The most recent of these reports suggest a single population of $GABA_A$ receptor-channels with complex gating (Mathers, 1985; Mathers & Wang, 1988; Macdonald *et al.*, 1989a; Weiss & Magleby, 1989). For other agonist-gated ion channels, such as the muscle nicotinic acetylcholine receptor-channel, kinetic analysis of single-channel currents activated by high concentrations of agonist have provided additional and complementary information to that obtained at low agonist concentrations (e.g. Sine & Steinbach, 1984a, 1987; Ogden & Colquhoun, 1985; Auerbach & Lingle, 1986, 1987; Colquhoun & Ogden, 1988). There are however, no published studies of $GABA_A$ single-channel currents activated by high concentrations of agonist. The aim of this chapter was to investigate properties of the $GABA_A$ receptor-channel by analysing single-channel currents activated by high concentrations of GABA in outside-out patches from rat superior cervical ganglion neurones.

4.3 *Basic features of responses to high concentrations of GABA*

Whole-cell current responses to GABA showed obvious desensitization at concentrations above 10μM. Fig. 4.1A shows a typical whole-cell response to 80μM GABA in a superior cervical ganglion (SCG) neurone held at -60mV. The current was reduced to approximately 15% of the peak amplitude within 90s. Desensitization was also apparent in the single channel records, as illustrated in Fig. 4.1B. The initial application of a desensitizing concentration of GABA (50μM in the example) to an outside-out patch resulted in the simultaneous opening of several channels (up to four, in this patch). However, in the continued presence of GABA the receptors desensitized, such that apparently only one channel was active at a time. In the example illustrated this occurred within about 7s of GABA application. Under these conditions the other receptors had entered long-lived desensitized states (or the number of functional receptors had fallen). In a desensitized outside-out patch such as the one depicted in Fig. 4.1C, the openings occur in prolonged clusters each of which can last several seconds, and these clusters are separated by long silent intervals (1s-480s). For example, the clusters illustrated in Fig. 4.1C were separated by shut periods of between 7.6 and 51s. At 50μM GABA the mean cluster length was 3.8 ± 3.7s (mean ± S.D., n = 19 clusters) for clusters which opened mainly to the 30pS conductance level.

In the present study, analysis of the probability of being open was restricted to those clusters that opened mostly to a 30pS level, since this was the most frequently occurring conductance state. Bursts within clusters were defined as a series of openings separated by closed intervals shorter than some critical value, t_c (see Methods). A typical burst from within one of the clusters in Fig. 4.1C, is illustrated on an expanded time base in Fig. 4.1D. At 50μM GABA the mean burst length (± S.D.) was 439 ± 434ms (n = 40, t_c = 50ms), and the apparent number of openings per cluster was about 350. The apparent mean open time and mean shut time were 8.9ms and 3.66ms respectively (at 50μM GABA). It is highly likely that all openings occurring during such a single cluster arise from the continued activity of the same receptor-channel (see later). The probability of being open, p_o, during bursts within clusters has been analysed as a function of GABA concentration (see below).

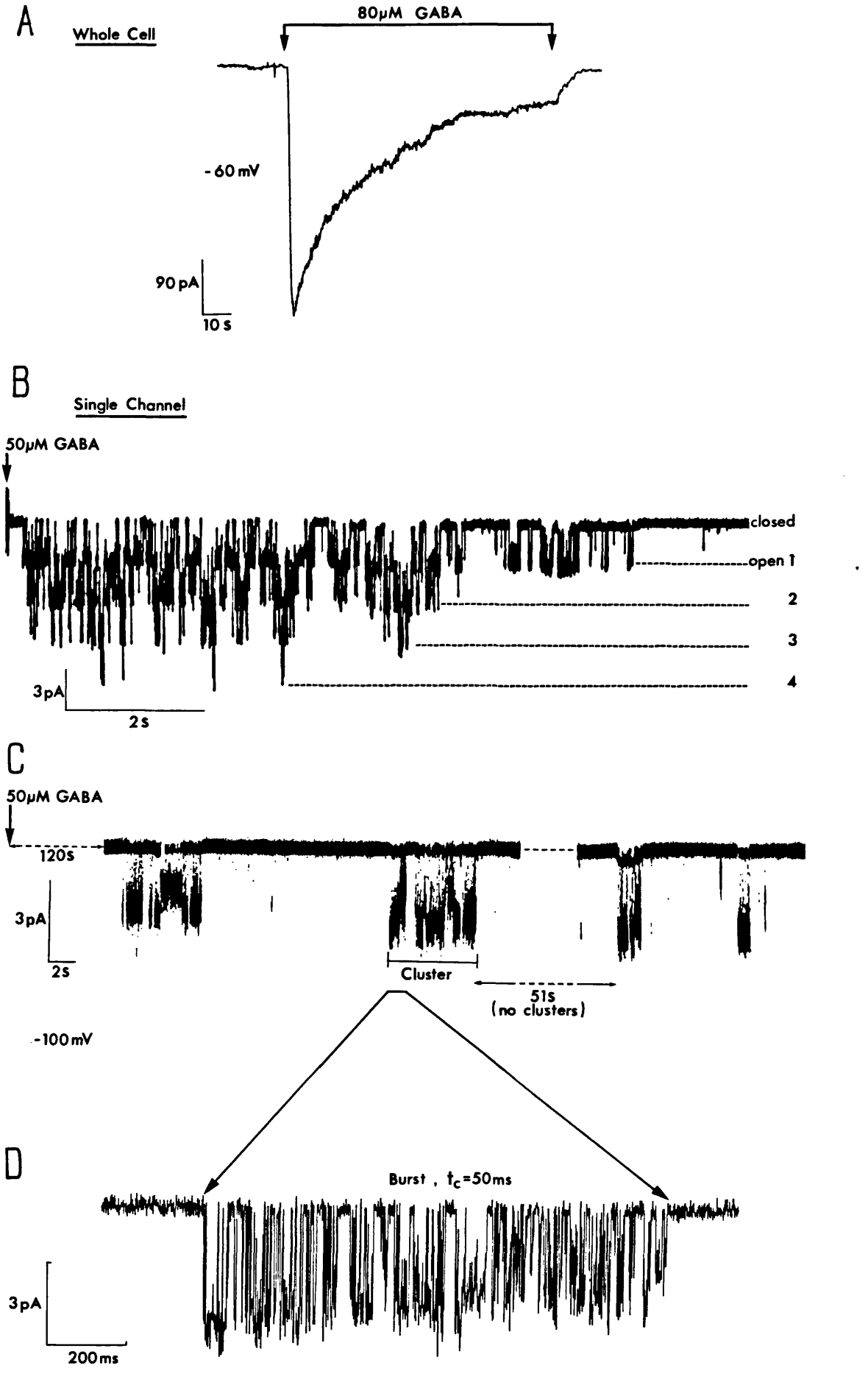
A
Whole Cell
80μM GABA
-60 mV
90 pA
10 s
B
Single Channel
50μM GABA
closed
open 1
2
3
4
3pA
2s
C
50μM GABA
120s
3pA
2s
Cluster
51s
(no clusters)
-100mV
D
Burst , t_c=50ms
3pA
200ms

Fig. 4.1 Desensitization of GABA-responses in whole-cell and outside-out patches. A, whole-cell current response of a cell held at -60mV, showing desensitization in the continued presence of 80μM GABA. Calibration 90pA and 10s. B, Application of 50μM GABA (drug perfusion starts at the beginning of the trace) to an outside-out patch, causing simultaneous opening of up to 4 channels. The number of open channels are indicated on the right hand side. After 5-10s in the continued presence of 50μM GABA only one channel is active at a time. Calibration 3pA and 2s (V_m = -80mV). C, examples of 'desensitization clusters' of openings produced by 50μM GABA. The four consecutive clusters were recorded in the continued presence of GABA and approximately 120s after the initial GABA application. Individual clusters are separated by long silent intervals of 7-51s (V_m = -100mV). Calibration 3pA and 2s. D, an example of a single burst shown on an expanded time base. As indicated, this burst is the first one in the second cluster in trace C, and exceeds 2s in duration (defined by a t_c of 50ms). Note that the effective filtering of the plot is 890Hz (-3dB). Calibrations 3pA and 200ms. T = 22°C.

4.4 *Multiple conductance states*

Many different conductance levels of the $GABA_A$ receptor-channel were observed in all patches and at all GABA concentrations (10-2000μM), ranging from 7-35pS. These conductance states were often difficult to resolve, apparently because the levels were too close together and too short-lived, and because of the exceptionally large open channel noise (relative to the shut-channel noise). In terms of these various conductance levels, clusters of channel openings fell into three general categories: (1) within a single cluster the channel may appear to 'wobble' between many different conductance levels, (2) there may be a few clear, large changes in conductance within a cluster, which were obvious from open point amplitude and mean low-variance amplitude histograms, and (3) there may be whole clusters which have pretty consistent levels, that clearly differ from one cluster to another in the same patch. The following three Figures (Figs. 4.2, 4.3 & 4.4) illustrate examples of each of these categories of channel openings within clusters.

It is clear from the single channel records in Fig. 4.2A & B that the same channel appears to open to many different ill-defined conductance levels, none of which correspond to the overall mean open channel amplitude (2.45pA) determined from the mean low variance amplitude histogram of this cluster (Fig. 4.2D). Fig. 4.2B also shows that the current during an individual channel opening was much noisier than the baseline (shut channel).

Discrete multiple conductance levels could not be resolved as discrete peaks from the open point amplitude distribution in Fig. 4.2C. Open point amplitude histograms were generated from the amplitudes of individual data points of the digitized current record, during periods when the channel was open. The presence of a wide range of conductance levels was, however, reflected by the much larger standard deviation (S.D.) of the open point amplitude distribution, compared with the (S.D.) of the shut point amplitude distribution, both of which could be fitted reasonably well with single Gaussian functions. The S.D. of the open and shut point amplitude distributions in this example were 0.54pA and 0.11pA respectively, so the excess open channel noise variance is 23-fold greater than the shut channel variance. The mean amplitude of 2.5pA corresponds to a conductance of 21pS. Fig. 4.2D illustrates that multiple conductance levels could also not be detected as obvious discrete peaks from the mean low-variance amplitude histogram. This histogram consisted of the mean amplitudes of sections of digitized current record (10 points) that had a variance as low as that of the

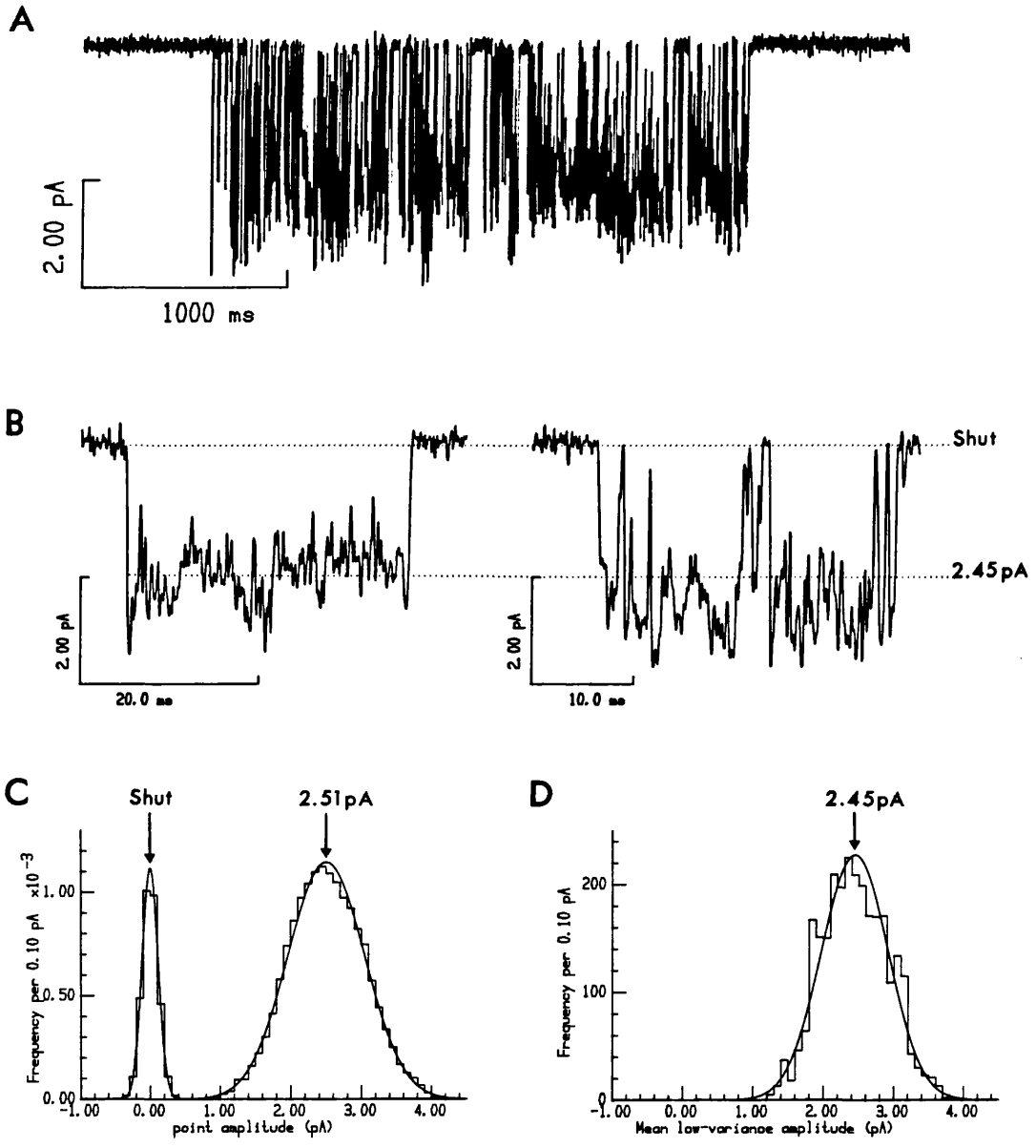
A
2.00 pA
1000 ms
B
Shut
2.45pA
2.00 pA
20.0 ms
2.00 pA
10.0 ms
C
Shut
2.51pA
Frequency per 0.10 pA x10^-3
1.00
0.50
0.00
-1.00
0.00
1.00
2.00
3.00
4.00
point amplitude (pA)
D
2.45pA
Frequency per 0.10 pA
200
100
0
-1.00
0.00
1.00
2.00
3.00
4.00
Mean low-variance amplitude (pA)

Fig. 4.2 A, a selected record to illustrate repeated transitions between multiple conductance levels occuring during a single cluster (50μM GABA, outside-out patch, V_m = -120mV). Long shut periods, >56s, occurred on either side of the cluster (not shown). Calibration 2pA and 1s. B, sections of the cluster in A, on an explanded time scale, to illustrate what appear to be transitions between discrete conductance states. The dotted lines indicate the shut level and the mean open level of 2.45pA (equivalent to 20.4pS), as obtained from the low-variance amplitude distribution (D). Calibration 2pA and 10ms; records filtered at 2kHz, -3dB. C, amplitude histograms for open and shut points during the cluster. Each histogram was fitted with a single Gaussian; mean open point amplitude of 2.51pA, (equivalent to 20.9pS). Note that multiple conductance states were not discernable as discrete peaks from the point amplitude distribution, although the width of the open point amplitude distribution (S.D. of 0.54pA) was far greater than that of the shut point distribution (S.D. 0.11pA). Currents used for the histogram were filtered at 2kHz, -3dB. Frequency scale refers to the open point histogram. D, mean low-variance amplitude histogram for the open states of the cluster in A. The histogram was fitted with a single Gaussian, mean open level 2.45pA (equivalent to 20.4pS). Currents used for the histogram were filtered at 2kHz, -3dB. T = 22°C.

shut channel. The histogram shown in Fig. 4.2D has been fitted with a single Gaussian distribution; although there is some sign of multiple peakes in the histogram, these are not clearly defined, and were not consistent from one cluster to another.

The amplitudes of various conductance levels of the $GABA_A$ receptor-channel could, however, be clearly resolved when the channel opened to one level for a large proportion, or all of the open time during a cluster (examples of which are illustrated in Figs. 4.3 & 4.4). Fig. 4.3A shows an example of a cluster that opens initially to a current level (or levels) of 1.68-2.15pA. After approximately 1.8s the current dropped to 0.76pA; it returned briefly to the higher level, and then continued at 0.76pA for a further 3.5s. Fig. 4.3B illustrates direct transitions between current levels of 0.76pA and the higher level (1.68-2.15pA) on a faster sweep speed. The presence of such transitions and of direct closures from the higher level, indicate that these events are due to multiple-conductances of a single channel, rather than superimposed openings from several channels. Fig. 4.3C & D illustrate that the 0.76pA level and the higher level could be clearly resolved as discrete peaks both from their open point, and mean low-variance amplitude histograms. In both cases the 0.76pA histogram was compiled from the data separately from the other histograms and fitted with a single Gaussian distribution. It is clear from Fig. 4.3C &D that the higher level may consist of two or more conductance states, since the point amplitude, and mean low-variance amplitude histograms of the higher level could not be well fitted with a single Gaussian. It can be seen by comparing the histograms in Fig. 4.3C & D that the appearance of more than one component in rather more obvious in the mean low-variance amplitude plot than in the open point amplitude plot. Both are fitted reasonably well by the sum of two Gaussians, and the estimates of the two discrete higher levels (1.68 and 2.15pA from the former and 1.71 and 2.21pA from the latter) agree well, especially in view of the fact that the distributions are not, in principle expected to be described exactly by a sum of Gaussians. It can be seen that the lines drawn in Fig. 4.3B at the 1.68 and 2.15pA level correspond only roughly with discrete conductance levels in the data, so it may well be that the description in terms of two discrete levels is an oversimplification. The levels suggested in Fig. 4.3 (*viz* 0.76, 1.7 and 2.2pA) correspond to single channel conductances of 7.6, 17 and 22pS respectively.

Fig. 4.4 A,B,C and D illustrates four representative clusters (from

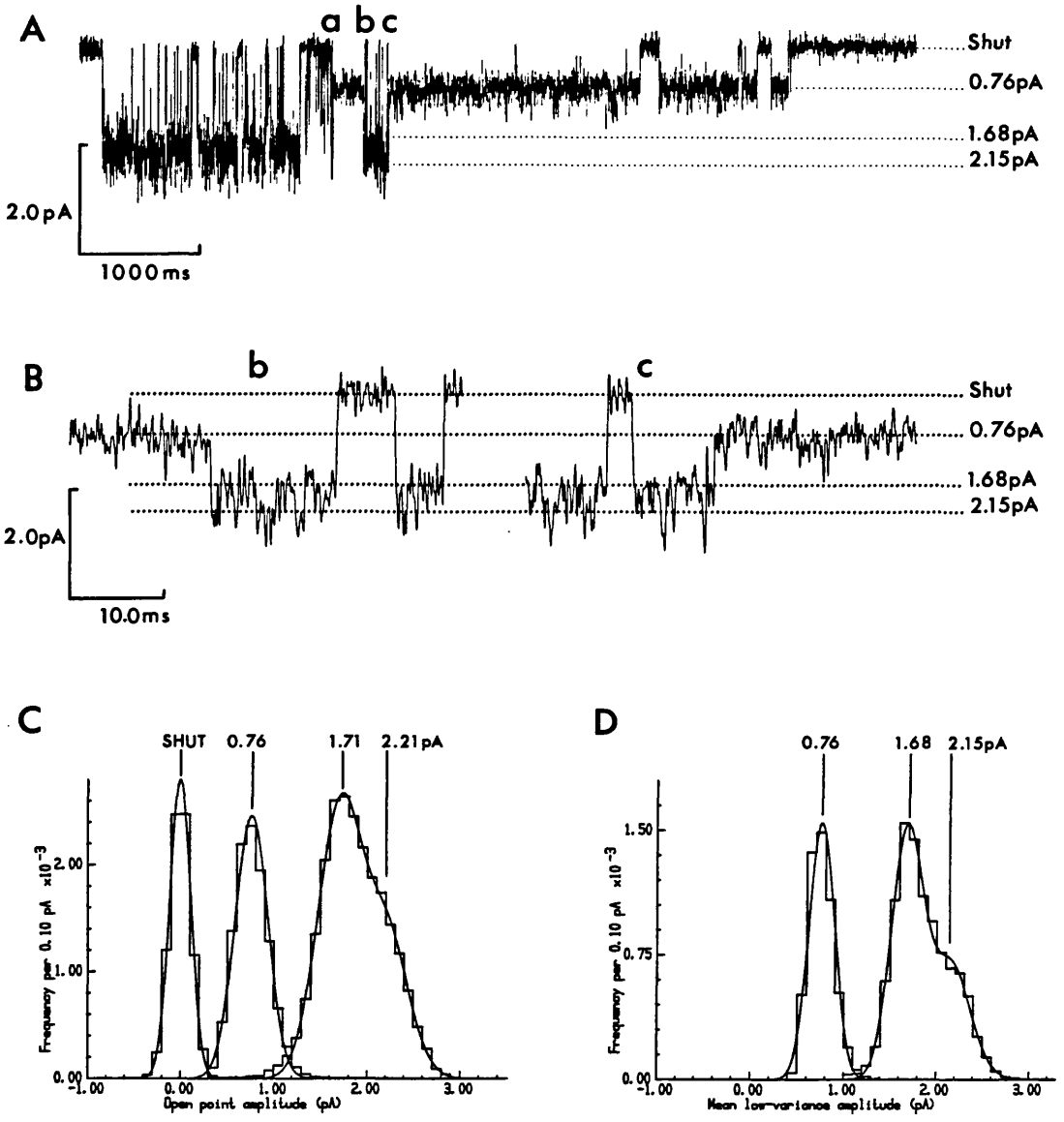
A
a b c
Shut
0.76pA
1.68pA
2.15pA
2.0pA
1000ms
B
b
c
Shut
0.76pA
1.68pA
2.15pA
2.0pA
10.0ms
C
SHUT
0.76
1.71
2.21pA
Frequency per 0.10 pA x10^-3
Open point amplitude (pA)
D
0.76
1.68
2.15pA
Frequency per 0.10 pA x10^-3
Mean low-variance amplitude (pA)

Fig. 4.3 A, a single cluster selected to illustrate switching between high conductance and low conductance levels. The low level is about 0.76pA and the high level may actually consist of two rather closely spaced levels (1.68 and 2.15pA; suggested by the sublevel detection plot in D). These levels are indicated by dotted lines (outside-out patch, 2mM GABA, V_m = -100mV). Long shut periods occurred on either side of this cluster. At points a, b and c during the cluster, the channel switched between distinct conductance states (7.6pS, 17-22pS and closed). Calibration 2pA and 1s. B, section b and c of the cluster in A, shown on an expanded time scale. The dotted lines indicate the shut level and the conductance levels of 7.6, 16.8 and 21.5pS. Calibration 2pA and 10ms; (filter 2.5kHz, -3dB). C, point amplitude histograms for the cluster shown in A. Single Gaussians were separately fitted to the shut point amplitude histogram and to the left hand open point amplitude distribution (mean amplitude 0.76pA). The sum of two Gaussians was fitted to the right hand open point amplitude distribution (mean amplitudes, 1.71 an 2.21pA). The frequency scale refers to the right hand distribution (maximum frequency of the 0.76pA distribution was 11,000 per 0.1pA). Current record filtered at 2.5kHz, -3dB. D, mean low-variance amplitude distributions of the open states of the cluster in A. The left hand distribution was fitted with a single Gaussian (mean amplitude 0.76pA); the sum of two Gaussians was fitted to the right hand histogram (mean amplitudes 1.68 and 2.15pA). Current record filtered at 2kHz (-3dB). The frequency scale refers to the right hand distribution (the maximum frequency of the 0.76pA peak occured at 11,000 per 0.1pA).

different patches), during which the $GABA_A$ receptor-channel opened to only one level, or to two closely spaced conductance levels. Fig. 4A,B illustrates two clusters which appeared to open mainly to one distinguishable level, since the open point amplitude histogram of each of these clusters was adequately fitted by a single Gaussian function (though, as always; its S.D. was much greater than that for the shut point amplitude histogram). The estimated conductance levels were 32.5pS (Fig. 4.4A) and 30.4pS (Fig. 4.4B) for a reversal potential of 0mV. Fig. 4.4C, D shows two clusters each of which appeared to open to at least two closely spaced conductance levels for large proportions of their open time, as judged by their open point amplitude histograms, which were fitted with the sum of two Gaussians. The estimated conductance levels for the cluster illustrated in Fig. 4C were 19.3pS and 25.1pS (relative areas 0.61 and 0.39, respectively); the estimated conductance levels for the cluster shown in Fig. 4D were 15.8pS and 19.9pS (relative areas 0.62 and 0.38, respectively). It was common to see clusters which had pretty consistent amplitudes that clearly differed from one cluster to another in the same patch.

The amplitudes of the different, closely-spaced (separated by only a few pS), and often ill-defined, conductance levels of the $GABA_A$ receptor-channel were infered by fitting of point amplitude, and mean low-variance amplitude histograms of clusters which opened only to one level for the whole of the cluster (e.g. Fig 4.4A & B), or which opened to a few conductance levels, and remained at each of these levels for a large proportion of the channel open time (e.g. Fig. 4.3). Estimates of the amplitudes of the various conductance levels were not made from clusters such as the one depicted in Fig. 4.2, since the levels were ill-defined. The most frequently occurring conductance levels were in the range 28.5-30.5pS. However conductance levels of approximately 15-18pS and 22-23pS were also frequently observed, and levels of roughly 33-36pS and 7-9pS were reliably, but only ocassionally observed.

In the present study, the analysis of the probability of being open p_o, as a function of GABA concentration was restricted to those clusters during which the channel was open to the main state conductance for at least 95% of the open time during the cluster. The amplitude of the main conductance level was 29.6 ± 0.34pS (mean ± S.E.M., n=47 clusters). An example of a cluster which opened mainly to this conductance level is illustrated in Fig. 4.4B. The question of whether p_o is the same at the other, less common, conductance levels has not been investigated.

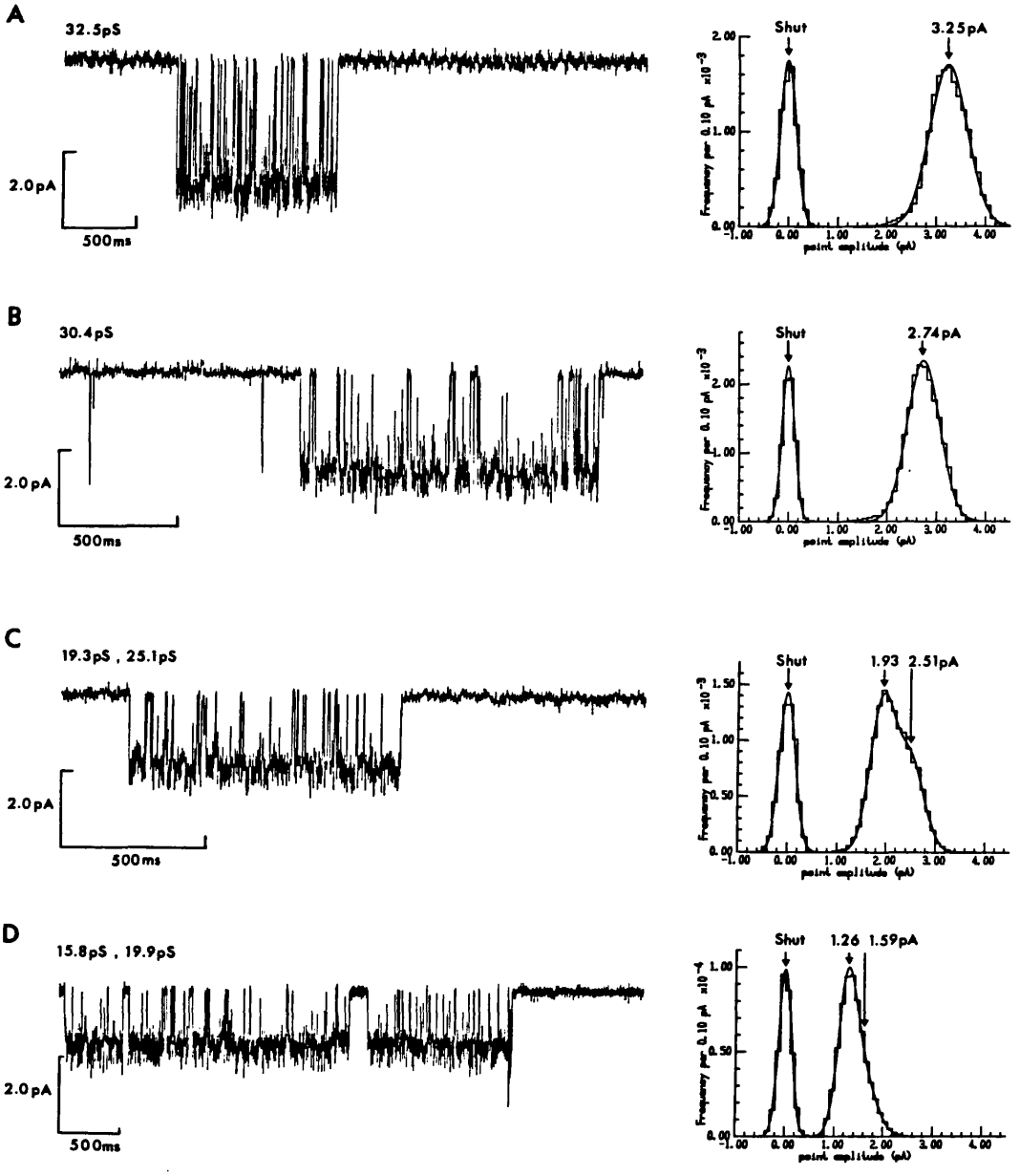
A
32.5pS
2.0pA
500ms
Shut
3.25pA
B
30.4pS
2.0pA
500ms
Shut
2.74pA
C
19.3pS , 25.1pS
2.0pA
500ms
Shut
1.93
2.51pA
D
15.8pS , 19.9pS
2.0pA
500ms
Shut
1.26
1.59pA

Fig. 4.4 Selected clusters in which the channel opens to a single conductance level, or to two closely spaced conductance levels. The shut and open point amplitude histograms are shown to the right of their corresponding current records. A, cluster recorded from an outside-out patch in 2mM GABA (V_m = -100mv). The open point amplitude histogram was fitted with a single Guassian distribution; mean amplitude of 3.25pA (equivalent to 32.5pS). B, a cluster in a patch exposed to 50μM GABA (V_m = -90mV). A single Gaussian was fitted to the corresponding open point amplitude histogram; mean amplitude 2.74pA (30.4pS). C, a cluster in the presence of 2mM GABA, (V_m =-100mV). The corresponding open point amplitude histogram was fitted with the sum of two Gaussians; mean amplitudes 1.93 and 2.51pA (19.3 and 25.1pA; relative areas 0.61 and 0.39 respectively). D, a cluster in the presence of 100μM GABA (V_m = -80mV). The corresponding open point amplitude histogram was fitted with the sum of two Gaussians; mean amplitudes 1.26 and 1.59pA (15.8 and 19.9pS; relative areas 0.62 and 0.38, respectively). Calibration for A-D: 2pA and 500ms. T = 22-23°C. Shut point amplitude histograms were fitted with single Gaussians (mean 0pA). The frequency scales refer to the open point amplitude histograms. Channel records low-pass filtered at 1kHz (-3dB) for illustrative purposes.

4.5 *Probability of being open as a function of GABA concentration*

4.5.1 ***Shut time distribution and choice of critical gap length.*** The aim of p_o determinations is to define the equilibrium response to specified agonist concentrations of an individual receptor-channel, after elimination, as far as possible, of the effects of desensitization. In order to achieve this it is necessary to identify sections of the record (bursts) during which one individual channel shows repeated activations without entering any desensitized state (and without interference from the opening of any other channel). The division of the observed record into clusters, which probably all originate from the same channel (see below), is quite clear. It is very likely that all the GABA channels in the patch are in long-lived desensitized states during the long silent periods that separate clusters, as in the case of the nicotinic receptor (Sakmann *et al.*, 1980; Sine & Steinbach, 1987; Colquhoun & Ogden, 1988).

Greater ambiguities arise in trying to decide whether the briefer shut periods, within clusters, are spent in (short-lived) desensitized states or whether they are spent in the resting (i.e. activateable) state between activations of a non-desensitized receptor. This problem is, of course, particularly acute at lower agonist concentrations (when intervals between individual activations are longer), which is one of the reasons why p_o values are not given for GABA concentrations below 10μM. In the case of the nicotinic receptor there are clearly shut periods (gaps) within clusters that are spent in short-lived desensitized states (Sakmann *et al.*, 1980), and the same is probably also true of GABA-receptors. It is therefore necessary to define a critical gap length, t_c, to define bursts, that is short enough to exclude most such brief desensitized periods, but to include most of the gaps between individual channel activations. In the case of the nicotinic receptor it was suggested by Cachelin & Colquhoun (1989) that the long gaps between clusters correspond with the microscopic component of desensitization that has a time constant of a few seconds, (Katz & Thesleff, 1957; Feltz & Trautmann, 1982) whereas the briefer desensitized periods within clusters correspond with 'ultra-fast' macroscopic desensitization with a time constant of the order of 100ms (e.g. Bekkers, 1986; Brett *et al.*, 1986). Unfortunately relatively little is known about GABA desensitization, even on the macroscopic scale (although see Akaike *et al.*, 1986; Cash & Subbarao, 1987; Ikemoto *et al.*, 1988). In particular, nothing is known about ultra-fast desensitization, so the choice of critical gap length, t_c, could not be unambiguous, and must be based

largely on inspection of the distributions of intracluster shut times (i.e. shut times within clusters).

4.5.2 ***Intracluster shut times.*** Frequency histograms of intracluster shut times were constructed using the intervals measured by the 50% threshold crossing routine (low pass filtered 2kHz -3dB, filter rise time 167μs). These histograms were fitted with probability density functions from 250μs to 2000ms by the method of maximum likelihood (Colquhoun & Sigworth, 1983).

Fig. 4.5 illustrates a typical distribution of the logarithm of intracluster shut times (see McManus, Blatz & Magleby, 1987; Sigworth & Sine, 1987) which were measured from six clusters, all recorded from the same outside-out patch, and exposed to 50μM GABA. Each exponential component appears as a peaked function, the maximum of which corresponds to the time constant of the exponential. In this example, the histogram was fitted with four exponentials, with time constants of 0.15, 2.26, 25.2, and 1210ms (relative areas 0.63, 0.28, 0.08, and 0.006 respectively). The fit is not very clearly defined, which is not surprising in view of the other evidence given here that $GABA_A$ receptor-channels do not show homogenous kinetic behaviour; there may well be far more than four time constants. Although the time constants of distributions cannot, in general, be equated with the mean lifetimes of particular states, or sets of states, it is necessary to postulate some approximate physical significance to the time constants in order to proceed. The fastest two components are likely to represent, primarily, spontaneous shut periods within single channel activations, because we have found similar time constants at lower GABA concentrations, at which individual channel activations are better separated: for example with 2-5μM GABA we find time constants of about 0.25 ± 0.07ms and 1.6 ± 0.34ms (mean ± S.D., n = 7). Comparable values, for shut periods within single channel activations, have been found for $GABA_A$ channels in other preparations, including cultured mouse spinal and chick cerebral neurones (Mathers, 1985; Weiss, 1988; Macdonald *et al.*, 1989a; Weiss & Magleby, 1989), as well as for bovine chromaffin cells (Bormann & Clapham, 1985), and cultured astrocytes from rat cerebral hemispheres (Bormann & Kettenmann, 1988). In addition, similar duration 'within-activation-gaps' have been found for other agonist-activated channels, including nicotinic channels (Colquhoun & Sakmann, 1981, 1985; Sine & Steinbach, 1984a, 1986), and glutamate channels (Cull-Candy & Parker, 1982; Howe *et al.*, 1988).

It is reasonable to suppose that the next slowest time constant

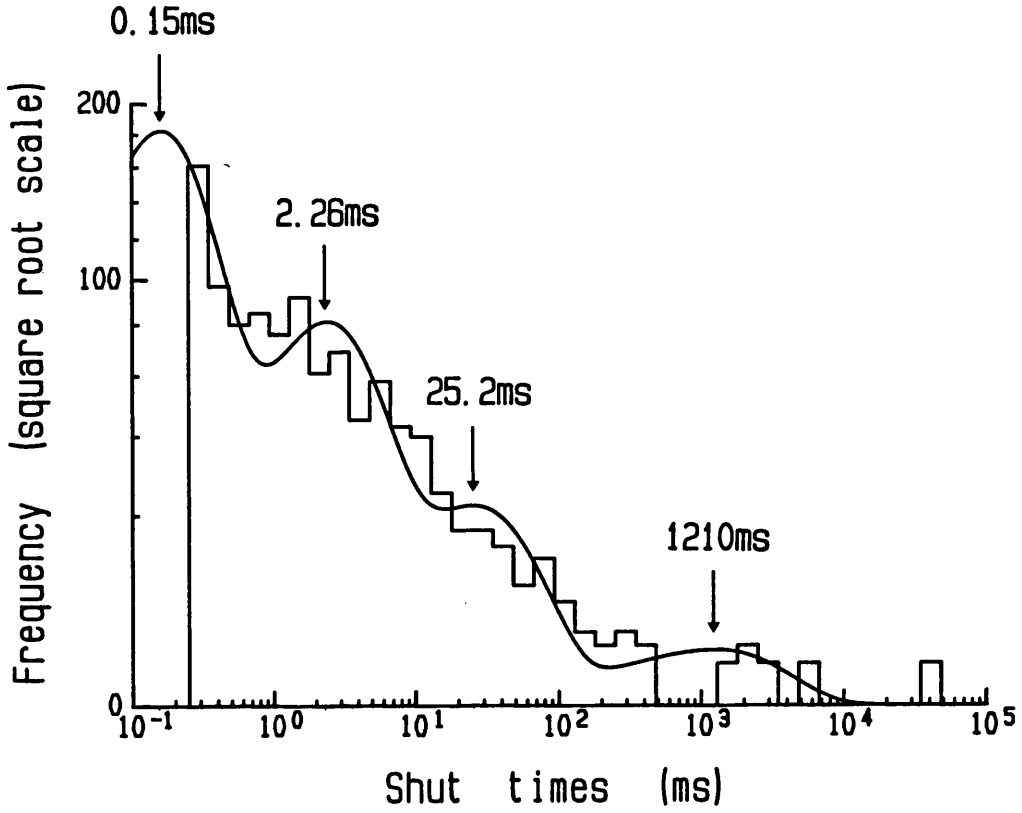

Fig. 4.5 Frequency histogram of all intracluster shut times, measured from 6 clusters (from the same patch), which opened mostly to the 30pS level; patch exposed to 50μM GABA; V_m = -70mV; T = 22°C. The histogram shows the distribution of log shut times, with the ordinate on a square root scale, for display purposes. The untransformed shut times were simultaneously fitted with four exponentials from 0.25 to 2000ms (continuous curve). The time constants were 0.15, 2.26, 25.2 and 1210ms; relative areas were 0.63, 0.28, 0.08 and 0.006 respectively. Currents filtered at 2kHz, -3dB; resolution set at 250μs. Note that the fit is not very clearly defined.

represents, primarily, gaps between channel activations (though at high concentrations these may not be distinguishable from intra-activation gaps). Thus it seems reasonable to use a critical gap length of about 50ms to define bursts with 50μM GABA, only the longest intracluster time constant in Fig. 4.5 being excluded.

4.5.3 *Estimates of p_o curves.* As expected, increasing the concentration of GABA resulted in an overall increase in the probability of being open, p_o. Fig. 4.6B shows the increase in mean probability of being open during bursts (of at least 100ms), over the GABA concentration range 10-2000μM; the t_c value used, and the number of bursts analysed are indicated for each concentration. The results were pooled from different outside-out patches held at -60 to -100mV, and include a total of 270 bursts. The mean probabilities (± S.D.) of being open were 0.35 ± 0.17 (10μM, n=14 bursts), 0.29 ± 0.22 (20μM, n=60) 0.43 ± 0.19 (30μM, n=10), 0.80 ± 0.12 (40μM, n=20), 0.77 ± 0.16 (50μM, n=95), 0.83 ± 0.11 (100μM, n=31), and 0.83 ± 0.1 (2000μM, n=40). It is apparent from Fig. 4.6B that the maximum mean p_o falls well below 1.0, even at the high concentration of 2mM GABA (where the mean maximum p_o value was 0.83). Furthermore, even at these high concentrations, the main state conductance was sitll approximately 30pA, indicating that rapid open channel block by the GABA molecule itself was not responsible for the low maximum p_o.

A striking feature of the p_o *vs* GABA concentration relationship is the wide range of p_o values observed for any given agonist concentration. Fig. 4.6A shows the probability of being open for 270 individual bursts, the mean of which are indicated in fig. 4.6B. For example, at a concentration of 50μM GABA the probability of being open ranged from 0.26 to 0.99 (95 bursts), and at 20μM GABA the range was 0.01-0.79 (60 bursts). Such a wide range of p_o values has not previously been seen for populations of agonist-activated channels which are homogeneous (see for example, Sakmann, Patlak & Neher, 1980; Cull-Candy, Miledi & Parker, 1981; Colquhoun & Ogden, 1988).

4.5.4 ***Expected spread of p_o for a homogeneous population of receptor-channels.*** It is not immediately obvious how much variability would be expected in p_o, from one burst to another, if the receptors behaved in a homogeneous manner. Simulations have therefore been performed in order to determine the anticipated spread of p_o values. To date there are no consistent models of $GABA_A$ receptor-channel gating

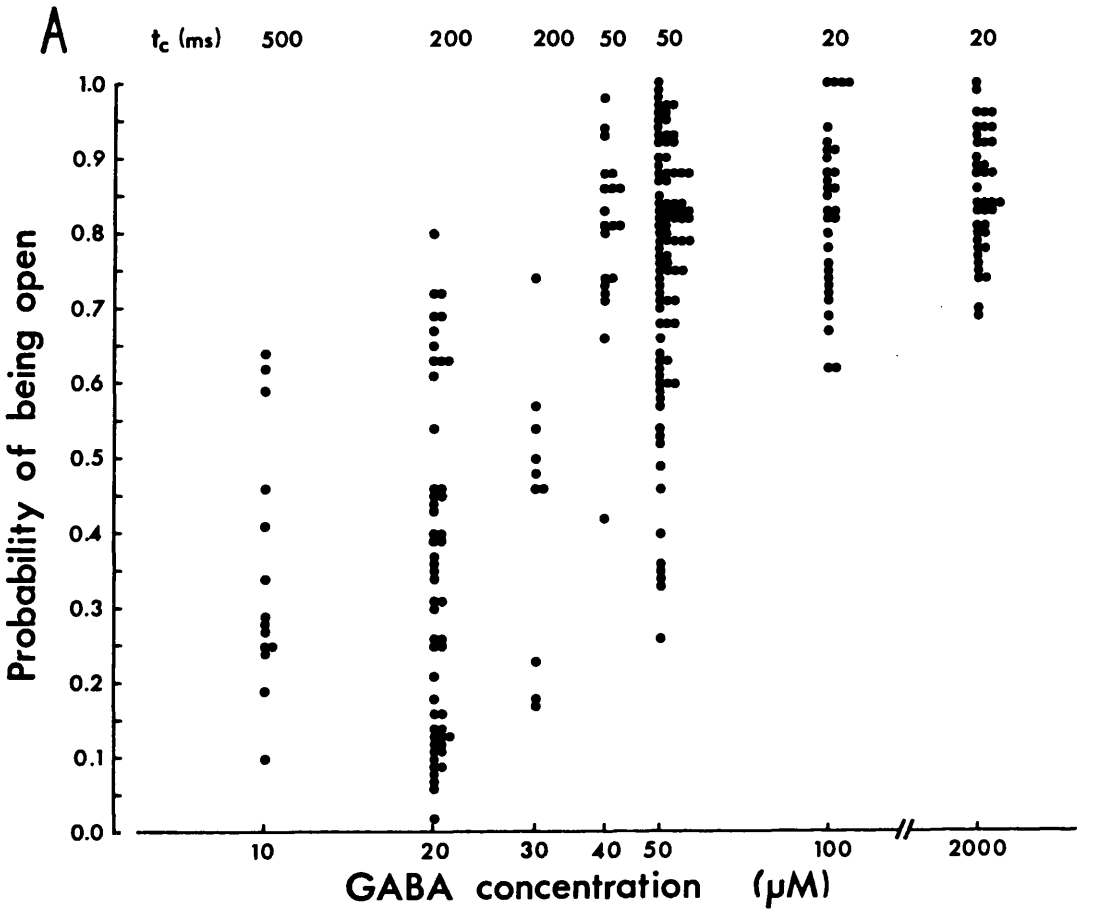
A
t_c (ms) 500 200 200 50 50 20 20
Probability of being open
1.0
0.9
0.8
0.7
0.6
0.5
0.4
0.3
0.2
0.1
0.0
10 20 30 40 50 100 2000
GABA concentration (μM)

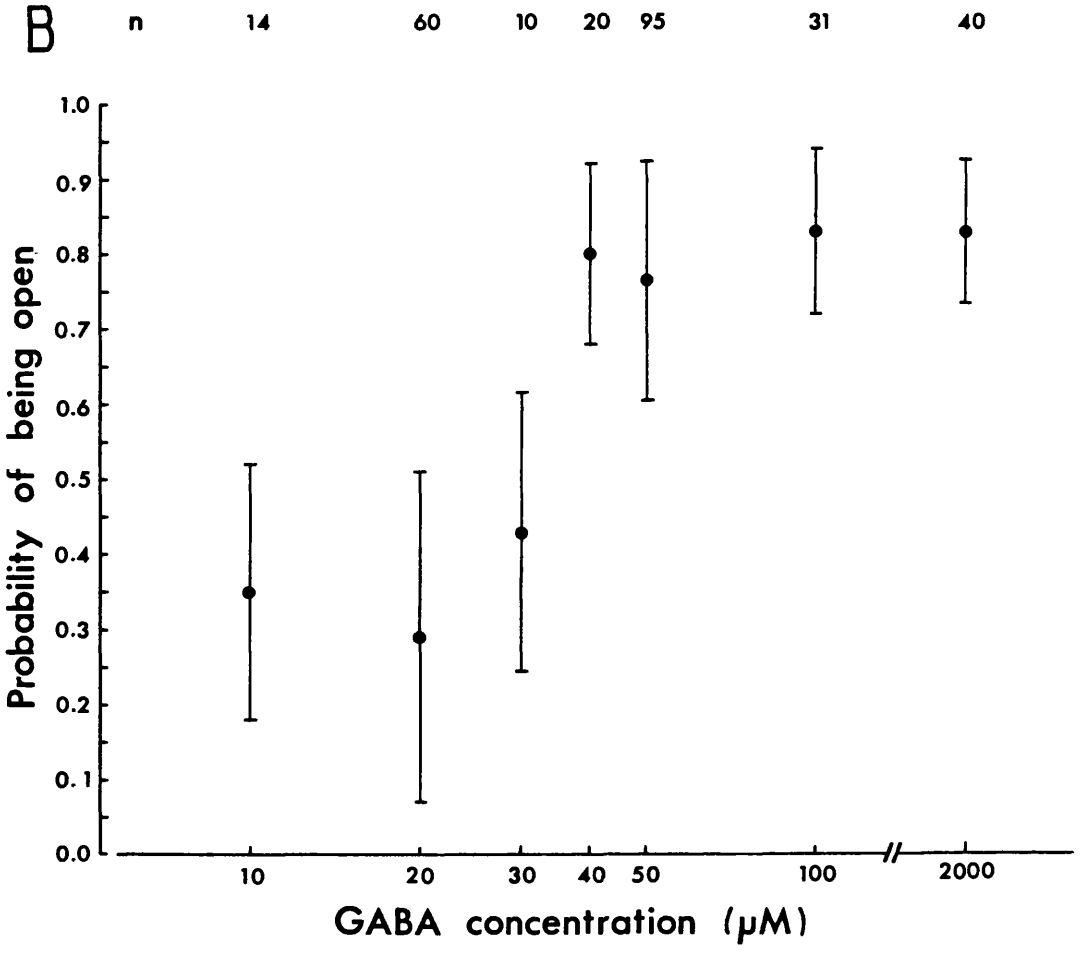
B
n 14 60 10 20 95 31 40
Probability of being open
1.0
0.9
0.8
0.7
0.6
0.5
0.4
0.3
0.2
0.1
0.0
10 20 30 40 50 100 2000
GABA concentration (μM)

Fig. 4.6 Dependence of probability of being open (during bursts within clusters) on GABA concentration. A, probability of being open as a function of GABA concentration (10-2000μM). Each point represents a single burst; the number of bursts, n, at each concentration, were 10μM (n = 14), 20μM (n =53), 30μM (n =10), 40μM (n = 20), 50μM (n = 95), 100μM (n = 31) and 2000μM (n = 40). Results were pooled from five different outside-out patches held at -60 to -100mV, T = 22-23° C. The critical gap length, t_c, used to define the bursts is given above each concentration. Note the range of p_o values at each concentration. The concentration axis is not continuous. B, mean p_o *vs* GABA concentration (same data as in A). The vertical bars represent ± S.D.; the number of bursts (n) averaged for each point is given at each concentration; the t_c value used to define the bursts is the same as in A. Note the large S.D., due to the wide scatter of p_o values, and that p_o increases with increasing GABA concentration up to approximately 40-50μM.

(although see Macdonald *et al.*, 1989a; Weiss & Magleby, 1989), and in particular no models of $GABA_A$ receptor-channel gating in peripheral neurones. Therefore the simplest mechanisms of channel gating that could produce bursting behaviour were used, *viz.*

$$C_L \underset{k_{-1}}{\overset{k_{+1}}{\rightleftharpoons}} C_S \underset{\alpha}{\overset{\beta}{\rightleftharpoons}} 0 \qquad (1)$$

and

$$C_L \underset{\alpha}{\overset{\beta'}{\rightleftharpoons}} 0 \underset{k_{-B}}{\overset{k_{+B}}{\rightleftharpoons}} C_S \qquad (2)$$

where 0 represents an open channel, C_L represents a long-lived shut state (entry into which will end a burst) and C_S represents a short-lived shut state. The transition rates (k_{-1} , k_{+1} , β, β', α, k_{+B} , and k_{-B}) shown in both (1) and (2) were selected to give the mean number of openings per burst as approximately 35, the mean open time as 8.9ms and the mean shut time as 3.66ms, with the p_o within bursts being 0.72. These are the values observed experimentally with 50μM GABA, using a t_C of 50ms (with the exception of p_o, where the mean observed p_o was 0.76). Thus for scheme (1) the transition rates were: for k_{-1}, 7.8s^{-1}; β, 265s^{-1}; α, 112s^{-1}; k_{+1} , 0.1 s^{-1} . For scheme (2) the rates used were: α, 3.2s^{-1}; β', 0.1s^{-1}; k_{+B} , 109.2s^{-1}; k_{-B} , 273s^{-1}. A random number generator (Wichman & Hill, 1985) was used to generate simulated records from these models, and the simulated records were divided into bursts using a critical shut time of 100ms; bursts were well separated because the mean lifetime of C_L was made very long (10^4ms). Bursts shorter than 100ms were discounted, as in the analysis of the real experiments, and a histogram of p_o values from the remaining bursts was constructed. The results for both models were (as usual) indistinguishable, so the results for model (1) only are shown in Fig. 4.7. The histogram of simulated p_o for model (1) is shown in Fig. 4.7A, and the histogram of the observed p_o obtained from the experimental data is shown in Fig. 4.7B, (the histograms of the simulated and observed data contain 304 and 87 bursts respectively). Clearly the expected spread of p_o values, for receptors that behave homogeneously, is much less than the observed spread (S.D. of p_o for the simulated and observed bursts were 0.057 and 0.16, respectively).

Two experimental problems could have contributed to the variability in p_o, namely, (1) inappropriate selection of t_C and, (2) undetected

A

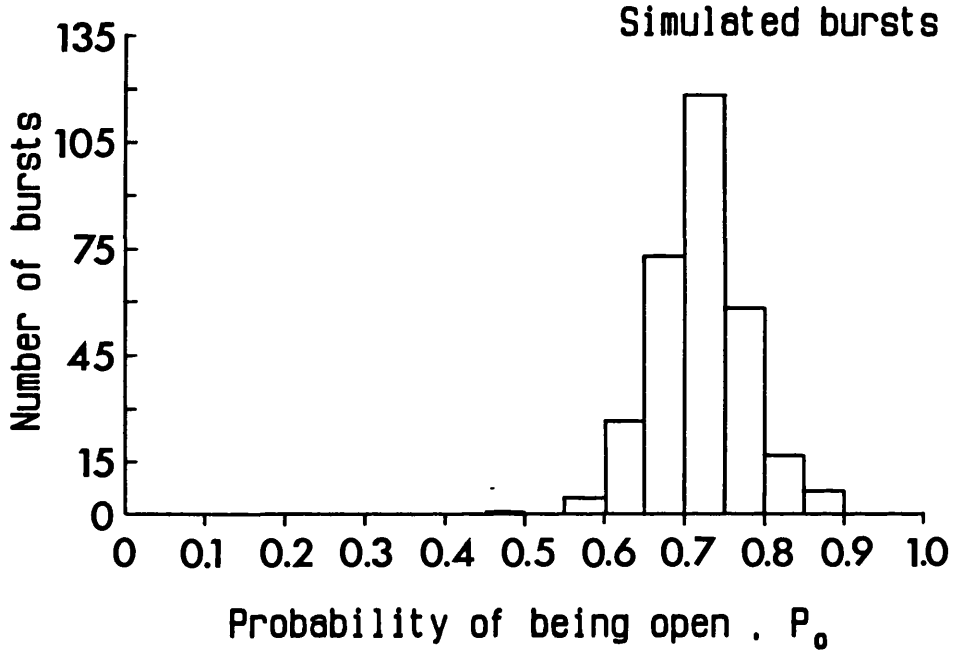
Simulated bursts
Number of bursts
135
105
75
45
15
0
0 0.1 0.2 0.3 0.4 0.5 0.6 0.7 0.8 0.9 1.0
Probability of being open . P_o

B

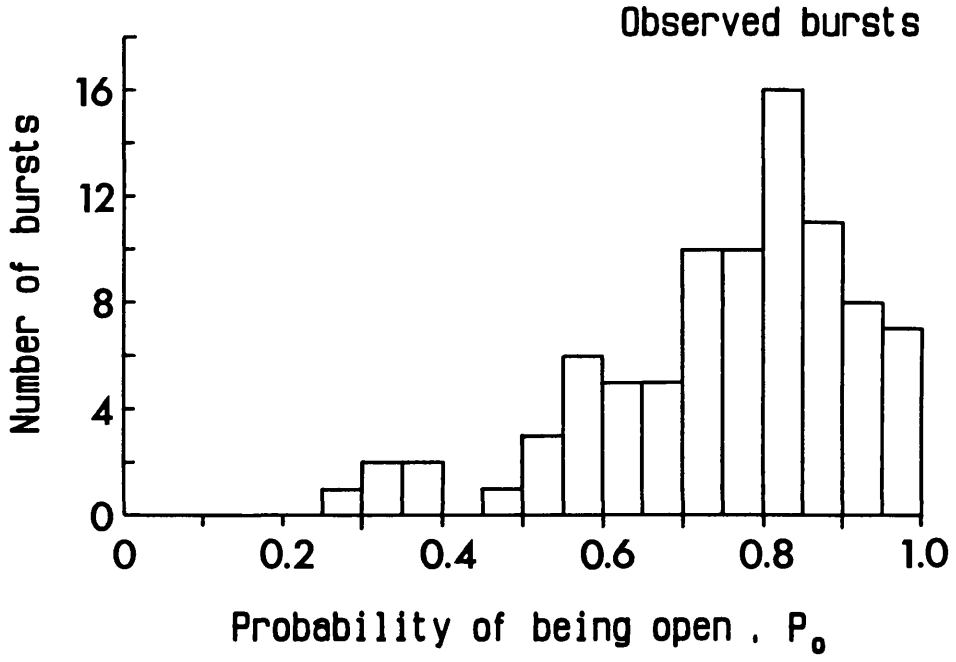
Observed bursts
Number of bursts
16
12
8
4
0
0 0.2 0.4 0.6 0.8 1.0
Probability of being open . P_o

Fig. 4.7 Comparison of the observed spread of probability of being open, p_o, with that expected for a population of identical and independent receptor-channels. A, histogram of p_o for 304 bursts of more than 100ms duration, obtained from a simulated record of channel opening and closing durations, using a t_c of 100ms (see text for details). Mean p_o was 0.72. B, histogram of p_o of 87 observed bursts (50μM GABA; t_c = 50ms; bursts more than 100ms duration; T = 22-23°C). Mean p_o was 0.76. Note the larger spread of p_o for the observed bursts, compared with the simulated bursts (S.D. of the p_o for the simulated bursts was 0.057, and for the observed bursts was 0.16).

presence of more than one active channel during part, or all, of some of the bursts. The possible contribution of these two artefacts will now be considered.

4.5.5 *Effect of t_C on the estimation of p_o.* Although only one value of t_C (for a given GABA concentration) can be optimum for estimation of the equilibrium concentration-response curve, it seems legitimate to inspect, empirically, the spread of p_o values obtained with each of a range of t_C values. This allowed us to check that the appearance of great heterogeneity is not critically dependent on t_C, the optimum value for which was often not certain. Histograms of p_o values for individual bursts were therefore calculated using a range (20-100ms) of critical gap durations, t_C (see Auerbach & Lingle, 1986). Fig. 4.8 illustrates the effect of selecting different values for t_C on the spread of p_o, and on the overall mean p_o, of bursts recorded in the presence of 50μM GABA.

The graph includes data from twenty clusters (at holding potentials of -60mV to -100mV). For each curve, bursts within the twenty clusters were defined by one of the t_C values, 20, 50, 100, 200 or 1000ms (indicated next to corresponding curve), and only bursts of more than 100ms duration were included. It is clear from Fig. 4.8 that, at 50μM GABA, there is a wide spread in p_o regardless of t_C. This suggests that bursts are heteogenous since the value of p_o varies from one bursts to another (see randomization test, below, for further analysis). Reducing the value of t_C obviously increased the number of bursts and reduced the length of each burst. However, at 50μM GABA the mean p_o was increased only slightly when the t_C value was reduced. Thus, the mean p_o was reduced from 0.81 to 0.71 when the t_C was increased from 20ms to 200ms. The change may reflect the inclusion of some of the brief desensitization gaps with the longer t_C or exclusion of some of the inter-activation gaps at the shorter t_C, or both.

4.5.6 *Two channels active simultaneously.* The length of experimentally observed runs of single openings (clusters without double events) was so long that the probability of two channels being active during a cluster is extremely low (Colquhoun & Hawkes, in preparation). For example, burst #13 of the cluster illustrated in Fig. 4.9 consisted of 41 openings with a p_o of 0.28. Even for this low observed p_o it is unlikely (P=0.01) that more than 24 consecutive single openings would be seen before the first double event, if there were actually two independent and identical channels active throughout the burst. Furthermore, there

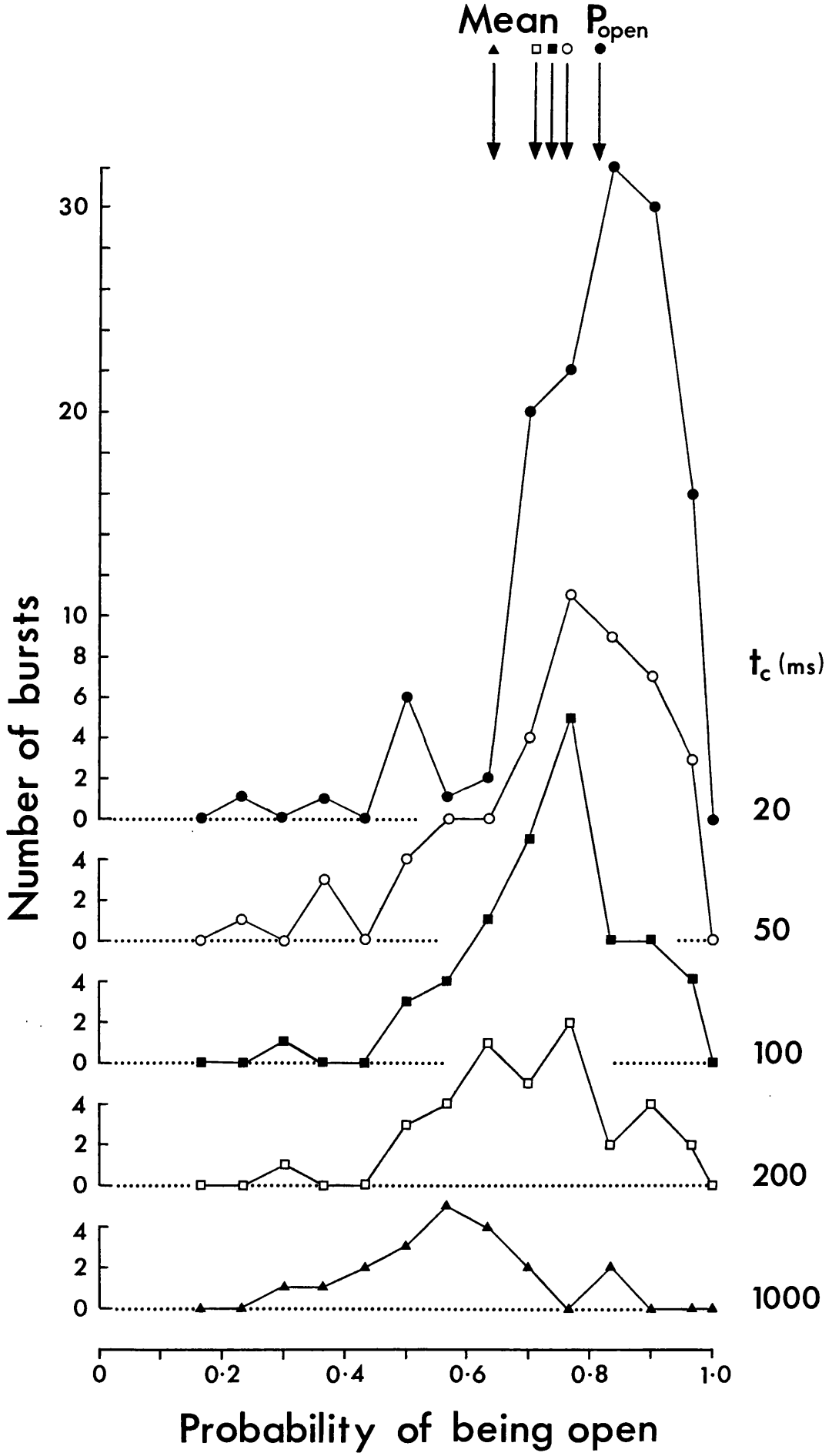
Mean P_{open}
Number of bursts
30
20
10
8
6
4
2
0
t_c (ms)
20
50
100
200
1000
0
0·2
0·4
0·6
0·8
1·0
Probability of being open

Fig. 4.8 Effect of selecting different values for the critical gap duration, t_c, on the spread of p_o values and on the overall mean p_o. Distributions of p_o for bursts within clusters, over a range of t_c (20-1000ms); the t_c value used in each plot is given on the right hand side (●, t_c 20ms; o, t_c 50ms; ■, t_c 100ms; □,t_c 200ms; ▲, t_c = 1000ms). The overall mean p_o for each t_c is indicated by the arrows (identified by their corresponding symbols) above the distributions: mean p_o = 0.64 (t_c = 1000ms; number of bursts, n=20), 0.71 (t_c = 200ms; n=37), 0.74 (t_c = 100ms; n=59), 0.76 (t_c = 50ms; n=84), and 0.81 (t_c = 20ms, n=131). Note the wide spread in p_o regardless of t_c, and that changing t_c from 20 to 1000ms shifts the mean p_o by only 0.17. Results represent data from 20 clusters recorded from outside-out patches (V_m = -60 to -100mV) exposed to 50μM GABA. Only bursts of more than 100ms duration were included. Each point represents the centre of a bin; bin width = 0.033; T = 22-23°C.

was no tendency for the p_o to be larger for bursts in the middle of a cluster, compared with bursts at the ends of a cluster, as would have been expected if there had been partial overlap of bursts of activity of two independent.

4.6 *Randomization test for heterogeneity of bursts*

The values obtained for p_o, as well as mean open time and shut time, for bursts within the same cluster and between different clusters, were compared by means of a randomization test (see Patlak, Ortiz & Horn, 1986). The aim of this test was to examine whether the wide variability in p_o could plausibly occur if all open and closed intervals came from the same population, that is, from channels showing homogeneous behaviour.

Values of p_o, and of mean open time and mean shut time, for pairs of bursts of at least 200ms duration (more that 40 openings) were compared at the same agonist concentration. Figure 4.9 shows an example of such an analysis applied to two clusters of openings. The single channel records (Fig. 4.9A) show two clusters (cluster 1, and cluster 2) recorded from a single patch in the presence of 50μM GABA. These two clusters have been selected to illustrate markedly different p_o values for bursts within the same cluster, and for bursts from different clusters. Cluster 2 occurred 2.8s later than cluster 1. Together the two clusters were divided into 13 bursts using a t_c of 50ms. The p_o values for the six bursts in cluster 1 ranged from 0.70 - 0.96, while the p_o values of the seven bursts in the second cluster ranged form 0.20 - 0.49.

Fig. 4.9B indicates the result of comparing, with the randomization test, the values of p_o, mean open time and mean shut time of bursts number 2 and 3 from the same cluster (Fig. 4.9A, cluster 1). Burst 2 had a p_o of 0.70 while the p_o of bursts 3 was 0.96. The histograms of randomized scatter (randomized *S*) were obtained under the null hypothesis that the two bursts were homogenous, by generating 1000 pairs of bursts, by use of randomization (see Methods). There is good evidence that both the p_o and the shut time, differed between the two bursts, since the estimated proportion of randomized *S* values which exceeded the observed *S* value for p_o and also for shut times, was zero (i.e. none of the 1000 randomized *S* values exceeded the observed *S*). However the proportion of randomized *S* which exceeded the observed *S* for the open times was 0.123, so there was no compelling evidence that the open times differed between these bursts. Figure 4.9C shows a

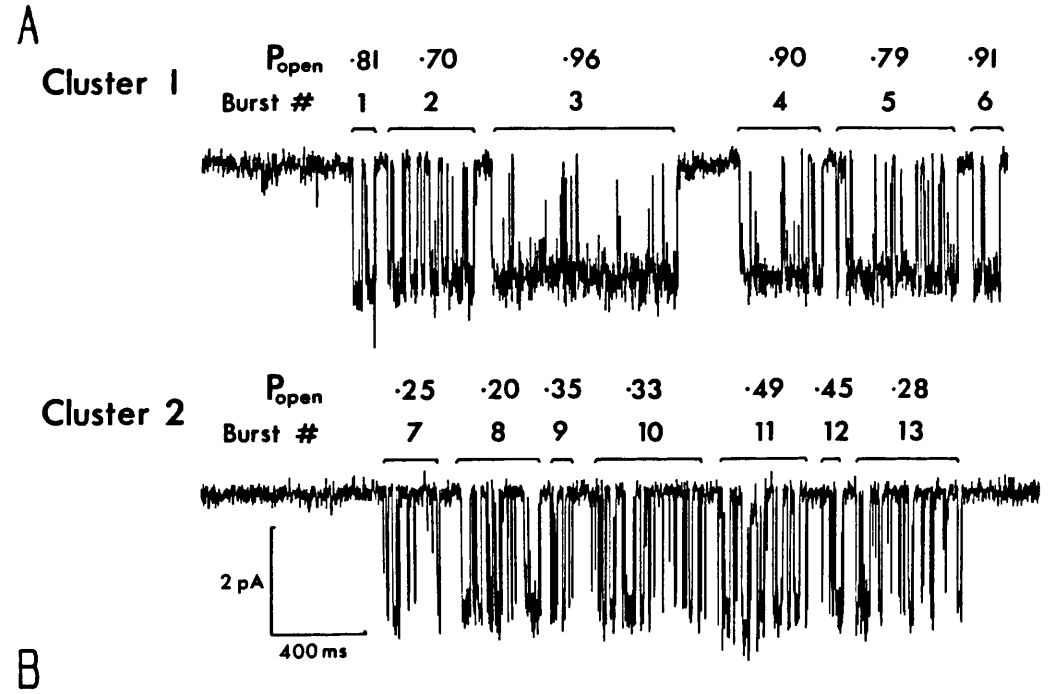

B

Comparison of bursts 2 and 3, from the same cluster

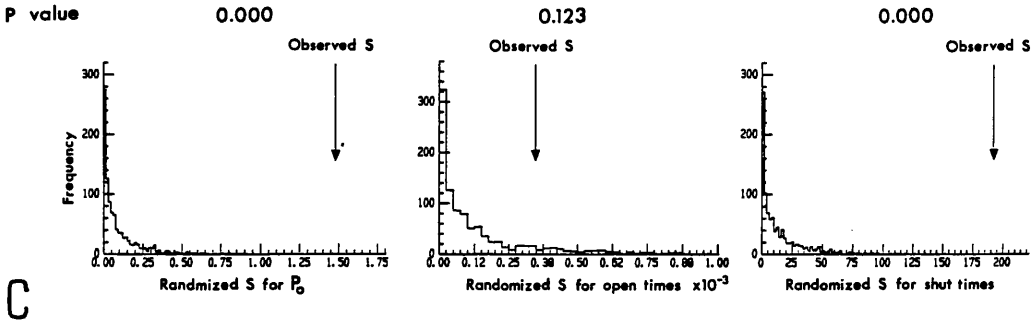

C

Comparison of bursts 3 and 13, from different clusters

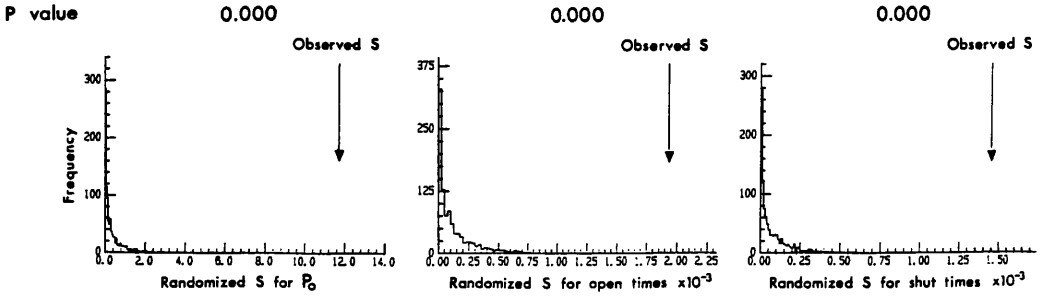

Fig. 4.9 Randomization test to compare bursts within a cluster and bursts from different clusters. A, records selected to illustrate different p_o values for bursts within a cluster and for bursts from two different clusters, in the same outside-out patch. The record shows two successive clusters. The first cluster (upper trace) occurred 2.8s before the second cluster (lower trace; 2.8s gap not shown). The two clusters have been subdivided into 13 bursts (numbered burst # 1-13 above each burst) using a t_c of 50ms. Corresponding p_o values are also given (50μM GABA, V_m = -80mV; T = 22°C; effective filter ing 670Hz, -3dB). B, histograms showing randomized scatter for p_o (left), for open times (middle) and for shut times (right) obtained under the null hypothesis that bursts #2 and #3 are homogenous (see text for details). 1000 pairs of artificial bursts were compared. The arrows indicate the level of the observed scatter for burst #2 and burst #3. The proportion of randomized S values which exceed the observed S values is indicated above each histogram (P values). C, histograms of randomized scatter for p_o (left), for open times (middle) and for shut times (right) obtained when comparing two bursts (3 and 13) from different clusters.

similar comparison for bursts number 3 and number 13 (i.e. bursts from different clusters). Burst number 3 contained 64 openings and had a p_o of 0.96, while the p_o of burst number 13 was 0.28 and consisted of 41 openings. Using 1000 pairs of artificial bursts (produced by randomization), the *P* values for p_o, mean open time and mean shut time, were all 0.000, indicating a difference in the kinetic properties of the two bursts.

Values of p_o, and of mean open time and mean shut time, have been compared for sets of 2-20 bursts, considering bursts of more than 200ms duration (more than 40 openings) and at a single agonist concentration. In order to eliminate any bias in selecting bursts, all bursts recorded from any particular outside-out patch, which satisfied the criteria previously indicated (in terms of amplitude, and of duration), were compared. Figure 4.10 shows the result of such a randomization test, used to compare all of the bursts that were longer than 200ms (20 in total) recorded from a single patch exposed to 50μM GABA. The bursts were defined by a t_c of 50ms and originated from six clusters. The p_o of the 20 observed bursts ranged from 0.56 to 0.89, and the grand mean p_o was 0.73. The randomization proceedure was used to generate 10^4 sets of 20 artificial bursts, in order to construct histograms of randomized *S* for p_o, and for the open times and shut times. In this example the estimated *P* values were: 0.0001 for shut times, 0.0003 for p_o, and 0.0000 for open times, indicating that all three parameters were significantly different for bursts within and between the clusters, recorded in this particular patch.

In summary, the p_o, mean open time, and mean shut time have been found to differ between one channel and another (i.e. between clusters), and for the same channel at different times (i.e. between bursts within the same cluster).

4.7 *Whole-cell dose -response relationship*

The p_o *vs* GABA concentration relationship was necessarily obtained from single-channel current recordings in which the $GABA_A$ receptor-channels were desensitized (so that clusters of openings, resulting from the activity of individual channels, were well separated). Therefore a whole-cell GABA dose-response relationship was obtained for comparison with the plot of p_o *vs* GABA concentration.

The whole-cell dose-response relationship illustrated in Fig. 4.11 contains data pooled from 12 cells (clamped at -60mV). The normalized responses are the peak amplitudes of the current responses expressed

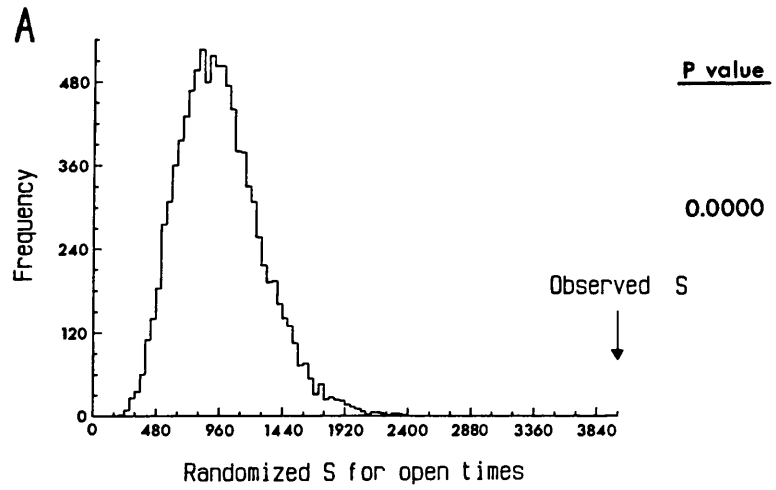
A
P value
0.0000
Observed S
Frequency
480
360
240
120
0
0
480
960
1440
1920
2400
2880
3360
3840
Randomized S for open times

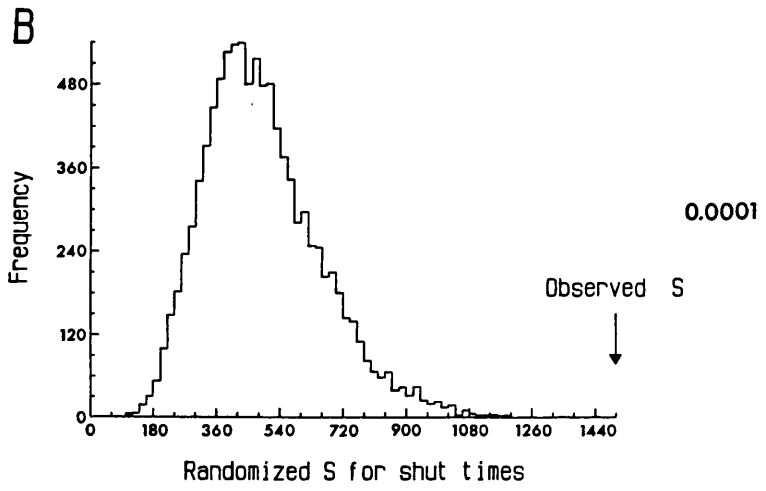
B
0.0001
Observed S
Frequency
480
360
240
120
0
0
180
360
540
720
900
1080
1260
1440
Randomized S for shut times

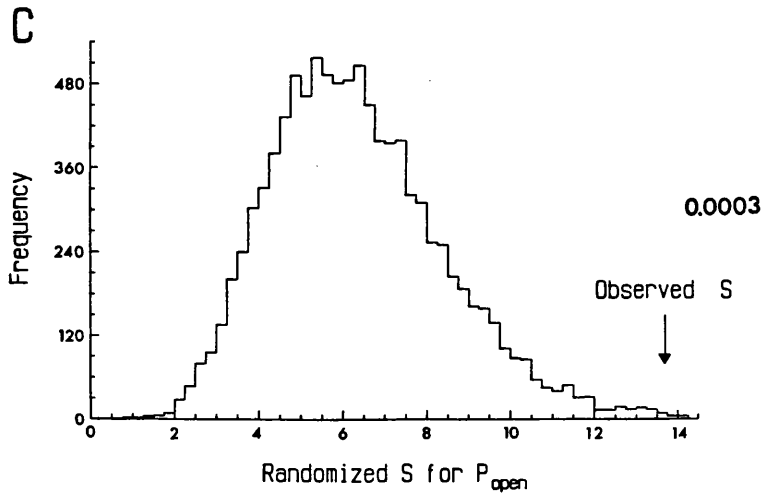
C
0.0003
Observed S
Frequency
480
360
240
120
0
0
2
4
6
8
10
12
14
Randomized S for P_{open}

Fig. 4.10 Randomization test to compare 20 bursts from 6 clusters, recorded from one patch exposed to 50μM GABA; V_m = -70mV; T = 22°C. Bursts were defined by a t_c of 50ms. The histograms are of randomized scatter (Randomized S) of A, open times, B, shut times, and C, p_o, obtained under the null hypothesis than the 20 bursts are homogenous, and using 10^4 randomizations (see Methods for details). Arrows indicate the level of the observed scatter (Observed S). The proportion of randomized S values which exceeded the observed S value is shown to the right of each histogram (as P values). Note the larger scatter in open times, shut times, and p_o, for the observed bursts compared to that expected for receptor-channels showing homogeneous behaviour.

as a percentage of the peak response to 10μM GABA in the same cell. This was necessary since the absolute amplitude of current responses to a given concentration of GABA, (at a particular holding potential), varied from cell to cell (up to a two fold difference). It is apparent from the relationship that at concentrations of GABA below 20μM, the normalized responses did not vary greatly from cell to cell, in contrast to the wide variability in responses to concentrations above 20μM. Part of this variability is undoubtedly due to differences in the extend of desensitization at the apparent peak of the whole-cell current responses.

Fig. 4.11B illustrates three representative whole-cell currents recorded from the same cell in response to 5, 10 and 20μM GABA. There was no apparent desensitization below 10μM GABA, but above this concentration there was pronounced desensitization. The whole-cell dose-response relationship flattens above 30μM GABA, probably partly as a result of attenuation of the peak response by desensitization. By comparing Figs. 4.6 and 4.11 it can be seen that the lowest concentration of GABA used to determine the p_o *vs* GABA concentration relationship (10μM) is close to the apparent EC_{50} of GABA in these cells. The EC_{50} of GABA was taken as the concentration which produced a response of approximately 50% of the apparent maximum response (Fig. 4.11A).

4.8 *Effect of guanosine 5' triphosphate (GTP)*

In addition to $GABA_A$ receptors, $GABA_B$ receptors have also been found in mammalian superior cervical ganglion (SCG) neurones (Balcar *et al*, 1986). In cultured rat, mouse and chick dorsal root ganglion (DRG) neurones, activation of $GABA_B$ receptors has been shown to inhibit voltage-activated calcium channel currents, *via* activation of membrane-bound GTP binding proteins (Dunlap & Fischback, 1981; Deisz & Lux, 1985; Dolphin *et al*, 1986; Dolphin & Scott, 1987; Holz *et al*, 1986; Green & Cottrell, 1988). Furthermore, voltage activated Ca^{2+} currents in cultured and freshly dissociated SCG neurones are inhibited by the non-hydrolysable GTP analogue, guanosine 5'-0(3-thio) triphosphate, GTP-γ-S, (Wanke *et al*, 1987; Dolphin & Scott, 1989). In contrast, in rat and guinea-pig hippocampal pyramidal cells, $GABA_B$ receptors are coupled to K^+ channels *via* a GTP-binding protein (Newberry & Nicoll, 1984; Gähwiler & Brown, 1985; Inoue *et al*, 1985; Andrade, Malenka & Nicoll, 1986). It was therefore of interest to determine whether the wide variability in p_o of $GABA_A$ receptor-channels (at a given agonist concentration) was the result of modulation of these receptor-channels

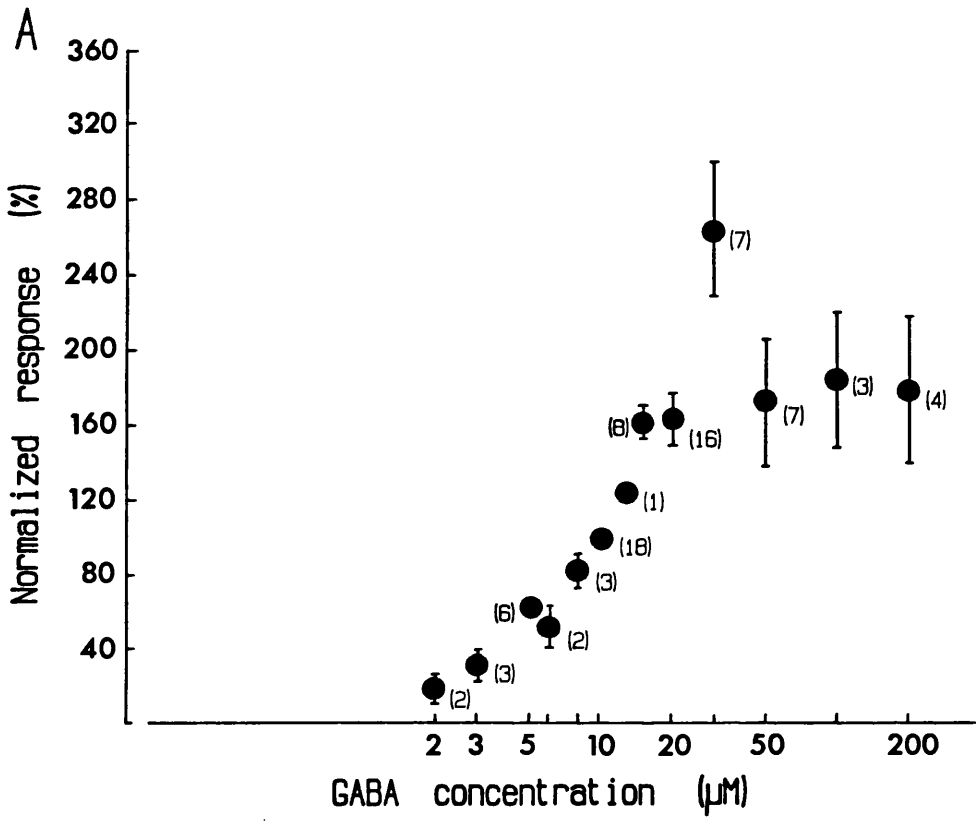
A
360
320
280
240
200
160
120
80
40
Normalized response (%)
(2)
(3)
(6)
(2)
(18)
(3)
(1)
(8)
(16)
(7)
(7)
(3)
(4)
2 3 5 10 20 50 200
GABA concentration (μM)

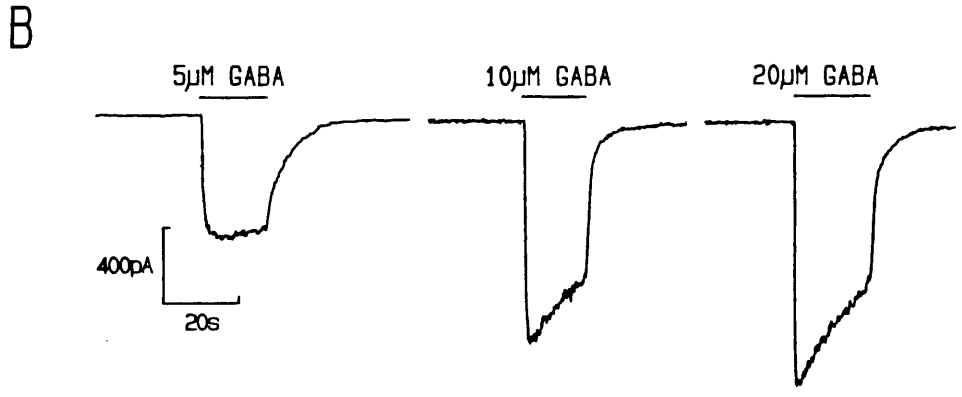
B
5μM GABA
10μM GABA
20μM GABA
400pA
20s

Fig. 4.11 A, whole-cell dose-response relationship for data pooled from 12 cells (V_m = -60mV). In each cell peak responses were normalized with respect to the peak response to 10μM GABA. The numbers in parenthesis indicate the number of responses averaged for each point. Vertical bars represent ± S.E. (where these values are larger than the symbol). The concentration of GABA which produced a response of approximately 50% of the apparent maximum response, was about 10μM; the plateau of the dose-response relationship occurred above 30μM GABA. B, representative current responses from one cell (used in A) evoked by 5, 10 and 20μM GABA. Calibration 400pA, 20s.

by membrane-bound GTP binding proteins activated by GABA via $GABA_B$ receptors.

Guanosine 5' triphosphate (GTP), rather than the non-hydrolysable analogue guanosine 5'-0(3-thio)triphosphate (GTP-γ-S) was used in these experiments because, in the case of voltage-activated calcium channels in DRG neurones, GTP-γ-S has an additional agonist-independent effect on these channels (Scott & Dolphin, 1986; Dolphin & Scott, 1987).

Figure 4.12A illustrates p_o values for bursts in the absence and presence of 1mM GTP inside the pipette. The patches were exposed to 50μM GABA, and the t_c value used to select bursts was 50ms. Each graph includes data from four different outside-out patches (eight in all), held at -60 to -100mV. It is clear from Fig. 4.12A that inclusion of 1mM GTP inside the pipette did not reduce the amount of variability in p_o values. The S.D. of p_o values in the presence of intracellular GTP was practically the same as the S.D. in the absence of GTP (0.18 and 0.16 respectively). From Fig. 4.12A it appears that intracellular GTP reduces the overall mean p_o from 0.76 to 0.47 ($P<0.05$, Student's t-Test). However, this difference may well result from the use of a small number of patches. In addition there may be several different types of $GABA_A$ receptor-channels in these neurones with different kinetics, such that not all types of the receptor-channel were active in each patch. In support of this, it was found that for some of the patches, the overall mean p_o of a particular patch was significantly different ($P<0.05$, t-Test) from the overall mean p_o of a different patch under identical conditions.

4.9 *Effect of adenosine 5' triphosphate and pentobarbitone*

Adenosine 5' triphosphate (ATP) was included in the patch pipette (plus magnesium ions) during one experiment to ascertain whether the wide variability in p_o could have resulted from internal phosphorylation of the $GABA_A$ receptor-channel by a membrane-bound Mg-ATP dependent phosphorylating protein. In addition to GABA, pentobarbitone (at a concentration which did not directly activate the $GABA_A$ receptor-channels) was added to the extracellular surface of the outside-out patch, to determine if the wide variability in p_o was altered by a drug that is thought to increase channel open time (Study & Barker, 1981; Jackson *et al*, 1982b; Macdonald *et al.*, 1989b). Since Mg-ATP was included inside the pipette during the same experiment in which pentobarbitone was also used (only one experiment) no attempt was made to determine the effects of these agents individually, on say the overall mean p_o. Figure 4.12B depicts p_o for bursts (produced by

50μM GABA) in the absence or presence of 4mM Mg-ATP inside the pipette, plus 10μM pentobarbitone in the extracellular medium. Only bursts of more than 100ms duration were used in the analysis (t_c of 50ms was used throughout). The control data (50μM GABA) was obtained from four outside-out patches, and the data for pentobarbitone and Mg-ATP was recorded from one patch (different from the control patches). It is apparent from Fig. 4.12B that the presence of intracellular Mg-ATP and extracellular pentobarbitone did not reduce the wide variability in p_o values. In control conditions the S.D. was 0.16, while in the presence of Mg-ATP plus pentobarbitone, the S.D. was 0.13. Although Mg-ATP plus pentobarbitone produced an apparent reduction in the overall mean p_o (from 0.76 to 0.57), this again probably reflects the small number of patches used and the possible presence of several kinetically different $GABA_A$ receptor-channels, (see GTP Results).

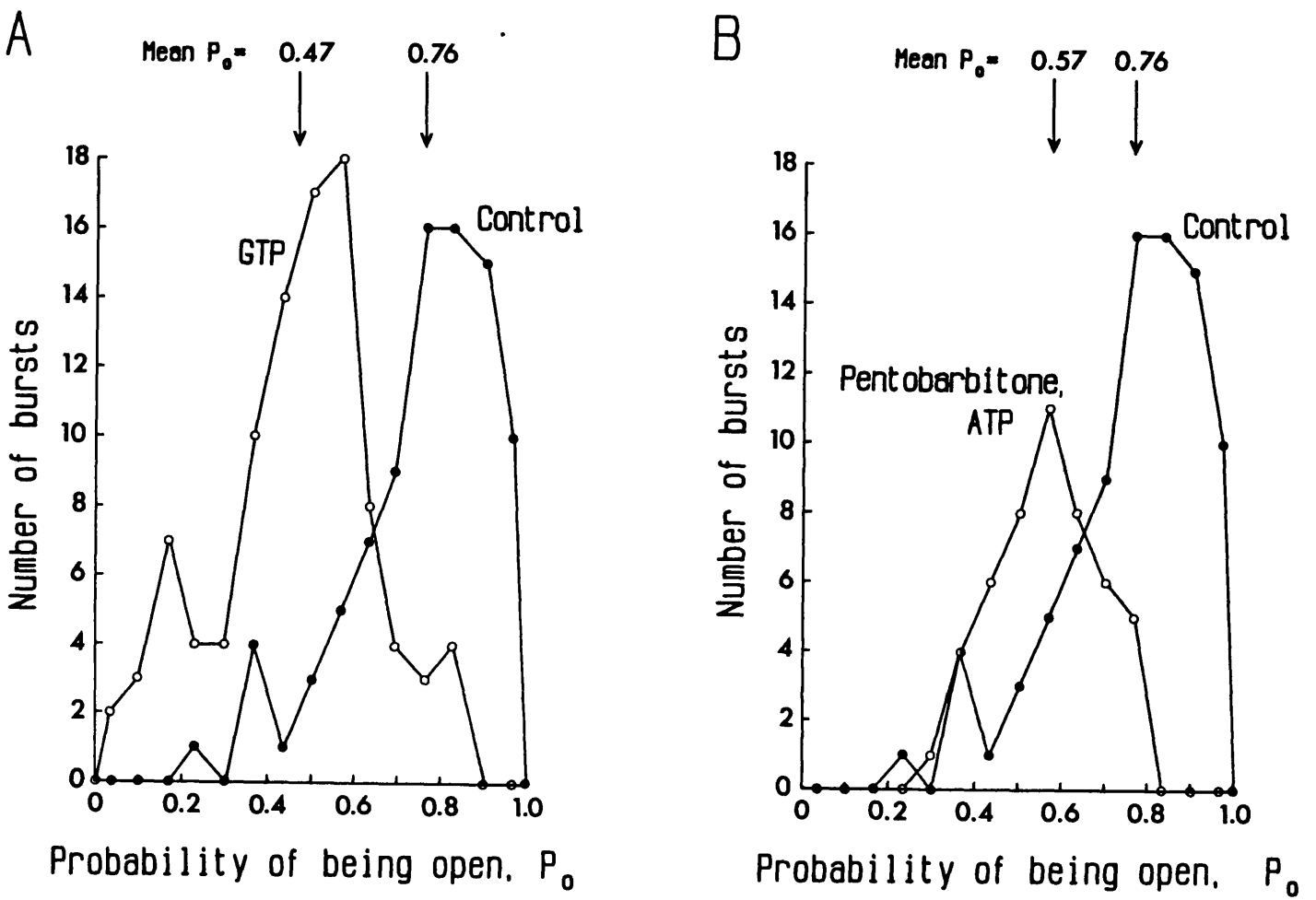
A
Mean P_o= 0.47
0.76
GTP
Control
Number of bursts
Probability of being open, P_o
B
Mean P_o= 0.57
0.76
Pentobarbitone, ATP
Control
Number of bursts
Probability of being open, P_o

Fig. 4.12 A, distribution of p_o for bursts (> 100ms duration) recorded in the absence and presence of 1mM GTP contained in the pipette solution; patch exposed to 50μM GABA; V_m = -60 to -100mV; t_c = 50ms. Mean p_o in the absence of GTP (closed circles) was 0.76 ± 0.16 (mean ± S.D., n=87 bursts); mean p_o in the presence of GTP (open circles) was 0.47 ± 0.18 (mean ± S.D., n = 98 bursts). Each distribution includes data from a different set of four patches. Each point marks the centre of a bin; bin width = 0.067. B, distribution of p_o (bursts > 100ms duration) recorded in the absence or presence of 4mM Mg-ATP contained in the patch pipette and with 10μM pentobarbitone in the bathing medium: patch exposed to 50μM GABA. Mean p_o in the presence of GABA alone (closed circles) was 0.76 ± 0.16 (mean ± S.D., n = 87 bursts, 4 patches); mean p_o in the additional presence of Mg-ATP, plus pentobarbitone (open circles) was 0.57 ± 0.13 (mean ± S.D., n = 50 bursts, 1 patch). Each point marks the centre of a bin; bin width = 0.067.

4.10 *Multiple conductance states*

A conductance level of about 30pS was the most common in the present work, and values of about 22-23pS, 15-18pS and 7-9pS could also be seen with reasonable reliability. However, the results are such that this cannot be regarded as an exhaustive list. For much of the time, open channels were not in any clearly-identifiable discrete conductance level, but rather appeared noisy. Some of this noisy appearance may result from the channel oscillating relatively quickly between various closely spaced and discrete conductance levels. However the only evidence for closely spaced discrete conductance levels in these neurones is that (1) the open point amplitude histograms and mean low-variance amplitude histograms could, in many cases, be fitted with the sum of two or more Gaussians which had closely spaced means, and (2) when considering clusters of pretty consistent amplitude, the amplitudes clearly differed from one cluster to another in the same patch, and often by only a few pS. It is interesting to note that nicotinic acetylcholine receptors in rat sympathetic neurones also appear noisy in their open state (Mathie *et al*, 1988). In contrast, various groups have reported that $GABA_A$ receptor-channels, in other vertebrate neurones, open to a number of discrete but more widely spaced multiple conductance levels (see Table 4.1 for references). Table 4.1 lists the conductance levels of $GABA_A$ receptor-channels measured from various cell types, and also lists the relative frequency of occurrence of these levels (when given), and the chloride concentrations used. Since the methods of measuring the amplitudes of single channel currents in some of these studies were of relatively low resolution, it is not possible to determine whether there was evidence that these $GABA_A$ receptor channels opened to closely spaced discrete conductance levels. Other amino acid activated channel types, such as mammalian central glutamate receptor-channels, and glycine receptor channels appear far less noisy than $GABA_A$ receptor channels and also have more discrete-looking subconductance levels (Hamill *et al*, 1983; Bormann *et al*, 1987; Cull-Candy & Usowicz, 1987, 1989b; Jahr & Stevens, 1987; Cull-Candy, Howe & Ogden, 1988).

Although the conductance levels of $GABA_A$ receptor-channels in other preparations are reported to be more discrete than in the present work, there is little agreement in the amplitudes reported for the various conductance levels (range 6-45pS). This may result, in part,

TABLE 4.1:

Conductance states of the $GABA_A$ receptor-channel

PREPARATION	CONDUCTANCE AMPLITUDES (pS) IN ORDER OF FREQUENCY OF OF OCCURRENCE (IF KNOWN)	CHLORIDE CONCENTRATIONS (mM)	REFERENCE
Cultured mouse spinal cord neurones	19 > 30 > 44, 12	145*s*	Hamill, Bormann & Sakmann 1983.
Xenopus oocytes injected with total mRNA from chick optic lobe	30 >> 28.5, 1.5	unknown *i*	Miledi, Parker & Sumikawa, 1983
Dissociated bovine chromaffin cells	28.9 ± 1.3 >> 17, 37	148*e* 144*i*	Cottrell, Lambert & Peters, 1985.
Cultured embryonic mouse spinal cord	29 ± 2.8	145*s*	Mathers, 1985.
Cultured rat (embryonic) hippocampal neurones	19	142*s*	Allen & Albuquerque 1987.
Cultured mouse spinal neurones	30 >> 19, 12 >>44	145*s*	Bormann, Hamill & Sakmann, 1987.
Cultured mouse cerebellar neurones	31 > 19	145*s*	Huck & Lux, 1987.
Cultured rat cerebral astrocytes	29 > 12, 21, 43	148*e* 146*i*	Bormann & Kettenmann, 1988

Cultured chick cerebral neurones	21 > 10-13, 6-8, 27-32	136*e* 131*i*	Weiss, Barnes & Hablitz, 1988.
Cultured mouse brain and spinal cord neurones	27.2 ≏ 15.9	150*s*	Macdonald, Rogers & Twyman, 1989.
Cultured embryonic chick spinal cord neurones	26 >> 10	147*e* 145*i*	Yang & Zorumski, 1989.
Dissociated 17-day rat sympathetic neurones	31-33	145*e* 142*i*	Cull-Candy & Mathie, 1986
Cultured procine intermediate lobe endocrine cells	23-31 > 19 >> 45	147.5 to 172*e* 144*i*	Taleb, Trouslard, Demeneix, Feltz, Bossu, Dupont & Feltz, 1987
Dissociated rat sympathetic neurones	30 > 22-23, 15-18, 7-9	159*e* 142*i*	present study

THE CHLORIDE CONCENTRATIONS ARE GIVEN AS *i*, FOR INTRACELLULAR, AND *e*, FOR EXTRACELLULAR, OR *s* FOR SYMMETRICAL.

from differences in experimental conditions, such as temperature (21-26°C for the cited papers), pH, and chloride activities (the concentrations used ranged from 120 to 150mM and were symmetrical about the cell membrane). We have found that both temperature and pH alter the single-channel conductance of $GABA_A$ receptor channels in rat sympathetic neurones. Increasing the temperature resulted in an increase in the amplitude of the main conductance level (Q_{10} approximately 1.3; effect of temperature on the amplitude of the other conductance levels was not investigated). Increasing the pH resulted in a decrease in conductance of the main level (we observed that an increase of 3pH units, from 5.3 to 8.3, reduced the single-channel conductance from approximately 40pS to 25pS). Thus only modest differences would be expected to result from differences in these conditions.

An alternative explanation for the reported differences in the amplitudes of the conductance levels is that different forms of the $GABA_A$ receptor are present in different cell types.

4.11 *Heterogeneous properties of $GABA_A$ receptors in rat* superior cervical ganglion *neurones*

The probability of being open, as well as the mean open times and mean shut times have been found to differ not only between one channel and another (i.e. between clusters), but probably for the same channel at different times (i.e. between bursts within a cluster). These differences have been shown to be far greater than those expected for a channel which behaves homogeneously. The fact that there are kinetic differences between bursts within a single cluster strongly suggests that there is at least one homogeneous population of $GABA_A$ receptors whose activity changes relatively slowly with time. The finding that the channel kinetics were different between bursts from different clusters indicates that there may, in addition, be two or more distinct $GABA_A$ receptor-channel types which exhibit different kinetics.

Many groups have studied the kinetics of $GABA_A$ receptor channels in various vertebrate cell types, by the use of patch-clamp techniques, and employing low agonist concentrations. These include cultured mammalian neurones and astrocytes (Sakmann *et al*, 1983a; Bormann & Clapham, 1985; Mathers, 1985; Mathers & Wang, 1988; Macdonald *et al*, 1989a), cultured chick neurones (Weiss, 1988; Weiss & Magleby, 1989) and dissociated frog neurones (ffrench-Mullen *et al*, 1988). At low concentrations of GABA (below 5μM) the main conductance state of the

$GABA_A$ receptor channels in these preparations appears to behave homogeneously. However, in none of these studies were responses to high agonist concentrations recorded. So it is not known whether $GABA_A$ channels in other preparations show the sort of heterogeneity of open and shut times reported here.

A channel which can switch between different kinetic 'modes' is not unprecedented. The word 'mode' is used here merely to refer to a subset of open and closed states of the receptor-channel within which the channel may oscillate for relatively long periods of time, before switching to a different subset ('mode') in which open times and/or closed times are different. Rare, but sudden, changes in the kinetics of an individual channel have been observed for other agonist-activated channels, including glutamate receptors in locust muscle (Patlak *et al*, 1979; Cull-Candy *et al*, 1981), nicotinic acetylcholine receptors in *Xenopus* myocytes (Auerbach & Lingle, 1986), and glutamate receptors in cerebellar granule neurones (Howe *et al*, 1988). Voltage activated ion channels also occasionally switch between different kinetic states, as observed for sodium channels in adult frog skeletal muscle (Patlak *et al*, 1986) and calcium channels in cardiac cells (Hess *et al*, 1984). Similarly, Blatz & Magleby (1986) have reported the existence of two kinetic modes of spontaneous 'fast' chloride channels in cultured rat skeletal muscle, though one mode contained only 1% of all open and shut intervals. The present work, however, is the first report of this sort of behaviour of single $GABA_A$ receptor-channels in a mammalian neurone.

The presence of two (or more) kinetically distinguishable populations of $GABA_A$ receptors, rather than one type with modal behaviour, has been suggested by a few groups. Cash & Subbarao (1987) detected two phases of desensitization of $GABA_A$ receptors, each with first-order kinetics, when measured by the transmembrane flux of $^{36}Cl^-$ in sealed rat brain membrane vesicles, using quenched-flow techniques. The two phases were thought to originate from two separate populations of $GABA_A$ receptors since, at a concentration of GABA below saturation level, the relative Cl^- flux activities during the two phases were concentration independent. Yasui *et al* (1985) had previously suggested the presence of kinetically distinguishable populations of $GABA_A$ receptors in frog sensory neurones, based on results from the separate analysis of GABA current noise during the peak and the steady state phases of whole-cell responses in these neurones. The analysis was based on the parabolic relationship

$$\sigma^2 = Ni^2 p_o (1-p_o)$$

where i is the single channel current amplitude, N is the total number of channels, and p_o is the probability of being open of individual channels. The relationship can be written

$$\sigma^2 = (i - \bar{I}/N)\ \bar{I}$$

where $\bar{I} = Nip_o$ is the whole-cell current amplitude. The non-linearity of a plot of $\sigma^2/\bar{I}$ *vs* $\bar{I}$ was taken to indicate heterogeneity of the $GABA_A$ receptor, the different subtypes being present in different numbers and having different conductances (approximately 4, 13 and 25pS). However, it is well documented that multiple conductance levels often originate from the same $GABA_A$ receptor-channel, rather than originating from different channel types, as observed in rat and mouse brain and spinal cord neurones (Bormann *et al*, 1987; McBurney *et al*, 1988; Weiss *et al*, 1988; Macdonald *et al*, 1989a). Akaike *et al.* (1986) also interpreted their results in terms of the presence of at least two types of kinetically distinguishable $GABA_A$ receptor-channels present in frog sensory neurones. The rate of activation of whole-cell GABA currents was found to be composed of two exponential components which had different concentration dependencies. The finding that these two components recovered from desensitization with different time courses, was taken as evidence for at least two receptor subtypes.

There is much indirect evidence for the existence of structurally distinct populations of $GABA_A$ receptors. Numerous groups have described the existence of multiple brain binding sites for benzodiazepine ligands, including Lippa *et al* (1985) who demonstrated that flunitrazepam labelled at least three distinct macromolecules in mouse cerebellar membranes (see Lippa *et al.*, 1985, for further references). More recently Duggan & Stephenson (1988) have shown heterogeneity in benzodiazepine binding sites when using purified $GABA_A$ receptors from bovine brain (as well as membrane bound $GABA_A$ receptors). The displacement of [^{3}H]-flunitrazepam binding activity to the purified $GABA_A$ receptors, by ethyl-β-carboline-3-carboxylate (a benzodiazepine ligand) was best described by a two site model. Furthermore, differences in the relative potencies of agonists and antagonists on $GABA_A$ receptors from vertebrates and invertebrates suggests the presence of different $GABA_A$ receptor types (for reveiw see Nistri & Constanti, 1979).

Molecular biology has recently provided direct evidence for the existence, in mammalian and chick brain, of multiple isoforms of the α, β and γ subunits which constitute the $GABA_A$ receptor-channel (Fucks &

Sieghart, 1988; Levitan *et al*, 1988; Pritchett *et al*, 1989). Furthermore, Levitan *et al* (1988) have demonstrated that different α subunit isoforms, when expressed in *Xenopus* oocytes with a singel type of β subunit, formed functional receptors for which GABA had apparently different potencies. There is therefore a possibility that structurally distinct types of the $GABA_A$ receptor channel exist in superior cervical ganglion neurones.

The present work provides strong evidence for at least one structurally homogeneous population of $GABA_A$ receptor channels whose activity changes. The results also suggest the possibility that, in rat superior cervical ganglion neurones, there are two or more structurally distinct populations of $GABA_A$ receptor-channels which exhibit different kinetics.

4.12 *General features of the p_o curve*

The maximum p_o value that could be achieved at high GABA concentrations, 0.83, was clearly less than 1.0. It is unlikely that this resulted from rapid open channel block by GABA, since the apparent conductance of the single channels was not reduced by high concentrations of GABA. This is in contrast to the effect of high concentrations of acetylcholine acting at nicotinic acetylcholine receptor channels in frog muscle; in this case there is an obvious reduction in the apparent channel conductance, because both open and shut (blocked) times are too brief to be fully resolved by the recording system (Ogden & Colquhoun, 1985). One possible explanation for the low maximum p_o is that short desensitization gaps have been inadvertently included in the bursts. As discussed in the Results, ambiguities arose in trying to decide whether the briefer shut periods within clusters (of less then 100ms) were spent in short lived desensitized states or whether they were spent in the resting (i.e. activatable) state of the non-desensitized receptor. A more likely explanation for the low maximum p_o is that GABA may be a partial agonist. That is, the opening rate of the agonist bound receptor-channel may be little greater than the shutting rate into the bound but activatable state, (i.e. low β/α; see Colquhoun & Ogden 1988); a maximum p_o of 0.83 corresponds with β/α = 4.9.

Several groups have inferred low values of β/α (between 2.8 and 6.6) from observations of the activation of $GABA_A$ receptors by low concentrations of GABA, in bovine chromaffin cells, mouse spinal neurones, and cultured rat cerebral astrocytes (Sakmann *et al*, 1983b;

Bormann & Clapham, 1985; Bormann & Kettenmann, 1988). In all three cases the $GABA_A$ receptor-channel gating at low agonist concentration could be described by a simple sequential reaction scheme, based on that originally proposed by Del Castillo and Katz (1957) for agonist-activated channels, *viz*

$$A+R \underset{k_{-1}}{\overset{2k_{+1}}{\rightleftharpoons}} AR+A \underset{2k_{-1}}{\overset{k_{+1}}{\rightleftharpoons}} A_2R \underset{\alpha}{\overset{\beta}{\rightleftharpoons}} A_2R^*$$

where A is the agonist molecule, R is the receptor, AR and A_2R are mono-and biliganded closed states respectively, A_2R^* is the only open state of the receptor-channel, and k_{+1} , k_{-1} , β and α are the transition rate constants between the various states. In each case, the histograms of shut times at low agonist concentrations were fitted with two exponential components, the shortest of which were interpreted as *nachschlag* gaps (Colquhoun & Sakmann, 1981). The sum of two exponential components was also adequate to describe the histograms of burst lengths, the shortest component taken to represent isolated brief openings, and the longer component corresponding to bursts of re-openings. Values of β and α were dervied using these results together with the number of *nachschlag* gaps per burst, according to Colquhoun & Hawkes (1977, 1982). Recently, however, comprehensive analysis of $GABA_A$ single channel currents has led Macdonald *et al.* (1989a) and Weiss & Magleby (1989) to propose that the kinetics of the main conductance state of $GABA_A$ receptor-channels is far more complex than can be described by the sequential scheme given above. In fact both studies report at least 3 open states and 3 shut states for $GABA_A$ receptor-channels in cultured chick cerebral and mouse spinal neurones (and propose kinetic schemes which would fit their data). It is therefore difficult, at present, to give definite values for β/α, since the gating of $GABA_A$ receptors appears more complex than in the scheme given above, and the models proposed by Weiss & Magleby (1989) and Macdonald *et al* (1989a), have yet to be confirmed.

At high concentrations of GABA, it is observed that the gap between clusters usually greatly exceeds the duration of a cluster, even when there are several channels in the patch. It is therefore expected that one of the macroscopic desensitization time constants will be comparable to the mean cluster length, which in the present study was about 3.8s at 50μM GABA. This is similar to the most rapid time constant of macroscopic desensitization reported for frog spinal neurones (Akaike *et*

al, 1986) and for *Aplysia* neurones (Ikemoto *et al*, 1988).

In the present study, the GABA concentration *vs* whole-cell peak current relationship did not have a clearly defined maximum, probably as a result of attenuation of the peak current response by fast receptor desensitization. It was therefore not reasonable to estimate precisely the EC_{50} for GABA or the Hill coefficient for GABA, from this dose-response relationship. However, a GABA concentration of about 10μM produced a response that was approximately 50% of the apparent maximum response amplitude (i.e. EC_{50} was approximately 10μM). This value is in reasonable agreement with EC_{50} values determined for various isolated cell preparations in which the concentration of GABA was known (i.e. where there were no problems with GABA uptake, metabolism or diffusion of GABA). EC_{50} values of between 10 to 42μM have been reported for rat and frog dorsal root ganglion neurones (Akaike *et al*, 1985; Akaike *et al*, 1986; Hamann *et al*, 1988), chick neurones (Choi & Fischbach, 1981) and *Xenopus* oocytes which had been injected with mRNA coding for $GABA_A$ receptors (Sigel & Baur, 1987; Van Renterghem *et al*, 1987; Levitan *et al*, 1988). It is probable that fast desensitization of $GABA_A$ receptors also distorted the apparent dose-response relationships determined in at least some of these cases.

4.13 *Possible intracellular modulation of $GABA_A$ receptor-channels*

Several recent studies suggest that the $GABA_A$ receptor-channel can be modulated by various intracellular factors. The activation of protein kinase C was shown to inhibit $GABA_A$ mediated currents in acutely dissociated hippocampal neurones (Stelzer & Wong, 1989) and in *Xenopus* oocytes which had been injected with total mRNA from chick forebrain (Sigel & Baur, 1988). Furthermore, an ATP-dependent process appears to be necessary for the maintenance of $GABA_A$ receptor function in both acutely dissociated hippocampal neurones and cultured chick spinal cord neurones (Gyenes *et al*, 1988; Stelzer *et al*, 1988). These modulatory effects may be mediated *via* phosphorylation of the $GABA_A$ receptor, and several putative sites have been suggested. These include a cAMP-dependent kinase consensus sequence on the β subunit of the $GABA_A$ receptor-channel (Schofield *et al*, 1987) and a site on the α subunit which has been shown to be phosphorylated by a receptor-associated protein kinase (Sweetnam *et al*, 1988). Modulation of $GABA_A$ receptor-channels by receptor- or membrane-bound kinases or phosphatases, could conceivably occur in the present study when Mg-ATP was included in the pipette. However the observation that the

inclusion of Mg-ATP inside the pipette had no effect on the wide variability in p_o, suggests that the observed kinetic heterogeneity of the $GABA_A$ receptor channels did not result from modulation of these receptor channels by an ATP-dependent process, possibly involving membrane bound proteins.

Freely diffusible cytoplasmic factors have also been implicated in the modulation of $GABA_A$ receptor-channels. For example, Feltz *et al*, (1987) and Behrends *et al*, (1988) have reported that raising the intracellular calcium concentration (in the range 10^{-8}M to 10^{-6}M) depresses $GABA_A$ receptor-channel activity, in frog sensory neurones and in chick neurones. Modulation of the $GABA_A$ receptor channel by freely diffusible cytoplasmic factors seems unlikely in the present study, since all of the recordings were obtained from outside-out patches, and the patch pipette (intracellular) solution contained a very low, buffered calcium concentration (10mM EGTA + 1mM $CaCl_2$). Also, in most experiments, GTP, ATP, or any other factors thought to modulate other ion channels, were not included in the pipette solution.

In this study the presence of GTP on the cytoplasmic side of the membrane patch appeared to have no effect on the wide variability in p_o, so it appeared that GTP binding proteins have no pronounced effects on the kinetic behaviour of $GABA_A$ receptor-channels. If it were the case that the only route by which GTP binding proteins could be activated, were by activation of $GABA_B$ receptors, then the lack of effect of intracellular GTP could mean merely that there are no $GABA_B$ receptors in this preparation (although see Balcar *et al*, 1986), or that some intracellular factor is missing which is involved in the coupling of $GABA_B$ receptors to GTP binding proteins and to $GABA_A$ receptors. It is interesting to note that we did not observed a current response to baclofen (a selective $GABA_B$ agonist), in rat superior cervical ganglion neurones (in the whole cell configuration and at negative holding potentials), despite the observation by Balcar *et al*, (1986) of $GABA_B$ receptor binding in these cells. This apparent discrepency is not surprising in view of the composition of the recording solutions used in the present study. Firstly the use of Cs^+ in place of K^+ in the patch pipette solution would reduce any potassium conductance activated by baclofen. Secondly any effect of baclofen on voltage-activated calcium conductances was reduced by the inclusion of 10mM EGTA inside the patch pipette, and the exclusion of factors thought to be required to prevent 'wash-out' of voltage-activated calcium currents (Chad & Eckert, 1986; Byerly & Yazejian, 1986; Belles *et al*, 1988). Furthermore, the

experiments were not designed to observe voltage-activated calcium currents, or agonist gated potassium currents.

5. SOME GENERAL PHARMACOLOGICAL AND PHYSICAL PROPERTIES OF $GABA_A$ RECEPTOR-CHANNELS IN SYMPATHETIC NEURONES OF THE RAT

5.1 SUMMARY

1. The actions of three $GABA_A$ antagonists, and two putative $GABA_A$ potentiating ligands, on GABA currents in rat superior cervical ganglion neurones have been assessed using whole-cell patch-clamp techniques.

2. GABA-activated inward and outward currents were inhibited by 10μM picrotoxinin, 100μM penicillin and 10μM bicuculline.

3. Pentobarbitone, at a concentration below that which has a GABA mimetic effect on mammalian central neurones, potentiated GABA currents evoked in rat superior cervical ganglion neurones.

4. Glutamate, at a concentration which did not evoke a detectible current in these cells, had no effect on the amplitude of whole-cell GABA currents (inward or outward).

5. The whole-cell GABA current-voltage relationship in these neurones was virtually linear or showed slight outward rectification over the potential range +50 to -150mV.

6. The effects of temperature and pH on the amplitude of the main state conductance level of $GABA_A$ receptor-channels was measured from single-channel currents recorded from outside-out patches. Increasing the temperature or reducing the pH of the external solution increased the amplitude of the most frequently occurring conductance level. The Q_{10} was approximately 1.3, and a decrease of 3 pH units, from 8.3 to 5.3, increased the conductance from approximately 26pS to 40pS.

5.2 INTRODUCTION

This chapter includes a number of further properties of $GABA_A$ receptor-channels in superior cervical ganglion neurones, which were investigated during the course of this study. In general these topics were examined in less detail than the topics covered in the previous two sections, and have been included here as an (appendix) to the main experimental work.

One aim of this chapter was to determine whether peripheral $GABA_A$ receptor-channels resemble central ones in their current-voltage relationship.

A second aim of this chapter was to demonstrate that peripheral $GABA_A$ receptor-channels showed pharmacological similarity to those of mammalian central neurones. Therefore the effects of the well established $GABA_A$ antagonists, picrotoxinin, bicuculline, and penecillin, were tested on GABA responses in these neurones (for reviews see e.g. Krnjević, 1974; Kelly & Beart, 1975; Nistri & Constanti, 1979; Farrant & Webster, 1988). The effects of a low concentration of pentobarbitone (10μM) was also tested on GABA responses in these neurones. At low concentrations, depressant barbiturates such as pentobarbitone potentiate the inhibitory effects of GABA in the mammalian central neurvous system (Schmidt, 1963; Nicoll, 1972; Ransom & Barker, 1976; Macdonald & Barker, 1979). However at higher concentrations (above 50μM for pentobarbitone) some barbiturates directly activate chloride channels (e.g. Jackson, Lecar, Mathers & Barker, 1982). The effects of glutamate on GABA responses in these neurones were also investigated since it has been suggested that glutamate enhances GABA responses in mammalian neurones (Stelzer & Wong, 1989a).

Finally, the effects of temperature and pH on the $GABA_A$ single-channel conductance was also investigated (in outside-out patches).

5.3 *Pharmacological properties of the $GABA_A$ receptor-channel*

For this series of experiments, GABA was applied to the cell by ionophoresis, using brief pulses of between 5 and 20ms duration. The cells were continuously perfused at a constant rate, either with control external medium, or with this medium containing the appropriate concentration of antagonist or potentiating ligand.

5.3.1 *Bicuculline*

Bicuculline reversibly inhibited $GABA_A$ responses in rat superior cervical ganglion (SCG) neurones. A typical example of this antagonism is illustrated in Fig. 5.1, for a cell clamped at -80mV. Each downward deflection of the continuous whole-cell current trace shown in Fig. 5.1A is an inward current response to a 5ms pulse of GABA (applied every 0.7s). It is clear that perfusion of the cell with 2μM bicuculline greatly reduced the GABA responses. The peak response during steady-state inhibition was approximately 11% of the control amplitude. It is also clear from Fig. 5.1A that the inhibition by bicuculline was rapidly reversible. Three of the responses depicted in Fig. 5.1A are shown on an expanded time scale in Fig. 5.1B, to show the time course of these responses in more detail. These responses were recorded before, during, and after the application of 2μM bicuculline. Although there is no obvious difference in the time course of the responses in the presence of bicuculline, compared to the control, this was not investigated further.

5.3.2 *Penicillin*

Penicillin (1mM or 100μM) reversibly inhibited both inward and outward $GABA_A$ currents in rat SCG neurones. Examples of this are shown in Fig. 5.2. The continuous whole-cell current illustrated in Fig. 5.2A is from a cell held at -80mV, which was exposed to 1mM penicillin (during the period indicated). Inward current responses were evoked by 8ms ionophoretic pulses of GABA (applied every 1.2s) and appear as downward deflections of the current trace. It is clear from Fig. 5.2A that this dose of penicillin caused a large but reversible inhibition of the GABA responses. The peak response was reduced to 16% of the control amplitude by 1mM penicillin. It is apparent from Fig. 5.2B, which shows a continuous current trace from the same cell clamped at +50mV, that outward currents (which appear as upward deflections of the current trace) were also blocked by 1mM penicillin. It can be seen that

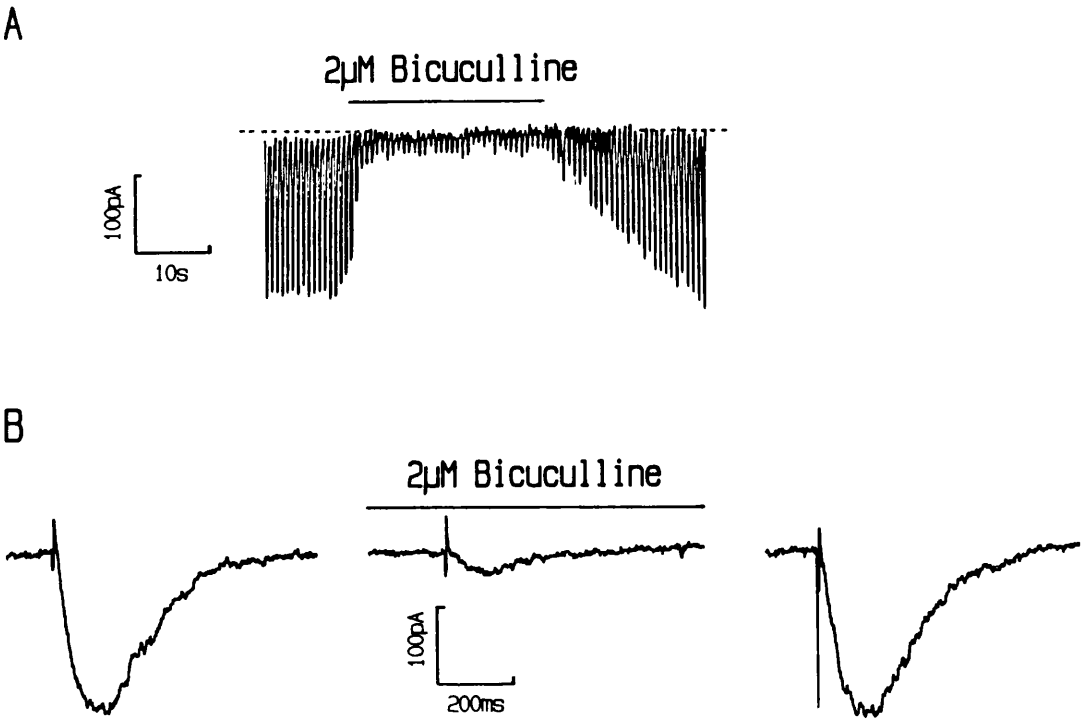

Fig. 5.1. A, continuous whole-cell current record showing inhibition of GABA currents by 2μM bicuculline. The baseline is indicated by the dashed line and each downward deflection is an inward current in response to an ionophoretic pulse of GABA (5ms pulses given once every 720ms, cell held at -80mV). 2μM bicuculline was bath applied during the period indicated by the horizontal bar. Calibration 100pA and 10s. B, three current responses from the trace in A on an expanded time scale to show the time course of the responses. The second response was recorded in the presence of 2μM bicuculline, while the first and third responses were recorded before and after bicuculline application, respectively. Calibrations 100pA and 200ms. Note that the artefact at the start of each response is due to the ionophoretic ejection current.

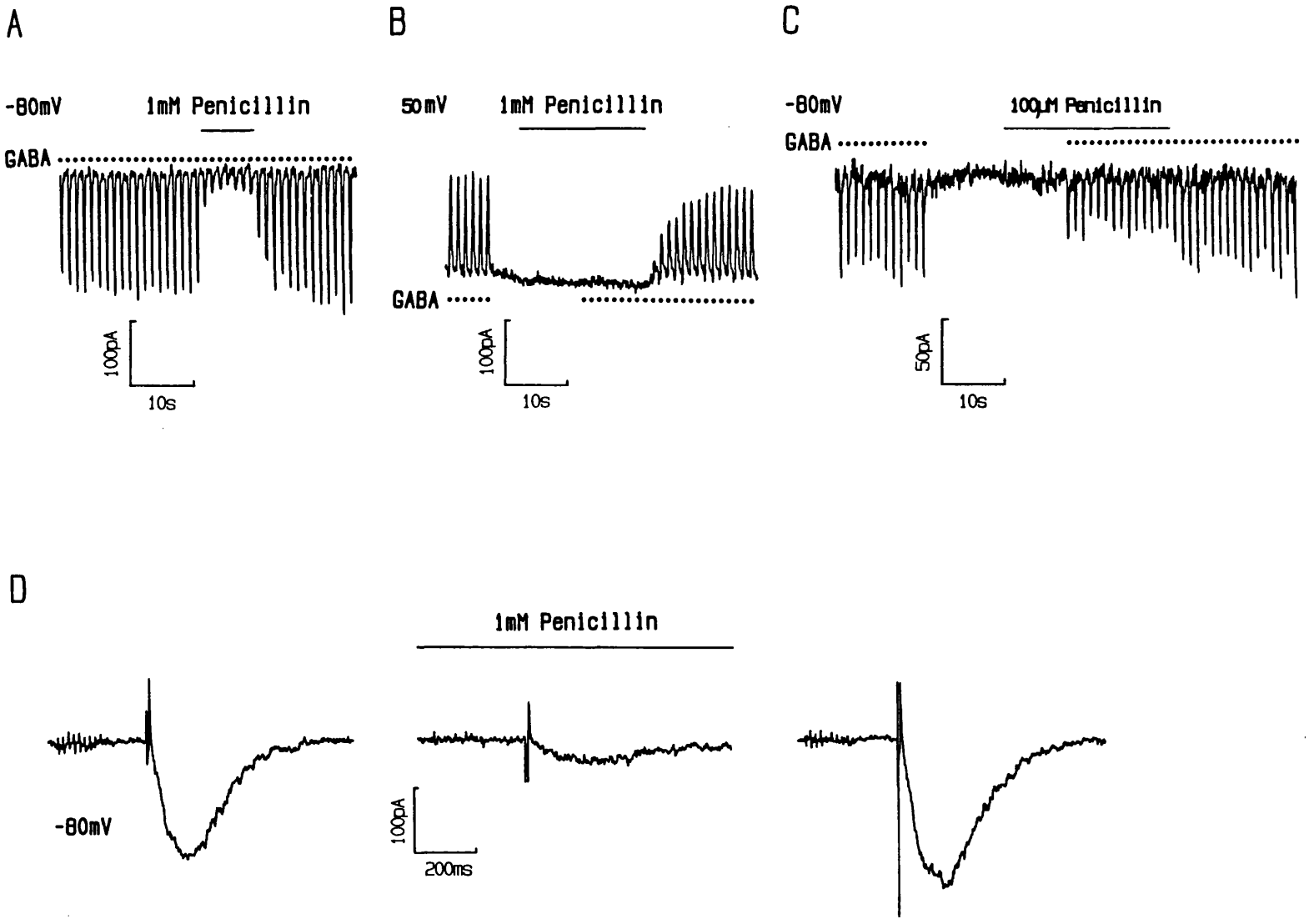
A
-80mV
1mM Penicillin
GABA
100pA
10s
B
50mV
1mM Penicillin
GABA
100pA
10s
C
-80mV
100μM Penicillin
GABA
50pA
10s
D
1mM Penicillin
-80mV
100pA
200ms

Fig. 5.2. A, continuous whole-cell current record showing inhibition of inward GABA responses by 1mM penicillin in a cell held at -80mV. Each downward deflection is an inward current response to an 8ms duration pulse of GABA. Pulses were applied to the cell every 1.2s (indicated by the dot above each response), and 1mM penicillin was bath applied during the period indicated by the horizontal bar. Calibrations 100pA and 10s. B, continuous whole-cell record showing the inhibition of outward GABA currents by 1mM penicillin, with the cell held at +50mV. 8ms pulses of GABA were applied every 1.2s, except for 5s before, and 10s during the initial application of 1mM penicillin. Penicillin was bath applied during the period indicated by the horizontal bar. Calibrations 100pA and 10s. C, continuous whole-cell current record showing inhibition of inward GABA currents by 100μM penicillin (cell clamped at -80mV, same cell as A). Pulses of GABA were applied every 1.2s except for 12s before and 11s during the initial bath application of 100μM penicillin. Note that the first GABA response in the presence of 100μM penicillin was maximally inhibited. Calibration 50pA and 10s. D, three responses from A, on an expanded time scale to show the time course in more detail, recorded (from left to right) before, during, and after the application of 1mM penicillin. Calibration 100pA and 200ms.

during bath application of 1mM penicillin, GABA did not elicit any detectible response, and the responses recovered to control amplitude following washout of the antagonist. For this particular cell penicillin appears to be a more potent inhibitor of outward rather than inward current responses, but this was not investigated further. Fig. 5.2C shows another current trace from the same cell, held at -80mV. Note that the control responses are smaller than those in Fig. 5.2A & B since the ionophoretic pipette was moved between these experiments. For the experiment illustrated in Fig. 5.2C the 8ms pulses of GABA were applied every 1.2s except for 12s before, and for the first 11s of the bath application of 100μM penicillin. It is clear from Fig. 5.2C that the first response to GABA elicited in the presence of 100μM penicillin was maximally inhibited, since the subsequent responses were of the same peak amplitude. This suggests that the action of penicillin is not use-dependent. Three responses from Fig. 5.2A are shown in Fig. 5.2D on an expanded time scale to illustrate the effect of penicillin on the time course and amplitude of the GABA currents. Note that the artefact at the start of each response is due to the ionophoretic ejection current.

5.3.3 *Picrotoxinin*

$GABA_A$ receptor-channels in rat SCG neurones were also inhibited by picrotoxinin. Fig. 5.3 shows the typical effect of bath application of 10μM picrotoxinin on GABA responses, evoked in a cell clamped at -80mV. 5ms duration pulses of GABA were applied every 1.2s. It is clear from the continuous current record shown in Fig. 5.3A that 10μM picrotoxinin produced a large and reversible inhibition of the $GABA_A$ responses, the peak amplitude during steady-state inhibition in this experiment was approximately 15% of the control amplitude. Fig. 5.3B shows three of these responses on an expanded time scale. These responses were recorded (from left to right) before, during and after, the bath application of 10μM picrotoxinin.

5.3.4 *Pentobarbitone*

A typical example of the effect of pentobarbitone on $GABA_A$ current responses in rat SCG neurones is illustrated in Fig. 5.4. Two whole-cell current traces recorded from the same cell (clamped at -80mV) are shown in Fig. 5.4A, the upper trace recorded in control medium, and the lower trace recorded in the presence of 10μM pentobarbitone. The inward current responses (downward deflections of the traces) were

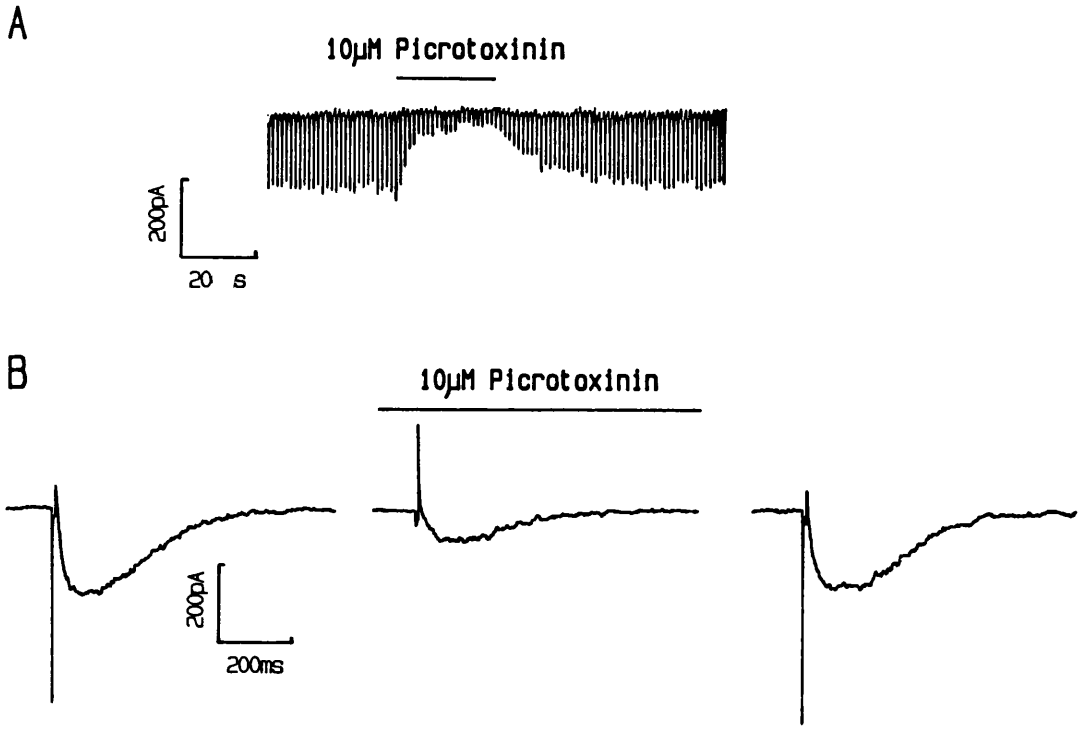

Fig. 5.3. A, continuous whole-cell current trace showing the inhibition of inward GABA currents by picrotoxinin. 5ms duration pulses of GABA were applied every 1.2s throughout the entire record, and 10μM picrotoxinin was bath applied during the period indicated by the horizontal bar. Each downward deflection of the trace is an inward current response (cell at -80mV). Calibrations 200pA and 20s. B, three responses (from A) on an expanded time scale, recorded (from left to right) before, during, and after the bath application of 10μM picrotoxinin. Calibration 200pA and 200ms.

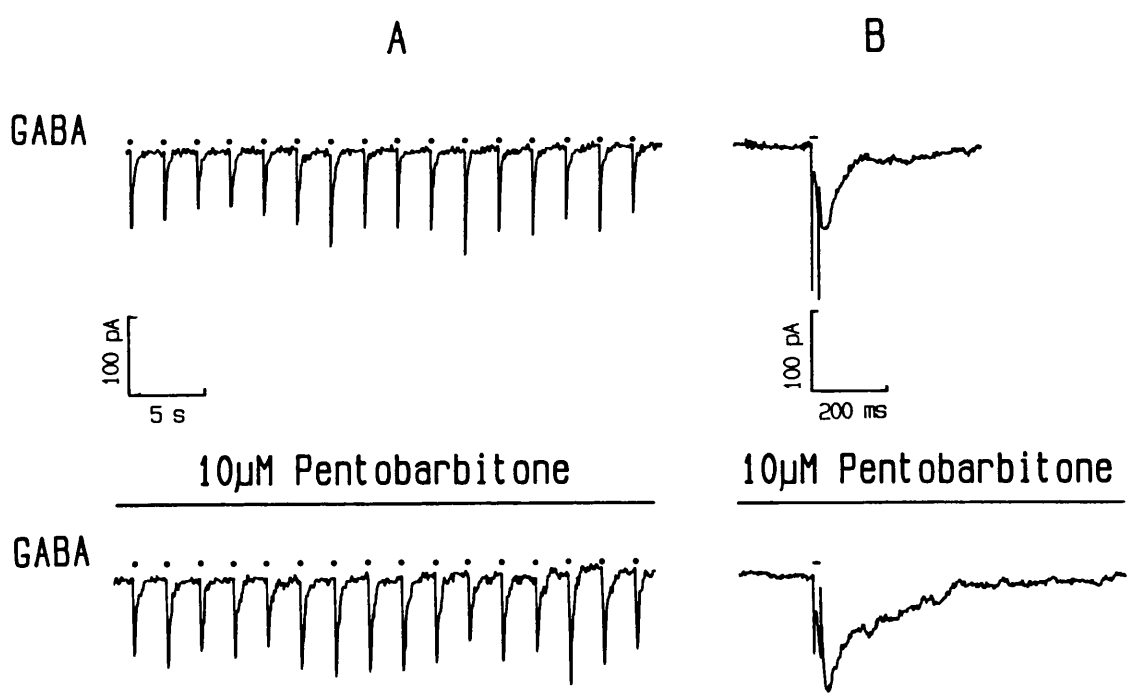

Fig. 5.4. A, two current records illustrating the effect of 10μM pentobarbitone on $GABA_A$ currents. The upper trace shows a continuous current record from a cell held at -80mV which was continuously perfused with control bathing medium. The lower trace was recorded under identical conditions except for the additional presence of 10μM pentobarbitone in the bathing medium. Each downward deflection is an inward current response to a 20ms ionophoretic pulse of GABA (indicated by dots). Calibrations (refer to both traces) 100pA, 5s. Note the variab le amplitude of the responses due to variability in the current passing properties of the ionophoretic pipette. B, single responses (from A) in the absence (upper trace) and presence (lower trace) of 10μM pentobarbitone, on an expanded time scale. The short bar above each trace indicates when GABA was applied. Calibrations refer to both traces; 100pA, 200ms.

evoked every 2.2s by 20ms duration ionophoretic pulses of GABA. In this example the peak amplitudes of the responses were not constant, due to variability in the current passing properties of the ionophoretic pipette. Even so, it is apparent from Fig. 5.4 that overall 10μM pentobarbitone produced a slight increase in the peak amplitude of the GABA responses. More obviously, pentobarbitone prolonged the responses, as illustrated more clearly in Fig. 5.4B which shows, on an expanded time scale, a response recorded in the absence (upper trace) and presence (lower trace) of 10μM pentobarbitone.

5.3.5 *Glutamate*

It has previously been reported that glutamate, at concentrations as low as 1μM, potentiates $GABA_A$ responses in adult guinea-pig hippocampal neurones (Stelzer & Wong, 1989a). In contrast to this however, 10μM glutamate did not have any detectible effect on $GABA_A$ current responses in rat SCG neurones. This lack of effect of 10μM glutamate on both inward and outward GABA currents is illustrated in Fig. 5.5, which shows whole-cell currents evoked by bath applied GABA to one cell clamped at -80mV or +60mV. It is apparent from Fig. 5.5A (cell at -80mV) that the inward current evoked by 10μM GABA in the simultaneous presence of 10μM glutamate (both drugs were applied in the bathing medium) was of the same amplitude as the responses recorded in the absence of glutamate. It is clear from Fig. 5.5B that at a holding potential of +60mV, 10μM glutamate did not evoke any detectible current response in these cells. Furthermore Fig. 5.5B illustrates that this concentration of glutamate had no effect on the amplitude of outward GABA responses, evoked by a submaximal concentration of GABA (10μM).

5.4 *Physical properties of the $GABA_A$ receptor-channel*

5.4.1 *Whole-cell current-voltage relationship*

Figure 5.6A. illustrates a typical whole-cell current-voltage relationship measured from a single rat SCG neurone which was clamped at potentials between +60 and -120mV. The responses were elicited by 8ms duration ionophoretic pulses of GABA applied every 2s from an ionophoretic electrode containing 0.1M GABA at pH 4.0 (constant ejection current used throughout). The cell was continuously perfused with external solution to prevent accumulation of GABA. Each point on the graph in Fig. 5.6A is the mean peak amplitude of between 1 and 9 responses (with ± S.E.M. where this was greater than the size of the

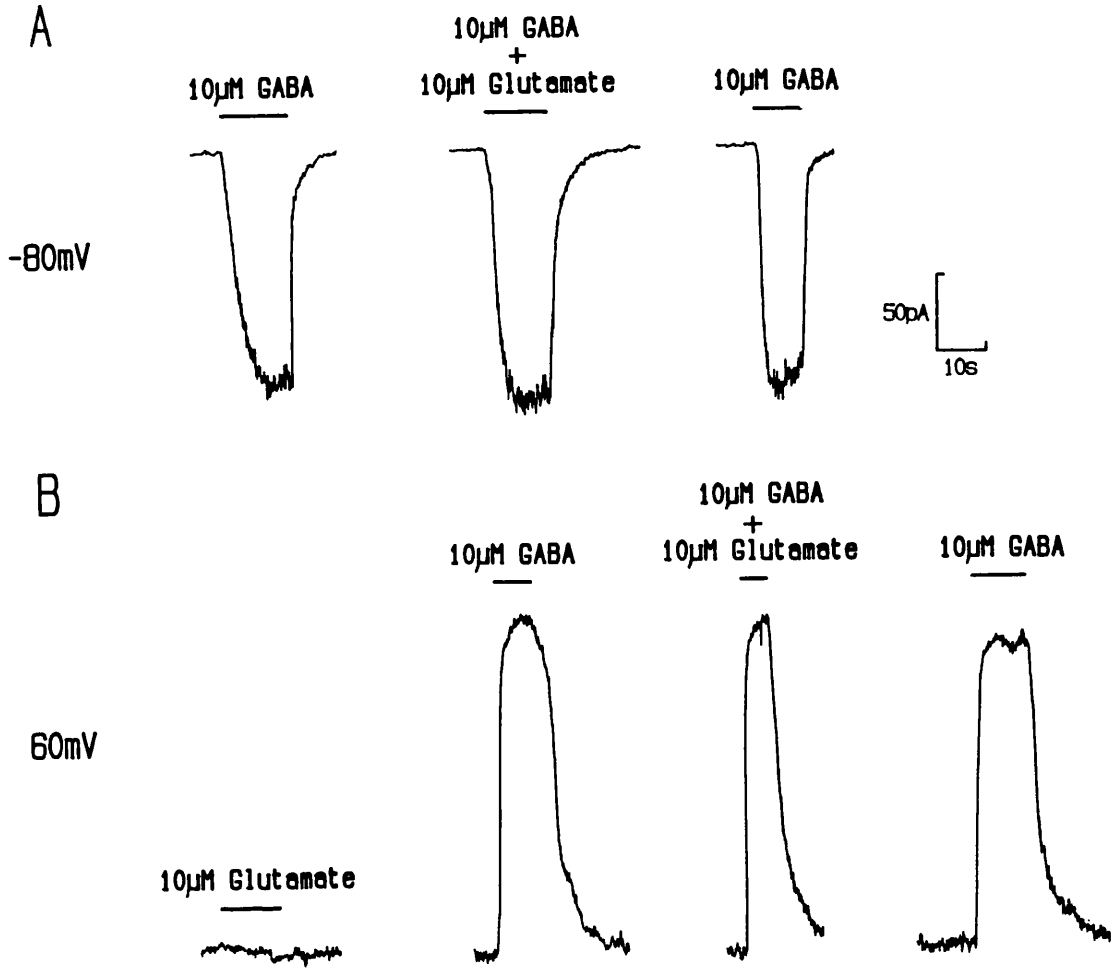

Fig. 5.5. Whole-cell current responses illustrating the lack of effect of glutamate on inward and outward GABA currents in rat SCG neurones. A, three inward current responses evoked by bath application of 10μM GABA, applied for between 9.2 and 13.5s (as indicated by the horizontal bars); cell at -80mV. The GABA responses were recorded, from left to right, before, during, and after the simultaneous bath application of 10μM glutamate. Calibrations (also apply to B) 10s, 50pA. B, consecutive whole-cell current responses evoked by bath application of 10μM glutamate, 10μM GABA, 10μM GABA plus 10μM glutamate, and then 10μM GABA (bath applied for the periods indicated by the horizontal bars); cell at +60mV.

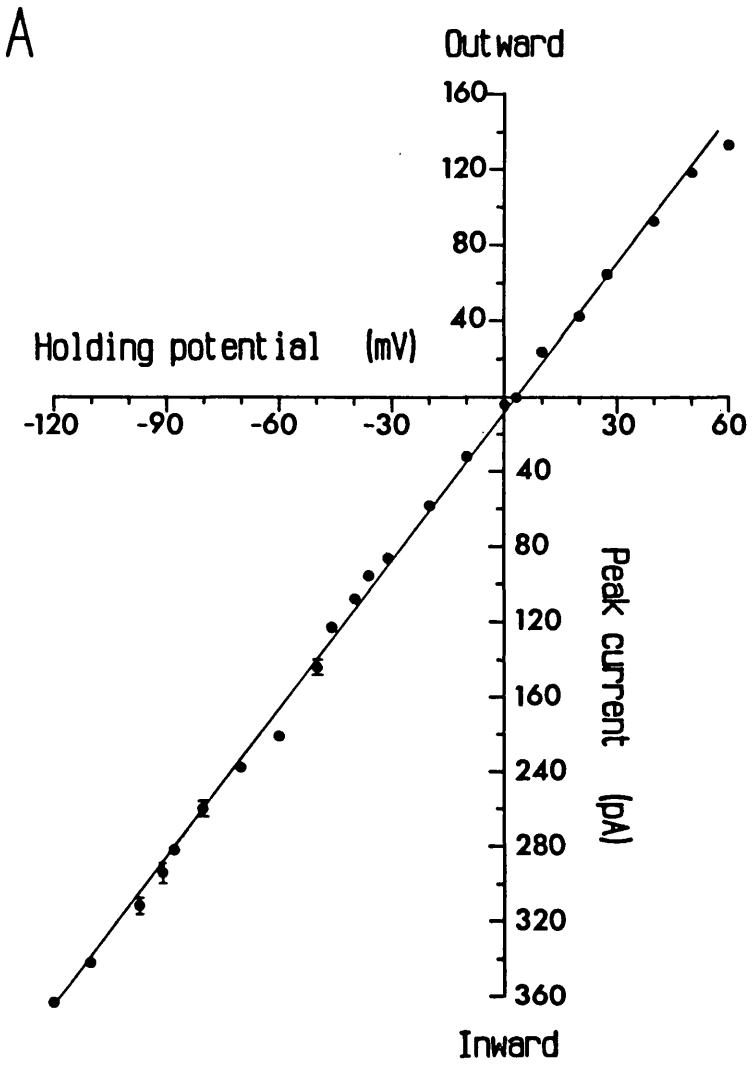
A
Outward
160
120
80
40
Holding potential (mV)
-120
-90
-60
-30
30
60
40
80
120
160
240
280
320
360
Peak current (pA)
Inward

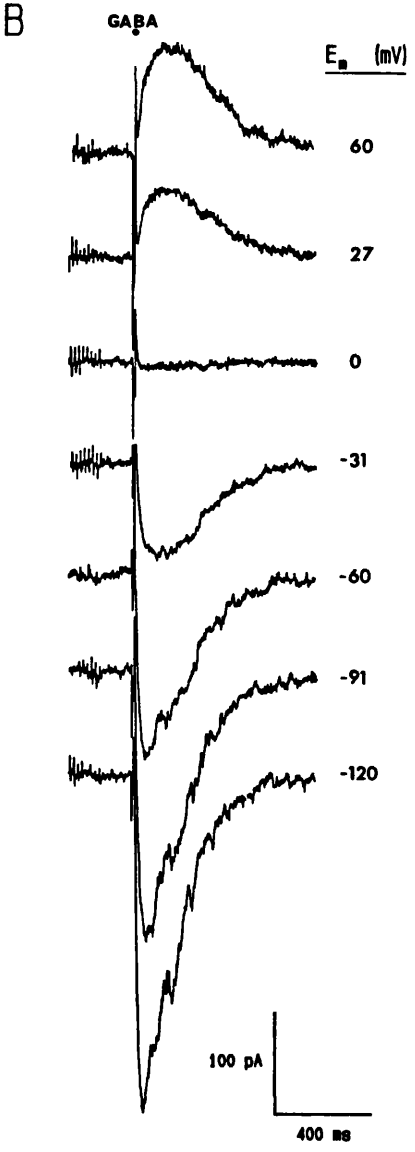
B
GABA
E_m (mV)
60
27
0
-31
-60
-91
-120
100 pA
400 ms

Fig. 5.6 A, whole-cell current-voltage relationship for a single cell. Each point is the mean peak amplitude of between 1 and 9 responses (± S.E.M., where this was greater than the size of the symbol). Each response was elicited by an 8ms duration ionophoretic pulse of GABA, applied every 2s with a constant ejection current. Note that the current-voltage relationship is approximately linear over the voltage range studied (+60mV to -120mV; line drawn by eye), and that the current reverses at +3mV. B, representative whole-cell currents evoked at various holding potentials (indicated to the right of each trace). The artefact at the start of each trace is due to the ionophoretic ejection current. Calibrations 50pA, 200ms (refer to all traces), and inward currents are downwards. T=21-23°C.

symbol). For this particular cell, the whole-cell current-voltage relationship was practically linear over the voltage range +60mV to -120mV. In all cells examined (8 cells) the whole-cell current-voltage relationship was linear or showed slight outward rectification. Fig. 5.6B. depicts example responses from this cell at potentials between +60mV and -120mV. As expected, with approximately symmetrical chloride concentrations, the responses were inward at hyperpolarized potentials and reversed close to zero mV. The reversal potential, estimated from whole-cell current-voltage relationships, ranged from 0mV to +3mV. The theoretical value, estimated from the chloride concentrations, rather than the chloride activities is, -2.8mV. Since the time to peak of the responses was relatively slow (approximately 100ms at -60mV in this example), and the rate of removal of GABA from the vicinity of the receptors was unknown, the rate of decay of the responses is expected to greatly exceed the burst length of the channel.

5.4.2 *Effect of temperature on single-channel conductance*

The effect of temperature on $GABA_A$ receptor-channels in rat SCG neurones was investigated using outside-out patches. A flow heater and a flow cooler (Grant Instruments, Cambridge) were used to change the temperature of the extracellular bathing medium from room temperature to as low as 4.5°C and to as high as 33°C. The fluid circulating the cooler and heater contained 20% antifreeze. This fluid was continuously circulated through a metal jacket surrounding the recording chamber (35mm diameter plastic dish) except for a 10mm diameter circular hole beneath the bath which was necessary for the microscope light. The cooled/heated fluid was also continuously circulated through a glass jacket. Within this jacket were several loops through which the extracellular medium passed just prior to entry into the recording bath. To help maintain a steady temperature in the vicinity of the patch, the perfusion outlet was only a few mm from the patch at one end, and near to the exit of the heated/cooled jacket at the other end. Furthermore, a small volume was maintained in the bath, and the bath was continuously perfused. The temperature in the bath was monitored with a thermister placed in the bathing medium a few mm from the patch. Rapid changes in temperature were not possible with this set-up, and therefore each patch was only exposed to one or two different temperatures. In all experiments investigating the effects of temperature, the pH of both the extracellular and intracellular solutions were maintained at pH 7.2.

The effect of temperature on the amplitude of the main

conductance state of $GABA_A$ receptor-channels in rat sympathetic neurones is illustrated in Fig. 5.7. Only this conductance level was considered because the other levels were less frequent and in some cases less discrete.The data displayed in the plot of cord conductance *vs* temperature (in °Celcius) in Fig. 5.7A. was pooled from 59 outside-out patches, which were clamped between -70mV and -200mV. The amplitude of the most frequently occurring conductance level in the single-channel currents recorded from each patch, was estimated from the corresponding open point amplitude histogram. Such histograms were obtained from the amplitudes of individual data points during periods when the channel was open, with subtraction of the mean shut-channel level. The conductance was calculated assuming a linear current-voltage relationship over the voltage range 0mV to -200mV, and taking the GABA reversal potential (E_{GABA}) as 0mV, since E_{GABA} estimated from whole-cell and single-channel current-voltage relationships was between 0mV and +3mV. It is clear from Fig. 5.7A that increasing the temperature increased the amplitude of the most frequently occurring conductance level. A Q_{10} was estimated from a linear regression fit to an Arrhenius plot of the data shown in Fig. 5.7A (*i.e.* a plot of ln conductance *vs* T^{-1}, in °Kelvin; not shown); the Q_{10} was approximately 1.3 (coefficient of regression, 0.9935).

For some patches, single-channel currents were recorded at several holding potentials, so that a comparison could be made between the estimated slope conductance and cord conductance. For example, although only 3 patches were maintained at approximately 7°C, a total of 18 estimates of cord conductance were obtained since single-channel currents were recorded from each patch at several different holding potentials. Fig. 5.7B shows two single-channel current-voltage plots obtained from two outside-out patches, one maintained at 7.5°C, the other at room temperature (22-23°C), and which were both clamped at potentials between -80mV and -190mV. The slope conductances were obtained from linear regression of the points between -80mV and -150mV, and also assuming the current reversed at 0mV. Note that there appears to be slight outward rectification at potentials more hyperpolarized than -150mV. The estimated slope conductances were 17.4pS at 7.5°C (regression coefficient, 0.9981), and 29.6pS at 22-23°C (regression coefficient, 0.9997), which closely agree with the cord conductances estimated at these temperatures. Fig. 5.7C shows example records of single-channel currents recorded at 7.5°C (upper trace) and 22-23°C (lower trace) from the two patches shown in Fig. 5.7B, clamped at

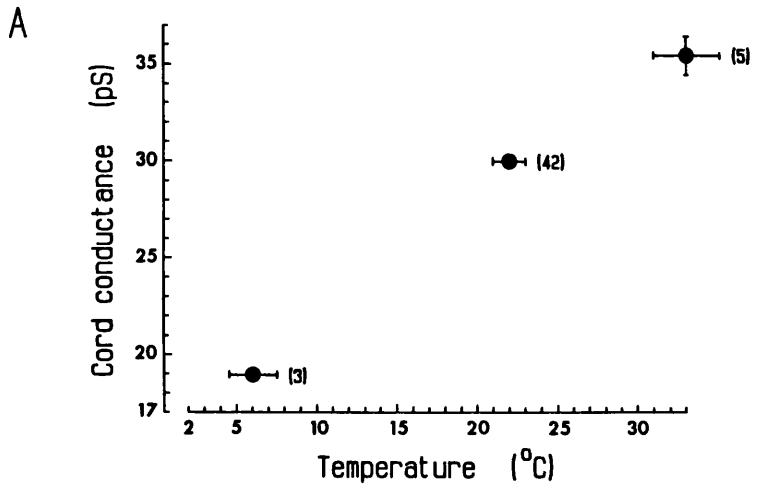
A
Cord conductance (pS)
35
30
25
20
17
(5)
(42)
(3)
2
5
10
15
20
25
30
Temperature (°C)

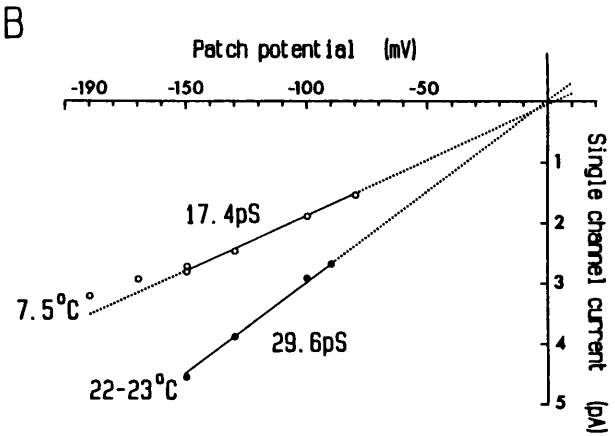
B
Patch potential (mV)
-190
-150
-100
-50
17.4pS
7.5°C
29.6pS
22-23°C
Single channel current (pA)
1
2
3
4
5

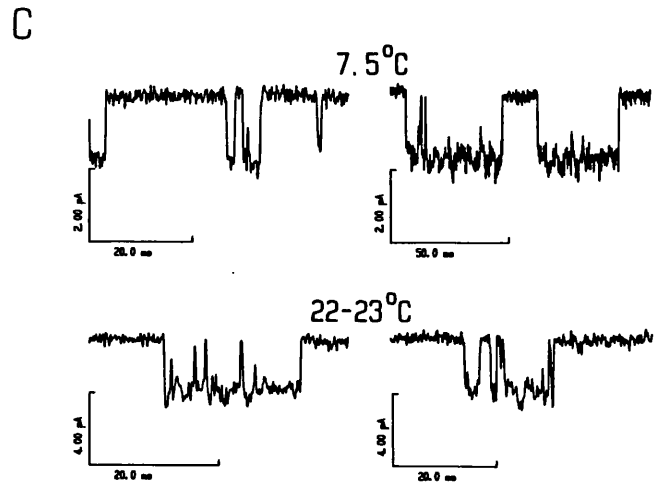
C
7.5°C
22-23°C

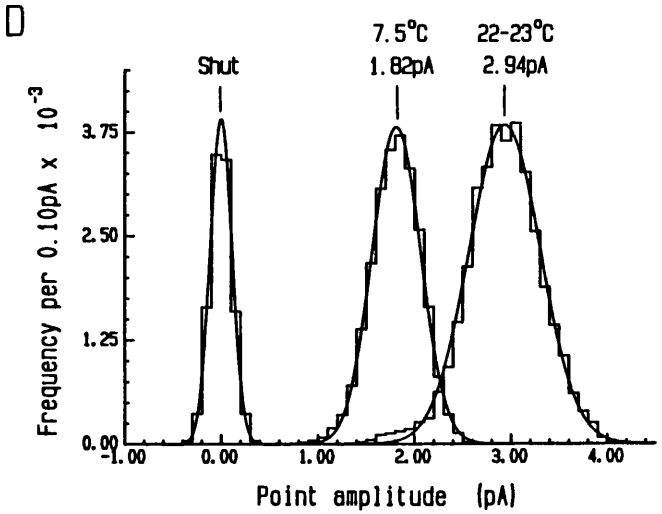
D
Shut
7.5°C
1.82pA
22-23°C
2.94pA
Frequency per 0.10pA x 10^-3
3.75
2.50
1.25
0.00
-1.00
0.00
1.00
2.00
3.00
4.00
Point amplitude (pA)

Fig. 5.7. Effect of temperature on the single channel conductance of $GABA_A$ receptor-channels. A, plot of the chord conductance *vs* temperature, assuming a linear current-voltage relationship, and current reversal at zero mV. Results were pooled from 59 outside-out patches, the number of patches averaged for each point is given in parentheses. For each patch the amplitude of the most frequently occuring conductance level was estimated from the corresponding open point amplitude histograms. Outside-out patches were clamped at -70 to -200mV. The vertical bars through each point are ±S.E.M. (where this is larger than the size of the symbol), while the horizontal bars give the temperature range. B, $GABA_A$ single channel current-voltage relationships measured at 7.5°C (o) and 22-23°C (•). The data was obtained from two different outside-out patches, and the amplitudes were estimated from the point amplitude histograms obtained at each potential. Slope conductances were obtained from linear regression of the points between 0mV and -150mV, assuming the currents reversed at 0mV. Slope conductances were 17.4pS at 7.5°C, and 29.6pS at 22-23°C. C, single channel current records from the two outside-out patches (in B) at 7.5°C (upper trace) and 22-23°C (lower trace); both at -100mV. D, typical point amplitude histograms for some of the data illustrated in A,B,C. Each histogram was fitted with a single Gaussian. At 7.5°C, -100mV, the mean amplitude was 1.82pA (equivalent to 18.2pS), while at 22-23°C, -100mV, the mean amplitude was 2.94pA (29.4pS). The frequency scale refers to the 1.82pA histogram; the maximum frequency of the 2.94pA histogram was 500 per 0.1pA.

-100mV. It is clear from Fig. 5.7C (note the different amplitude scales on each trace) and Fig. 5.7B, that the amplitude of the currents at 7.5°C were approximately 60% of the amplitude at 22-23°C. Example open point amplitude histograms for the most frequently occurring conductance level recorded at 7.5°C and at 22-23°C (and at -100mV),together with a shut point amplitude histogram, are shown in Fig. 5.7D (data from the same two outside-out patches used for Fig. 5.7B,C). The two open point amplitude histograms and the shut point histogram were individually fitted with single Gaussians (continuous curves on each histogram), with means at 0pA for the shut point histogram, at 1.82pA for the 7.5°C open point amplitude histogram, and at 2.94pA for the 22-23°C open point amplitude histogram. These are equivalent to chord conductances of 18.2pS and 29.4pS at 7.5°C and 22-23°C respectively. Note that the spread of the open point amplitude histograms are greater than that of the shut point amplitude histogram, probably as a result of open channel noise, and possibly from inclusion of conductance levels other than the most frequently occurring conductance level, in the open point amplitude histograms (see Chapter 4). Furthermore, the spread of the shut point amplitude histogram at 22-23°C was greater than the shut point amplitude histogram obtained at 7.5°C (which is the one illustrated in Fig. 5.7D).

In conclusion, the effect of increasing the temperature is to increase the conductance of the most frequently occurring conductance level of $GABA_A$ receptor-channels in rat sympathetic neurones. However it should be noted that other possible effects of changing the temperature (such as a change in the receptor-channel kinetics) were not investigated.

5.4.3 *Effect of pH on single channel conductance*

The pH of the extracellular medium, which was used to perfuse outside-out patches, was buffered at values between 5.3 and 10.8. HEPES buffer (10mM) was uesd for pH 7.0 and above, and MES buffer (10mM) was used for pH 6.0 and below. The pH of the extracellular solution was titrated by the addition of hydrochloric acid or sodium hydroxide. The pH of the intracellular medium was maintained at pH 7.2, and experiments were conducted at room temperature (22-23°C).

The effect of pH on the amplitude of the most frequently occurring conductance level of $GABA_A$ receptor-channels in rat SCG neurones is illustrated in Fig. 5.8. The cord conductance *vs* pH plot illustrated in Fig. 5.8A. contains data from 53 outside-out patches, which

were perfused with extracellular medium buffered at pHs between 5.3 and 10.8 (intracellular pH maintained at pH 7.2; temperature 22-23°C; holding potentials between -60mV and -90mV). The cord conductance of the single-channel currents recorded from each patch, were estimated from the corresponding open point amplitude histograms, assuming a linear current-voltage relationship and current reversal at 0mV. It is clear from Fig. 5.8A that the amplitude of the most frequently occurring conductance level was reduced when the pH was made more alkaline; the amplitude was reduced from approximately 40pS at pH 5.3 to about 25.5pS at pH 8.3. This point is also clear from Fig. 5.8B, which shows currents recorded from three outside-out patches (all clamped at -70mV) which were perfused with extracellular medium buffered at pH 5.3 (upper trace) pH 8.2 (middle trace) and pH 10.8 (lower trace). It appears from Fig.5.8A & B that there is a gradual decline in the amplitude of the most frequently occurring conductance level, with increasing pH. However, the possibility that there is a shift in the relative frequency of occurrence of the various conductance levels, with pH, cannot be excluded.

Examples of open and shut point amplitude histograms (obtained from two of the outside-out patches used for Fig. 5.8A, and clamped at -60mV) are illustrated in Fig. 5.8C. Each of the shut and open point amplitude histograms were fitted separately with single Gaussians. The mean of the Gaussian fitted to the pH 8.2 histogram was 1.43pA (corresponding to 23.8pS), while the mean of the pH 6.2 Gaussian was 2.04pA (equivalent to 34pS).

In conclusion, increasing the pH, reduces the amplitude of the most frequently occurring conductance level of $GABA_A$ receptor-channels in rat SCG neurones. However, possible additional effects of pH, say on the kinetics of $GABA_A$ receptor-channels, were not investigated.

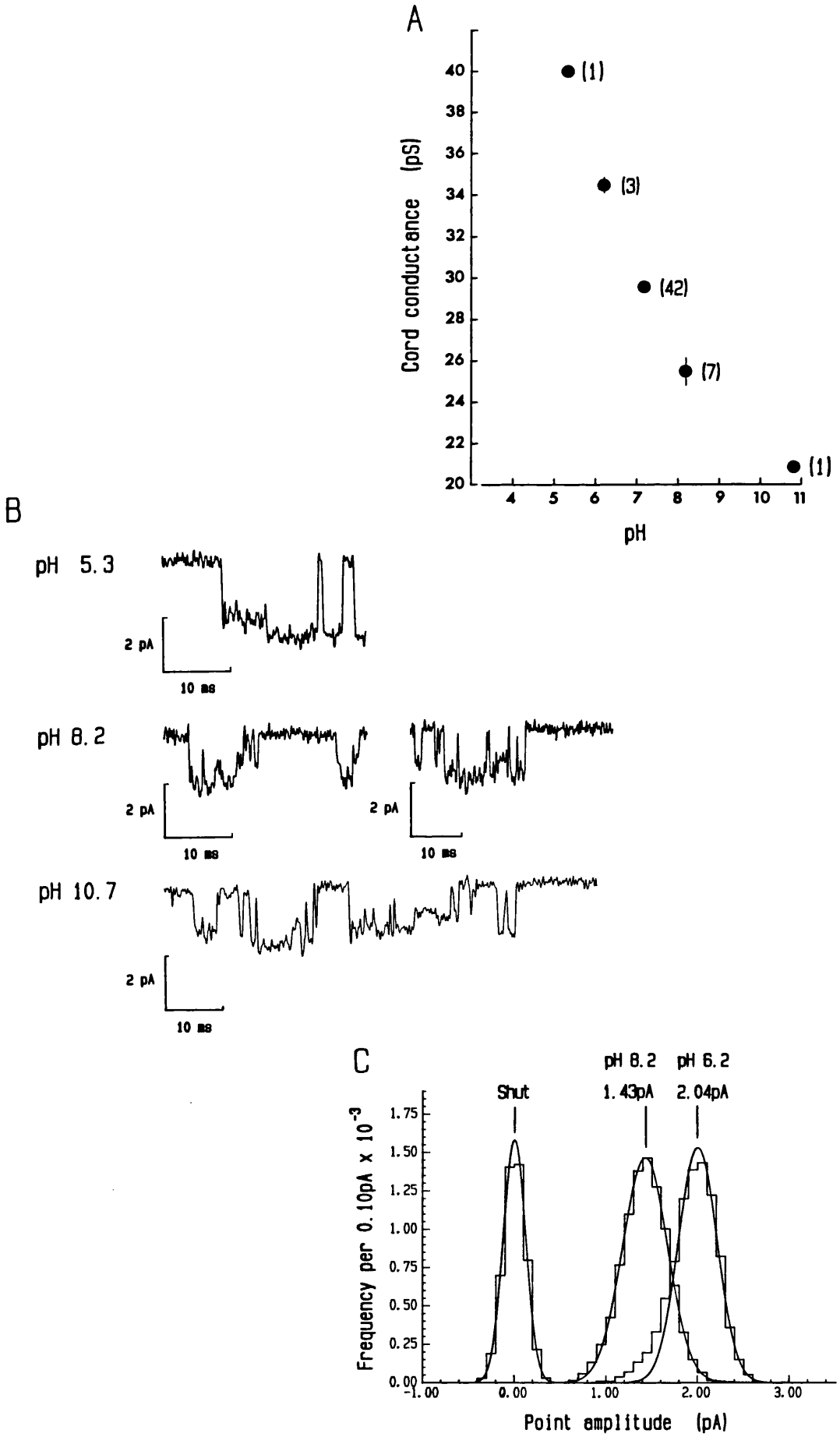
A
Cord conductance (pS)
40
38
36
34
32
30
28
26
24
22
20
(1)
(3)
(42)
(7)
(1)
4
5
6
7
8
9
10
11
pH
B
pH 5.3
2 pA
10 ms
pH 8.2
2 pA
10 ms
2 pA
10 ms
pH 10.7
2 pA
10 ms
C
Shut
pH 8.2
1.43pA
pH 6.2
2.04pA
Frequency per 0.10pA x 10^-3
1.75
1.50
1.25
1.00
0.75
0.50
0.25
0.00
-1.00
0.00
1.00
2.00
3.00
Point amplitude (pA)

Fig. 5.8. Effect of pH on the conductance of $GABA_A$ receptor-channels. A, plot of cord conductance (assuming linear current-voltage relationship and current reversal at 0mV) *vs* pH. Results were pooled from 54 outside-out patches, the number of patches averaged for each point is given in parentheses. The vertical bars represent ±S.E.M. (where larger than the symbol size). The holding potentials used were -60mV to -90mV, T=21-23°C. B, single channel currents recorded at pH 5.3, 8.2, and 10.8, as indicated (all currents were at -70mV, T=21-23°C). Calibrations are all 2pA and 10ms; the amplitude bar refers to all traces. C, point amplitude histograms for two of the outside-out patches included in A (both at -60mV). Each peak of the point amplitude histograms were fit individually with a single Gaussian. Mean amplitudes were 0, 1.43, and 2.04pA for the shut channel, openings at pH 8.2, and openings at pH 6.2 respectively. The shut point amplitude histogram was obtained from the patch at pH 8.2. Note the decrease in conductance with increasing pH value.

5.5 *Pharmacological properties*

The $GABA_A$ receptor-channels in rat superior cervical ganglion (SCG) neurones appear pharmacologically similar to those of mammalian central neurones, judging by the inhibition of GABA responses in SCG neurones by bicuculline, picrotoxin (see section 3), picrotoxinin and penicillin, and by the potentiation of these responses by pentobarbitone. Furthermore, in these neurones, the selective $GABA_A$ agonist, muscimol, was found to activate similar single-channel currents to those activated by GABA (results not shown). However, the lack of effect of 10μM glutamate on the amplitude of GABA currents in SCG neurones contrasts with observations from mammalian central neurones (Stelzer & Wong, 1989a). In acutely dissociated adult hippocampal neurones, glutamate enhances $GABA_A$ currents, at concentrations too low to evoke a detectible current, although these cells do respond to glutamate (Stelzer & Wong, 1989a). The reason for this discrepancy is unclear, although a likely explanation could be that this effect of glutamate requires the presence of glutamate receptors coupled to second messenger systems (reviewed by Berridge, 1987; Smart, 1989) or, less likely, that fast glutamate receptors are necessary for the effect. The glutamate receptors coupled to second messenger systems may be absent from peripheral neurones (which also lack fast glutamate channels). Alternatively, an intracellular factor necessary for the action of glutamate may be absent from our solutions; Stelzer & Wong (1989a) included ATP and leupeptin (a Ca^{2+} - activated neutral protease inhibitor) in the pipette (internal) solution, whereas these agents were not included in our internal solution.

5.6 *Physical properties*

The current-voltage relationship of $GABA_A$ receptor-channels in rat SCG neurones (both whole-cell and single-channel) are consistent with those observed in many types of mammalian neurone (Ashwood *et al.*, 1987; Bormann *et al.*, 1987; Robertson, 1989). The voltage sensitivity of $GABA_A$ receptor-channels in a variety of vertebrates and invertebrates is discussed in Chapter 6, where the effects of voltage on whole-cell and single-channel current-voltage relationships and on GABA noise and on the decay of GABAergic inhibitory post synaptic potentials, are discussed.

As expected, increasing the temperature (between about 5° and 33°C) resulted in an increase in the conductance of $GABA_A$ receptor channels in rat sympathetic neurones. In contrast to the present work,

most published studies have used noise analysis to investigate the effect of temperature on the conductance of agonist gated ion channels, but have yielded similar Q_{10} values. For example, Stettmeier & Finger (1983) reported a Q_{10} of approximately 1.6 for quisqualate activated channels in crayfish muscle, and Anderson *et al*, (1977) reported a Q_{10} of 1.2 (at temperatures above 6.6°C) for locust muscle glutamate receptors. The effect of temperature on single channel conductance has, however, been measured directly for channels activated by acetylcholine at the rat end-plate, where the Q_{10} was 1.3 (Mulrine & Ogden, 1989).

The present work also shows a direct effect of extracellular pH on the conductance of single $GABA_A$ receptor channels in rat sympathetic neurones. In agreement with this work, Gallagher *et al*, (1983) observed that an increase in extracellular pH reduced the amplitude of ionophoretically evoked GABA responses in cat dorsal root ganglion neurones. However, this effect could have resulted from an increase in glial cell GABA uptake (since intact ganglia were used) or from a change in affinity of GABA for the receptor, rather than from a change in single-channel conductance (or single-channel kinetics).

Extracellular pH has the opposite effect on the conductance of nicotinic acetylcholine receptor channels at the frog end-plate, possibly because the acetylcholine channel conducts cations rather than anions. Thus at the frog end-plate, the amplitude of acetylcholine evoked miniature end plate currents (m.e.p.c) or e.p.c, or the conductance estimated from acetylcholine noise, is reduced by a reduction in extracellular pH (Scuka, 1977; Landau *et al.*, 1981).

Changes in extracellular pH could alter the charge on specific groups close to the extracellular mouth of the channel (by protonation or deprotonation), or may change extracellular surface charge screening, both of which may be expected to alter the rate of transfer of ions through the channel. For example Imoto *et al*, (1988) reported that three anionic rings located (1) near the external mouth of the *Torpedo* acetylcholine receptor channel, (2) near the internal mouth, and (3) intermediate between these two, are major determinants of the rate of ion transport through this channel. Imoto *et al*, (1988) demonstrated that reducing the net negative charge on these rings (by point mutations) reduced the single channel conductance. This could explain the observed decrease in conductance of frog acetylcholine channels when the extracellular pH is reduced.

6. OVERALL DISCUSSION

6.1 *General properties of $GABA_A$ receptor channels*

The $GABA_A$ receptor channels present in various cells appear to be diverse, in terms of their kinetics, conductance states, and sensitivity to membrane potential. The apparent mechanism(s) and site(s) of action of antagonists and potentiating ligands also differs between cell type. There are also apparent differences in the relative potencies of various agonists and antagonists between cell types (for reveiw e.g. Nistri & Constanti, 1979). This variability may arise from real differences in the properties of the $GABA_A$ receptor channels in these different preparations. However, some variability may well also result from differences in the experimental conditions and analytical methods, some of which will be considered later.

6.1.1 *Noise analysis*

Noise analysis of agonist evoked currents has been widely used to estimate the kinetics and conductance of the underlying single channels. In the simple case where the channel can adopt only two kinetically distinguishable states the time constant determined from the half-power frequency of the single Lorentzian spectrum will correspond to the effective lifetime of the channel activation, provided that the intervals between channel activations are long, and the channel is open for most of the time during the activation (*i.e.* contains, at most, only brief shut gaps) (Katz & Miledi, 1972; Anderson & Stevens, 1973). It has become clear, however, that for most agonist activated ion channels there is more than one kinetically-distinguishable open state (as judged by their multi-exponential open time distributions), and the openings (at low agonist concentrations) tend to occur in bursts interupted by brief gaps. This type of behaviour is exhibited by muscle nicotinic acetylcholine receptor-channels (Colquhoun & Sakmann, 1981; Dionne & Leibowitz, 1982; Jackson *et. al.* ,1982a; Jakson *et. al.* ,1983; Auerbach & Sachs, 1983; 1984; Sine & Steinbach, 1984a; 1986), locust muscle glutamate receptor channels (Cull-Candy & Parker, 1982), mammalian neuronal glutamate receptor-channels (Cull-Candy, Howe & Ogden, 1988; Howe *et. al.*, 1988) and neuronal $GABA_A$ receptor-channels (Jackson, Lecar, Mathers & Barker, 1982; Sakmann, Hamill & Bormann, 1983a; Bormann & Clapham, 1985; Mathers, 1985; Allan & Albuquerque, 1987; Bormann & Kettenmann, 1988; ffrench-Mullen, Tokutomi & Akaike, 1988; Mathers &

Wang, 1988; Weiss, 1988; MacDonald *et al.*, 1989a; Weiss & Magleby, 1989). The time constants derived from noise analysis in these cases are expected, under the conditions mentioned above, to be good estimates of the mean burst length (Colquhoun & Hawkes, 1977). Indeed this appears to hold true for several types of agonist gated ion channels, including those activated by aspartate, in rat cerebellar granule cells (Cull-Candy, Howe & Ogden, 1988; Howe *et al.*, 1988); the time constants of the two slowest components determined from single-channel burst length distributions for the 50pS openings produced by aspartate (2.25 and 10.3ms) closely agree with the time constants estimated from the two Lorentzian spectra of whole-cell aspartate noise (3.1 and 15ms). Other examples include ion channels activated by glutamate analogues in locust muscle (Cull-Candy & Parker, 1983) and those activated by aspartate in large cerebellar neurones of the rat (Cull-Candy & Usowicz, 1989a, 1989b). Similarly, Cull-Candy *et. al.*,(1988) reported that in bovine chromaffin cells, the single Lorentzian time constant of nicotinic acetylcholine noise corresponded to the longer component of the burst length distribution determined by them in the same preparation. Previous noise analysis (Fenwick *et. al.*, 1982) and recordings of single channel currents in whole-cell voltage clamp (Clapham & Neher, 1984a, 1984b), in the same cell type, suggested slightly longer mean open times/burst lengths.

6.1.2 *Characteristics of $GABA_A$ channels from noise analysis*

Many groups have used noise analysis to make initial estimates of $GABA_A$ channel kinetics in a wide range of preparations. In early experiments most $GABA_A$ noise spectra were described by a single Lorentzian, although there was wide variability in the value of the time constant estimated from the half power frequency. Table 6.1 summarises the time constants estimated from $GABA_A$ spectra which were fitted with single Lorentzians, and also the frequency range which was considered, and the preparation. It is apparent from Table 6.1 that the time constants varied between 3 - 46ms. The finding in the present study that $GABA_A$ current noise in rat sympathetic neurones was described by the sum of two Lorentzians is consistent with more recent experiments in several different preparations and reflects improved frequency resolution. Table 6.2 summarises the results from several groups in which GABA spectra were described by the sum of two Lorentzians. It can be seen from Table 6.2 that the two time constants derived from analysis of GABA noise are fairly consistent for a range of preparations,

TABLE 6.1:
Characteristics of $GABA_A$ receptor channels from noise analysis: single Lorentzian

PREPARATION	TIME CONSTANT (ms)	CONDUCTANCE (pS)	FREQUENCY RANGE (Hz)	TECHNIQUE	REFERENCE
cultured embryonic mouse spinal neurones	20±6.6 (4 cells, 84 estimates)	19	D.C. to 100-150	2-microelectrode voltage-clamp (3M KCl)	McBurney & Barker, 1978
goldfish Mauthner cells (dissociated)	4.5-10.6	—	2-200	voltage noise, intracellular recording	Faber & Korn, 1980, 1982
isolated adult locust muscle	3-4 (at -80mV)	22 (at -80mV)	D.C. to 500	2-microelectrode voltage-clamp	Cull-Candy & Miledi 1981
cultured embryonic mouse spinal neurones	10-43	4.5-24	D.C. to 100-150	2-electrode voltage-clamp	Barker, McBurney & Macdonald, 1982
Xenopus oocytes injected with chick brain mRNA (total)	25	—	D.C. to 500		Miledi, Parker & Sumikawa, 1982
cultured embryonic rat hippocampal neurones	20-46 (V-dependent)	16.7±1.5 (n=15)	0.2-200	2-electrode voltage-clamp	Segal & Barker, 1984
isolated adult locust muscle	4±0.8 (at -80mV)	21.6±0.9 (at -80mV)		2-electrode voltage-clamp	*Cull-Candy, 1986
cultured chick spinal neurones	4.6		5-1250	patch-clamp	*Yang & Zorumski, 1989

*occasionally these noise spectra were best fit by the sum of two Lorentzians.
All experiments were at room temperature (18-26°C). In some cases mean values are given, ± S.D.

including crayfish muscle (Dudel *et. al.*, 1980) mammalian sympathetic neurones and bovine chromaffin cells (Cull-Candy & Mathie, 1986; Cull-Candy, Mathie & Newland, 1987; Cull-Candy, Mathie & Powis, 1988), bovine lactotrophs (Inenagah & Mason, 1987) and mammalian central neurones (Cull-Candy & Ogden, 1985; Cull-Candy & Usowicz, 1989a). The fast time constants are in the range 1-5ms, and the slow time constants in the range 10-53ms. The time constants of GABA noise in rat sympathetic neurones, determined in the present study, fall within these ranges, being 2.3 ± 1.4ms and 43 ± 17ms (mean S.D.; n=7; -60mV). As detailed in Table 6.2, neurones, in addition to those of rat sympathetic ganglia, exhibit a wide range of values for the fast and slow time constants estimated from noise. It seems reasonable that the single Lorentzian time constants from early studies reflect either the dominant component in the noise, or yield a value intermediate between short and long bursts. In this regard Inenagah & Mason (1987) reported that (for anterior pituitary cells) some of the noise spectra were described by the sum of two Lorentzians with time constants of 5 and 35ms, whereas for other spectra, a single Lorentzian with a time constant of 26ms provided an adequate fit. The observed variability in time constants derived from noise may reflect the presence of more than on type of $GABA_A$ receptor-channel, and this possibility is discussed elsewhere (Chapter 4). Furthermore, from analysis of single-channel currents (see below) it is clear that the two components which could be resolved in the spectra were not enough to describe the number of open and closed states observed.

6.1.3 *Characteristics of $GABA_A$ channels from the decay of inhibitory post synaptic currents, i.p.s.c.s*

For several agonist-activated channels, the decay of excitatory or inhibitory post synaptic currents (e.p.s.c. or i.p.s.c. respectively) are described by a single exponential whose time constant reflects the mean open time or the burst length of the underlying single channels. A good example of this is provided by the muscle nicotinic acetylcholine receptor.

The decay of GABAergic i.p.s.c.s in a range of preparations have been fitted with single exponentials, or with the sum of two exponentials (see Table 6.3 for references). Table 6.3 lists the time constants of single- and bi-exponential decays of GABAergic i.p.s.c.s for a number of cell types. As with the time constants derived from noise analysis, there are a wide range of values of the decay time constants for GABAergic

TABLE 6.2.
Characteristics of $GABA_A$ channels from noise analysis: two Lorentzian

PREPARATION	TIME CONSTANTS (ms) τ_1(fast)	τ_2(slow)	CONDUCTANCE (pS)	FREQUENCY RANGE (Hz)	TECHNIQUE	REFERENCE
dissociated crayfish muscle	5 (-100mV)	33 (-60mV)	9	1-200	2-microelectrode voltage-clamp	Dudel, Finger & Stetmeier, 1980
cultured rat cerebellar granule neurones	1.1-1.8 (at -30 to -90mV)	40-79	16	0.1-500	whole-cell patch-clamp	Cull-Candy & Ogden, 1985
dissociated rat sympathetic neurones	0.6-0.8	16-53		0.1-2000	whole-cell patch-clamp	Cull-Candy & Mathie 1986
isolated bovine lactotrophs	5	35		D.C.-800	whole-cell patch-clamp	Inenagah & Mason, 1987
dissociated rat sympathetic neurones	2.3±1.4 (n=7, at -60mV)	43±17	11.8±2.4 (n=7,=60mV)	0.1-500	whole-cell patch-clamp	Cull-Candy, Mathie & Newland, 1987
dissociated bovine chromaffin cells	1.73 (at -100mV)	10.9	31.6 (at -100mV)	0.1 to 500-2000	whole-cell patch-clamp	Cull-Candy, Mathie & Powis, 1988
cultured large cerebellar neurones	1.4 (+50mV) 1.9 (-110mV)	40.1 23.6	12±0.8	D.C.-500	whole-cell patch-clamp	Cull-Candy & Usowicz, 1989a

All experiments were at room temperature (18-26°C).
Where appropriate, time constants and conductances are given as mean±S.D., together with the number of estimates, n. In some cases, time constants were measured at specific holding potentials, and these are given in parentheses below the time constants.

TABLE 6.3.

The decay of GABAergic inhibitory post synaptic currents: single- or bi-exponential

PREPARATION		TIME CONSTANTS (ms) τ_1(fast)	τ_2(slow)	TECHNIQUE	REFERENCES
isolated crayfish muscle		15.6-22 (-40 to -100mV)		2-electrode voltage-clamp	Onodera & Takeuchi, 1976
isolated crayfish muscle		5 (at -60mV)	33	2-microelectrode voltage-clamp, voltage jump relaxations	Dudel, Finger & Stetmeier, 1980
isolated goldfish Mauther cell		3.5-11.9 (mean=6.65)		intracellular microelectrodes, potential (i.p.s.p.)	Faber & Korn, 1980
hippocampal slice CA1 region		8.3-16.2 (mean=11)		voltage-clamp, spontaneous i.p.s.c.	Collingridge, Gage & Robertson, 1984
cultured embryonic rat hippocampal neurones		26±4 (at hyperpolarized potentials)		2-microelectrode voltage-clamp	Segal & Barker, 1984
locust neuromuscular junction		7.6±0.7 (-80mV, mean±s.e., n=10)		2-microelectrode voltage-clamp, m.i.j.c & evoked i.j.c.	Cull-Candy, 1984, 1986
cultured chick cerebral neurones	68%	15-60 (at 40 to -80mV)		whole-cell voltage-clamp, spontaneous i.p.s.c.	Weiss, Barnes & Hablitz, 1988
	32%	9.5±5.7 (at -50mV, n=25)	66.6±27.5		
rat hippocampal CA1 pyramidal and granule neurones, thin slice		2 (-50mV)	>30	whole-cell voltage-clamp, m.i.p.s.c.	Konnerth, Edwards & Sakmann, 1989

All at room temperature (21-24°C). Values given as mean ± S.D.

i.p.s.c.s, ranging from 3.5 to 60ms for single exponential fits. It is therefore difficult to assess whether the time constants of the i.p.s.c. decays are identical with the time constants determined from GABA noise. However in cases where time constants for i.p.s.c. decay rate and for GABA current noise have been measured in the same preparation, there is usually reasonable agreement between these two estimates (Dudel *et. al.*, 1980; Faber & Korn, 1980; Cull-Candy, 1986). This suggests that in these preparations at least, the decay rate of GABAergic i.p.s.c.'s is governed by the closure of channels which are activated only once, and not by the removal of GABA from the synapse.

6.1.4 *Characteristics of $GABA_A$ channels from single channel currents: shut times, open times, and burst lengths*

It is only recently that it has become possible to analyse $GABA_A$ single channel currents in detail, as a result of the development of patch-clamp techniques to obtain low noise recordings from cultured (or dissociated) vertebrate neurones, or of *Xenopus* oocytes which have been injected with mRNA for $GABA_A$ receptor-channels. Distributions of open times and of burst lengths, measured directly from single channel current records from various preparations, have been fitted with one, or the sum of several, exponential decays. Table 6.4 lists the time constants of these exponential decays, and indicates the conductance state analysed (when specified), the filter frequency, and the resolution of the analysed data. The original estimates of the open times of $GABA_A$ receptor-channels probably rather reflect the burst length, or the mean open time, for several reasons. Firstly, the data was heavily filtered, and a low resolution was imposed on the data (*i.e.* the dwell times in the open or shut states had to be of a relatively long duration to be included in the analysis). Furthermore, no correction for missed events was made (see Colquhoun & Sigworth, 1983), and the presence of various conductance amplitudes was not considered. As a result, brief open and shut times were missed and estimates of the duration in the various open and shut states were inaccurate. From the most recent studies, which are of better resolution, and consider one conductance level at a time, it appears that $GABA_A$ receptor channels open to at least three open states and three burst states. As given in Table 6.4, the mean lifetimes of these three open states appear to be as follows; (1) less than 1ms, (2) between 2 and 5ms, and (3) around 6 to 12ms, while the apparent burst lengths are approximately 1ms, 6ms, and 30ms (Mathers, 1985; Mathers & Wang, 1988; MacDonald *et al.*, 1989a; Weiss & Magleby,

TABLE 6.4.
Kinetics of $GABA_A$ channels from single-channel currents: distributions of burst lengths (and *open times)

PREPARATION	ANALYSIS	FILTER (Hz); RESOLUTION (ms)	TIME CONSTANTS (ms) τ_1	τ_2	τ_3	t_c (ms)	REFERENCE
cultured mouse spinal neurones	MΩ seal resistance, fitted open times>10ms	60-150Hz	5.4±0.4 (one cell-attached patch)	35±5			Jackson, Lecar, Mathers & Barker, 1982
cultured mouse spinal neurones			*2.4	*29			Sakmann, Hamill & Bormann, 1983
Xenopus oocytes injected with chick brain total mRNA	131 openings measured from oscilloscope	500Hz	16				Miledi, Parker & Sumikawa, 1983
dissociated bovine chromaffin cells	outside-out patches	1000Hz	2.5	20		5	Bormann & Clapham, 1985
cultured mouse spinal neurones	outside-out patches	1000Hz	*4±1.3	*24±8.1			Mathers, 1985
cultured hippocampal neurones	inside-out patch	1000Hz (-3dB)	*0.5 4.3	*2.2		3	Allen & Albuquerque 1987
cultured porcine intermediate lobe		625-4000Hz	*3.86±1.0 (n=6;	*19.6±5.8 -80mV)			Taleb, Trouslard, Demeneix, Feltz, Bossu, Dupont & Feltz, 1987

cultured rat cerebral astrocytes	one inside-out patch		0.5	23		1.6	Bormann & Kettenmann, 1988
isolated frog dorsal root ganglion neurones			*1	*3.4			ffrench-Mullen, Tokutomi & Akaike, 1988
cultured embryonic mouse spinal neurones	outside-out patch, threshold crossing	1000Hz 500μs	*0.48±0.06 (for 1.25μM GABA)	*4.3±0.5			Mathers & Wang, 1988
cultured chick cerebral neurones	inside-out patch	1000Hz 170μs	*0.4±0.1	*2.1±0.9			Weiss, 1988
cultured embryonic mouse spinal neurones	27pS level only, outside-out patch, threshold crossing	1000Hz 260μs	*1±0.2 1±0.2	*3.7±0.4 5.5±0.2	*11.3±0.5 29.8±1.6	5	Macdonald, Rogers, & Twynam, 1989a
cultured chick cerebral neurones	4 outside-out patches, threshold crossing	800-1000Hz 180-225μs	*0.36	*1.83	*5.87		Weiss & Magleby, 1989
cultured embryonic chick neurones	26pS level only,	1500Hz 400-500μs	*0.82±0.18	*7.4±2.0			Yang & Zorumski, 1989

The time constants (τ_1 to τ_3) are for burst lengths, or for * open times.

1989), at least for $GABA_A$ receptor-channels in cultured embryonic chick and vertebrate neurones. Indeed MacDonald *et. al.* (1989a) and Weiss & Magleby (1989) have both proposed models for the behaviour of $GABA_A$ receptor channels in these preparations. In agreement, the present study shows that, for rat sympathetic neurones, the distributions of burst lengths are best described by the sum of at least three exponentials whose time constants are within the ranges given above.

It should be noted that in all of these studies, only currents evoked by low concentrations of GABA were analysed, and no mention was made of any heterogeneity, in terms of open and/or shut times (which would be difficult, if not impossible, to detect in low concentration experiments). This contrasts with the heterogeneity of open and shut times observed in rat superior cervical ganglion neurones in the presence of high concentrations of GABA (section 4). The differences in the open times and burst lengths estimated for $GABA_A$ receptor-channels from different preparations (see Table 6.4), may reflect the existence of different receptor subtypes, although differences in analytical techniques undoubtedly affect these estimates.

6.1.5 *Conductances estimated from GABA noise and single channel currents*

As discussed in chapter 4, $GABA_A$ receptor-channels in several types of mammalian neurones, including rat sympathetic neurones, open to several conductance levels, and the conductance state most frequently occupied is 27-31pS (in approximately 145mM symmetrical chloride solutions). The observation that in rat sympathetic neurones the conductance estimated from noise analysis is far lower than this, being 11.8 ± 2.4pS (mean ± S.D., n=7, -60mV), is consistent with the observation that these channels open to conductance levels lower than the approximately 30pS level for a large proportion of the channel open time. Similarly, the conductance estimated from noise in rat and mouse spinal cord neurones was only 4.5-24pS (McBurney & Barker, 1978; Barker, McBurney & Macdonald, 1982), although the main state conductance level measured directly from single channel currents in these cells was 27-30pS (Hamill, Bormann & Sakmann, 1983; Mathers, 1985; Bormann, Hamill & Sakmann, 1987; Macdonald *et al.*, 1989a). This difference, however, may partly be explained by differences in the ionic conditions; the single channel recordings were made in symmetrical chloride solutions of approximately 145mM, but the noise recordings were made using microelectrodes containing 3M KCl (for voltage clamp),

resulting in unknown intracellular chloride concentrations.

It has generally been found for other agonist gated ion channels that the conductance estimated from noise is lower than the largest conductance measured directly from single channel currents, when there is a high frequency of occurrence of lower conductance levels. For example, in rat central neurones, the agonists quisqualate and kainate activate two different receptor-channels (quisqualate and kainate receptor-channels respectively) which open to a 50pS conductance level for only a small proportion of the channel open time, the greater proportion of time being spent in lower amplitude conductance states (Cull-Candy & Usowicz, 1987; Jahr & Stevens, 1987). As a consequence the conductance amplitudes estimated from kainate or quisqualate noise in the same cells (or other types of rat central neurones), under similar ionic conditions, are far less than 50pS (Cull-Candy, Howe & Ogden, 1988). The conductance amplitudes estimated from noise can be the same as, or only slightly less than, the conductances measured directly from single channel currents when the channels only open to one conductance level. Included in this category are locust muscle glutamate receptors (Anderson, Cull-Candy & Miledi, 1978; Patlak, Gration & Usherwood, 1979; Cull-Candy, Miledi & Parker, 1981). However, even for channels which open to one conductance level, the conductance estimated from noise can be far less than that measured directly from single-channel currents. This is the case for acetylcholine receptors at the frog neuromuscular junction, where the conductance estimated from noise for several acetylcholine-like agonists (Colquhoun *et al.*, 1975; Dreyer *et al.*, 1976) are far lower than the conductance measured directly from single-channel currents (Gardner *et al.*, 1984).

6.2 *Sensitivity of $GABA_A$ receptor-channels to membrane potential*

6.2.1 *Macroscopic current-voltage relationship*

Macroscopic current-voltage relationships show varying degrees of outward rectification (*i.e.* larger currents at positive, compared with the equivalent negative potentials) in different cells. These include $GABA_A$ receptors from locust and crayfish muscle (Onodera & Takeuchi, 1976; Dudel, 1977; Cull-Candy & Miledi, 1981) mammalian neurones (Ashwood *et. al.*, 1987; Bormann *et. al.*, 1987; Robertson, 1989), frog neurones (Akaike *et. al.*, 1986), chick neurones (Weiss *et. al.*, 1988), turtle photoreceptor cells (Kaneko & Tachibana, 1986) and mammalian gland cells (Kehl *et. al.*, 1987). In the present study the whole-cell GABA current-voltage relation of rat sympathetic neurones were practically linear, or exhibited some

outward rectification ,over the voltage range +50 to -120mV. These current-voltage plots were constructed by measuring the peak amplitude of responses to ionophoretic pulses of GABA (so the extent to which they represent equilibrium current-voltage curves is uncertain); outward rectification was most prominent with long duration ionophoretic pulses (when the amplitude at the end of the pulse was measured). Yang & Zorumski (1989) reported that the whole-cell (macroscopic) GABA current-voltage relation for chick spinal neurones was linear, as also appears to be the case for *Aplysia* neurones (Ikemoto *et. al.*, 1988) and rat cerebral astrocytes (Bormann & Kettenmann, 1988).

Differences in experimental conditions or in the voltage-dependence of the burst length of $GABA_A$ channels may help to explain the apparent discrepancies between research groups. For example, Dudel (1977) concluded that the outward rectification that he observed when measuring the peak amplitude of GABA-mediated i.p.s.c.s in crayfish muscle (with K-acetate filled microelectrodes) largely resulted from changes in the intracellular chloride concentration. Furthermore, the constant field equation, and several energy barrier models for ion permeation through membrane channels, predict outward rectification when intracellular and extracellular concentrations of the permeating ion are unequal. Indeed, Kehl *et. al.* (1987) observed that whole-cell (macroscopic) GABA current-voltage relationships of rat *pars intermedia* cells, appear linear in symmetrical chloride solutions, but outwardly rectifying when the intracellular chloride concentration is lower than the extracellular chloride concentration. The use of non-symmetrical chloride solutions by other groups may also contribute to some of the apparent rectification (see Onodera & Takeuchi, 1976; Dudel, 1977; Cull-Candy & Miledi, 1981; Ashwood *et. al.*, 1987; Ikemoto *et. al.*, 1988). Discrepancies resulting from recording methods are exemplified by the results of Bormann *et. al.* (1987) and Robertson (1989). Both groups produced current-voltage plots by applying voltage steps during steady-state GABA current responses in symmetrical chloride solutions (using cultured mammalian neurones). It was found that the current-voltage relationships were linear when the instantaneous current following a voltage step was measured, but that the relationships were outwardly rectifying if the steady-state currents were measured. Further considerations include the possibility that GABA activates a channel other than the $GABA_A$ chloride channel, or regulates a voltage-dependent channel, via $GABA_B$ receptors. In this regard, activation of $GABA_B$ receptors in cultured rat, mouse, and chick dorsal root ganglion (D.R.G.)

neurones inhibits voltage-activated calcium channels, via activation of membrane bound GTP binding proteins (Dunlap & Fischbach, 1981; Deisz & Lux, 1985; Dolphin *et. al.*, 1986; Holz *et. al.*, 1986). In contrast, activation of $GABA_B$ receptors in rat and guinea-pig hippocampal cells, results in the opening of potassium channels (Newberry & Nicoll, 1984; Gähwiler & Brown, 1985; Inoue *et. al.*, 1985; Andrade *et. al.*, 1986). Furthermore, binding studies suggest the presence of $GABA_B$ receptors in rat superior cervical ganglion neurones (Balcar *et al.*, 1986). However, little contribution to the GABA current-voltage relation from calcium or potassium conductances would be expected in whole-cell patch-clamp recordings in which the patch electrode contained caesium in place of potassium, a high level of calcium buffer (*e.g.* 10mM EGTA), and none of the intracellular factors thought to be necessary to maintain calcium channel activity, such as ATP(Byerly & Yazejian, 1986; Chad & Eckert, 1986; Belles *et al.*, 1988).

Further insight into the possible voltage sensitivity of $GABA_A$ receptor-channels has been gained from analysis of GABA current noise, single channel currents, and GABAergic inhibitory post synaptic currents (i.p.s.c.'s).

6.2.2 *Single-channel current-voltage relationship*

Single-channel current recording techniques (Hamill, Marty, Neher, Sakmann & Sigworth, 1981) allow the extracellular and intracellular ionic compositions to be controlled. The present study has shown that, in rat sympathetic neurones, the single-channel current-voltage relation (of a particular conductance state) was linear over the voltage range 0 to -120mV, with approximately symmetrical chloride concentrations. Linear single-channel current-voltage (in symmetrical chloride solutions) have previously been observed for chick cerebral neurones, mouse spinal neurones and bovine chromaffin cells (Hamill *et. al.*, 1983; Cottrell *et. al.*, 1985; Bormann *et. al.*, 1987; Weiss *et. al.*, 1988). As predicted by various models of ion permeation through channels, single-channel current-voltage relationships are outwardly rectifying in non-symmetrical chloride solutions (Hamill *et. al.*, 1983; Bormann *et. al.*, 1987) .This would suggest that, in these preparations at least, any apparent rectification of whole-cell records (in symmetrical chloride) does not result from voltage-sensitivity of the single-channel conductance, although a shift in the relative frequency of occurrence of the various conductance levels cannot be excluded. In a different preparation however (adult guinea-pig hippocampal neurones) the

conductance of the $GABA_A$ receptor channels appears to be voltage-sensitive, since the single channel current-voltage plot (in symmetrical chloride) showed outward rectification (Gray & Johnston, 1985).

6.2.3 *Voltage dependence of $GABA_A$ kinetics; noise, i.p.s.c., single-channel*

Table 6.5 summarizes the effect of membrane potential on the time constant(s) estimated from GABA noise (τ_{noise}) or the decay of GABAergic i.p.s.c.'s (τ_{ipsc}), in a variety of preparations. The table indicates the voltage range considered and the depolarization required to produce an e-fold change in τ (where given). For the majority of cases, hyperpolarization decreases τ, hence, the duration of the openings or bursts underlying the response become briefer with hyperpolarization. This is consistent with the observed outward rectification of whole-cell equilibrium GABA currents. Thus, in crayfish and locust, depolarization prolongs the GABAergic i.p.s.c. (Dudel, 1977; Adams *et. al.*, 1981a) and prolongs τ_{noise} (Dudel *et. al.*, 1980; Cull-Candy & Miledi, 1981), with an e-fold change requiring approximately 200mV depolarization (Adams *et. al.*, 1981a; Cull-Candy & Miledi, 1981). A similar voltage sensitivity has been observed for τ_{ipsc}, τ_{noise}, and the decay of voltage-jump relaxations (τ_{jump}), recorded from mammalian neurones (Collingridge *et. al.*, 1984; Segal & Barker, 1984; Robertson, 1989). In the present study the slower time constant from the noise was also prolonged by depolarization (within a given cell). However, the two τ_{noise} va ried somewhat from cell to cell, making it unreasonable to pool results at a given potential.

In contrast McBurney & Barker (1978) and Barker *et. al.* (1982) observed little voltage-dependence of τ_{noise} in cultured spinal neurones. It is unclear whether these discrepancies reflect real differences in the $GABA_A$ receptor-channels in these preparations, or just differences in experimental techniques. The large variability in the values of τ_{noise} from cell to cell for any one preparation may have obscured the detection of small changes in τ_{noise} with potential, especially if only a rather narrow voltage range was considered.

The lack of voltage dependence of the open times measured directly from single channel currents in cultured chick cerebral neurones (Weiss, 1989) is difficult to reconcile with the general finding of a prolongation of τ_{noise} and τ_{ipsc} with depolarization. A possible explanation is that the burst length, but not the open time is prolonged

TABLE 6.5.
Voltage sensitivity of $GABA_A$ receptor kinetics: τ_{noise}, τ_{ipsc}, single-channel currents

PREPARATION	TECHNIQUE	VOLTAGE RANGE (mV)	VOLTAGE SENSITIVITY	VOLTAGE FOR e-FOLD CHANGE (mV)	REFERENCE
isolated crayfish muscle	i.p.s.c. decay	-30 to -150	τ_{ipsc} decreases with hyperpolarization		Onodera & Takeuchi, 1976
isolated crayfish muscle	i.p.s.c. decay, voltage-clamp, extracellular focal microelectrode recording	-20 to -150	τ_{ipsc} decreases with hyperpolarization		Dudel, 1977
cultured embryonic mouse spinal neurones	noise, D.C. to 100-150Hz, 2-microelectrode voltage-clamp	-10 to -90	little voltage sensitivity		McBurney & Barker, 1978
isolated crayfish muscle	noise, 1-200Hz	-20 to -150	τ_{fast} & τ_{slow} decrease with hyperpolarization		Dudel, Finger & Stetmeier, 1980
isolated crayfish stretch receptor	i.p.s.c. decay, 2-microelectrode voltage-clamp	0 to -140	slight decrease in τ_{ipsc} with hyperpolarization	226±14 (n=16)	Adams, Constanti & Banks, 1981a
isolated locust muscle	noise	10 to -75	τ_{noise} decreases with hyperpolarization	180	Cull-Candy & Miledi 1981

cultured embryonic mouse spinal neurones	noise, D.C. to 100-150Hz, 2-microelectrode voltage-clamp.	-50 to -100	little voltage sensitivity		Barker, McBurney & Macdonald, 1982
hippocampal slice	decay of spontaneous i.p.s.c.	40 to -120	τ_{ipsc} decreases with hyperpolarization	146±9.6	Collingridge, Gage, & Robertson, 1984
cultured rat hippocampal neurones	i.p.s.c. decay	10 to -60	τ_{ipsc} decreases with hyperpolarization		Segal & Barker, 1984
isolated locust muscle	m.i.j.c. decay, i.p.s.c. decay and noise		τ decreases with hyperpolarization	103±7.9	Cull-Candy, 1986
cultured chick cerebral neurones	single-channel, inside-out patch	-30 to -50	no effect on open times		Weiss, 1988
cultured chick cerebral neurones	decay of spontaneous i.p.s.c.,whole-cell voltage-clamp	40 to -80	τ_{ipsc} decreases with hyperpolarization		Weiss, Barnes & Hablitz, 1988
cultured rat and cat dorsal root ganglion neurones	voltage-jump relaxations	60 to -120	τ decreases with hyperpolarization	125-250 (mean=188)	Robertson, 1989
dissociated rat sympathetic neurones	noise, 0.1 to 250-500Hz	40 to -70	τ_{slow} slightly reduced by hyperpolarization		this thesis

by depolarization (say by increasing the number of openings per burst) since τ_{noise} and τ_{ipsc} probably reflect burst length rather than the duration of individual openings. This would be consistent with the observation that, in cultured chick cerebral neurones, depolarization increased the probability of finding the channel in an open state, where an e-fold change is produced by an approximately 100mV depolarization (Weiss, 1989).

In conclusion, voltage appears to alter the kinetics rather than the conductance of $GABA_A$ channels in a wide spectrum of cell types, such that the time spent in the open state is increased by depolarization.

REFERENCES

ADAMS, P.R. (1976). Drug blockade of open end-plate channels. *Journal of Physiology* **260**, 531-552

ADAMS, P.R. (1977). Voltage jump analysis of procaine action at frog end-plate. *Journal of Physiology* **268**, 291-318.

ADAMS, P.R. & BROWN, D.A. (1975). Actions of γ-aminobutyric acid on sympathetic ganglion. *Journal of Physiology* **250**, 85-120.

ADAMS, P.R., CONSTANTI, A. & BANKS, F.W. (1981a). Voltage clamp analysis of inhibitory synaptic action in crayfish stretch receptor neurons. *Federation Proceedings* **40**, 2637-2641.

ADAMS, P.R., CONSTANTI, A., BANKS, F.W. (1981b). Opposing actions of convulsants and anticonvulsants on GABA responses of crayfish stretch receptor. *In Amino Acid Neurotransmitters*; e.d. F.V. De Feudis & P. Mandel. Raven Press, New York.

AKAIKE, N., HATTORI, K., OOMURA, Y. & CARPENTER, D.O. (1985). Bicuculline and picrotoxin block γ-aminobutyric acid-gated Cl^- conductance by different mechanisms. *Experientia* **41**, 70-71.

AKAIKE, N., INOUE, M., KRISHTAL, O.A. (1986). 'Concentration-clamp' study of γ-aminobutyric-acid-induced chloride current kinetics in frog sensory neurones. *Journal of Physiology* **379**, 171-185.

AKAIKE, N. & OOMURA, Y. (1984). GABA-activated chloride channels in internally perfused frog dorsal root ganglion cells. *Biomedical Research* **5**, 115-132.

AKAIKE, N., YAKUSHIJI, T., TOKUTOMI, N. & CARPENTER, D.O. (1987). Multiple mechanisms of antagonism of γ-aminobutyric acid (GABA) responses. *Cellular and Molecular Neurobiology* **7**, 97-103.

ALLAN, C.N. & ALBUQUERQUE, E.X. (1987). Conductance properties of GABA-activated chloride currents recorded from cultured hippocampal neurones. *Brain Research* **410**, 159-163.

ANDERSON, C.R., CULL-CANDY, S.G. & MILEDI, R. (1977). Potential-dependent transition temperature of ionic channels induced by glutamate in locust muscle. *Nature* **268**, 663-665.

ANDERSON, C.R., CULL-CANDY, S.G. & MILEDI, R. (1978). Glutamate current noise: post-synaptic channel kinetics investigated under voltage clamp. *Journal of Physiology* **282**, 219-242.

ANDERSON, C.R. & STEVENS, C.F. (1973). Voltage clamp analysis of acetylcholine produced end-plate current fluctuations at frog neuromuscular junction. *Journal of Physiology*, **235**, 655-692.

ANDRADE, R., MALENKA, R.C. & NICOLL, R.A. (1986). A G protein couples seretonin and $GABA_B$ receptors to the same channels in hippocampus. *Science* **234**,1261-1265.

ARMSTRONG, C.M. (1971). Interaction of tetraethylammonium ion derivatives with the potassium channels of giant axons. *Journal of General Physiology* **58**, 413-437.

ASCHER, P., LARGE, W.A. & RANG, H.P. (1979). Studies on the mechanism of action of acetylcholine antagonists on rat parasympathetic ganglion cells. *Journal of Physiology* **295**, 139-170

ASCHER, P., MARTY, A. & NIELD, T.O. (1978). The mode of action of antagonists on the excitatory response to acetylcholine in *Aplysia* neurones. *Journal of Physiology* **278**, 207-235.

ASCHER, P. & NOWAK, L. (1988). The role of divalent cations in the N-methyl-D-aspartate response of mouse central neurones in culture. *Journal of Physiology* **399**, 247-266.

ASHWOOD, T.J., COLLINGRIDGE, G.L., HERRON, C.E. & WHEAL, H.V. (1987). Voltage-clamp analysis of somatic γ-aminobutyric acid respones in adult rat hippocampal CA1 neurones *in vitro*. *Journal of Physiology* **384**, 27-37.

AUERBACH, A. & LINGLE, C. (1986). Heterogeneous kinetic properties of acetylcholine receptor channels in *Xenopus* myocytes. *Journal of Physiology* **378**, 119-140.

AUERBACH, A. & LINGLE, C. (1987). Activation of the primary kinetic modes of large and small conductance cholinergic ion channels in *Xenopus* myocytes. *Journal of Physiology* **393**, 37-66.

AUERBACH, A. & SACHS, F. (1983). Flickering of a nicotinic channel to a subconductance state. *Biophysical Journal* **42**, 1-11.

AUERBACH, A. & SACHS, F. (1984). Single channel currents from acetylcholine receptors in embryonic chick muscle. Kinetic and conductance properties of gaps within bursts. *Biophysical Journal* **45**, 187-198.

AULT, B., EVENS, R.H., FRANCIS, A.O., OAKES, D.J. & WATKINS, J.C. (1980). Selective depression of excitatory amino acid induced depolarizations by magnesium ions in isolated spinal cord preparations. *Journal of Physiology* **307**, 413-428.

BALCAR, V.J., JOÓ, F., KÁSA, P., DAMMASCH, I.E., WOLFF, J.R. (1986). GABA receptor binding in rat cerebral cortex and superior cervical ganglion in the absence of GABAergic synapses. *Neuroscience Letters* **66**, 269-274.

BARKER, J.L., MCBURNEY, R.N., MACDONALD, J.F. (1982). Fluctuation analysis of neutral amino acid responses in cultured mouse spinal neurons. *Journal of Physiology* **322**, 365-387.

BARKER, J.L., MCBURNEY, R.N. & MATHERS, D.A. (1983). Convulsant-induced depression of amino acid responses in cultured mouse spinal neurones studied under voltage clamp. *British Journal of Pharmacology*, **80**, 619-629.

BEHRENDS, J.C., MARUYAMA, T., TOKUTOMI, N., AKAIKE, N. (1988). Ca^{2+}-mediated suppression of the GABA-response through mdoulation of chloride channel gating in frog sensory neurones. *Neuroscience Lettsers* **86**, 311-316.

BEKKERS, J.M. (1986). Studies on single ion channels: non-stationary sodium current fluctuations in squid axon and patch clamp analysis of acetylcholine channels in cultured rat skeletal muscle. PhD. Thesis, Cambridge University.

BELLES, B., MALÉCOT, C.O., HESCHELER, J. & TRAUTWEIN, W. (1988). "Run-down" of the Ca current during long whole-cell recordings in guinea-pig heart cells: role of phosphorylation and intracellular calcium. *Pflügers Archives*, **411**, 353-360.

BERRIDGE, M.J. (1987). Inositol triphosphate and diacylglycerol: Two interacting second messengers. *Annual Reveiw of Biochemistry* **56**, 159-193.

BERTOLINO, M., VICINI, S., & COSTA, E. (1978). Phencyclidine actions on modulation of the NMDA-activated cationic channel. *Society of Neuroscience Abstracts* **13**, 143.

BLATZ, A.L. & MAGLEBY, K.L. (1986). Quantiative description of three modes of activity of fast chloride channels from rat skeletal muscle. *Journal of Physiology*, **378**, 141-174.

BORMANN, J. & CLAPHAM, D.E. (1985). γ-aminobutyric acid receptor channels in adrenal chromaffin cells. A. patch-clamp study. *Proceedings of the National Acadamy of Sciences of the U.S.A.* **82**, 2168-2172.

BORMANN, J., HAMILL, O.P. & SAKMANN, B. (1987). Mechanism of anion permeation through channels gated by glycine and γ-aminobutyric acid in mouse cultured spinal neurones. *Journal of Physiology*, **385**, 243-286.

BORMANN, J. & KETTENMANN, H. (1988). Patch-clamp study of γ-aminobutyric acid receptor chloride channels in cultured astrocytes. *Proceedings of the National Academy of Sciences of the USA* **85**, 9336-9340.

BOWERY, N.G. & BROWN, D.A. (1974). Depolarizing actions of γ-aminobutyric acid and related compounds on rat superior cervical ganglia *in vitro*. *British Journal of Pharmacology*, **50**, 205-218.

BOWERY, N.G., COLLINS, J.F., HUDSON, A.L. & NEAL, M.J. (1978). Isoguvacine, isonipecotic acid, muscimol, and N-methyl isoguvacine on the GABA receptor in rat sympathetic ganglia. *Experientia* **34**, 1193-1195.

BRETT, R.S., DILGER, J.P., ADAMS, P.R. & LANCASTER, B. (1986). A method for the rapid exchange of solutions bathing excised membrane patches. *Biophysical Journal* **50**, 987-992.

BURGERMEISTER, W., CATTERAL, W.A. & WITKOP,B. (1977). Histrionicotoxin enhances agonist-induced desensitization of acetylcholine receptor. *Proceedings of the National Academy of Sciences of the USA* **12**, 5754-5758.

BYERLY, L. & YAZEJIAN, B. (1986). Intracellular factors for the maintenance of calcium currents in perfused neurones of the snail, *Lymnaea stagnalis*. *Journal of Physiology* **358**, 197-237.

CACHELIN, A.B. & COLQUHOUN, D. (1989). Desensitization of the acetylcholine receptors of frog end-plates measured in a vaseline-gap voltage clamp. *Journal of Physiology*, **415**, 159-188.

CAHALAN, M.D. (1978). Local anaesthetic block of sodium channels in normal and pronase-treated squid giant axon. *Biophysical Journal* **23**, 285-311

CASH, D.J. & SUBBARAO, K. (1987). Channel opening of γ-aminobutyric acid receptor from rat brain: molecular mechanisms of the receptor responses. *Biochemistry* **26**, 7562-7570.

CHAD, J.E. & ECKERT, R. (1986). An enzymatic mechanism for calcium current inactivation in dialysed *Helix* neurones. *Journal of Physiology* **378**, 31-51.

CHOI, D.W. & FISCHBACH, G.D. (1981). GABA conductance of chick spinal cord and dorsal root ganglion neurones in cell culture. *Journal of Neurophysiology*, **45**, 605-620.

CHOW, P. & MATHERS, D.A. (1986). Convulsant doses of penicillin shorten the lifetime of GABA-induced channels in cultured central neurones. *British Journal of Pharmacology* **88**, 541-547.

CLAPHAM, D.E. & NEHER, E. (1984a). Substance P reduces scetylcholine-induced currents in isolated bovine chromaffin cells. *Journal of Physiology* **347**, 255-277.

CLAPHAM, D.E. & NEHER, E. (1984b). Trifluoperazine reduces inward ionic currents and secretion by separate mechanisms in bovine chromaffin cells. *Journal of Physiology* **353**, 541-564.

COLLINGRIDGE, G.L., GAGE, P.W. & ROBERTSON, B. (1984). Inhibitory post synaptic currents in rat hippocampal CA1 neurones. *Journal of Physiology* **356**, 551-564.

COLQUHOUN, D. (1980). Competitive block and ion channel block as mechanisms of antagonist action on the skeletal muscle end-plate. *In Receptors for Neurotransmitters and Peptide Hormones*; e.d. G. Pepeu, M.J. Kuhar & S.J. Enna. Raven Press, New York.

COLQUHOUN, D., DIONNE, V.E., STEINBACH, J.N. & STEVENS, C.F. (1975). Conductance of channels opened by acetylcholine-like drugs in muscle end-plate. *Nature* **253**, 204-206.

COLQUHOUN, D., DREYER, F. & SHERIDAN, R.E. (1979). The actions of tubocurarine at the frog neuromuscular junction. *J. Phys.* **293**, 247-284.

COLQUHOUN, D. & HAWKES, A.G. (1977). Relaxation and fluctuation of membrane currents that flow through drug-operated ion channels. *Proceedings of the Royal Society of London* **B199**, 231-262.

COLQUHOUN, D. & HAWKES, A. (1982). On the stochastic properties of bursts of single ion channel openings and of clusters of bursts. *Philosophical Transactions of the Royal Society* **B300**, 1-59.

COLQUHOUN, D. & HAWKES, A. (1983). The principles of the stochastic interpretation of ion channel mechanisms. *In Single-Channel Recording*; e.d. Sakmann, B. & Neher, E., pp. 135-175. New York, Plenum.

COLQUHOUN, D. & HAWKES, A. (in press). Stochastic properties of ion channel openings and bursts in a membrane patch that contains two channels: Evidence concerning the presence of two channels when a record containing only single openings is observed. *Proc. Royal. Soc.* B.

COLQUHOUN, D. & OGDEN, D.C. (1988). Activation of ion channels in the frog end-plate by high concentrations of acetylcholine. *Journal of Physiology*, **395**, 131-159.

COLQUHOUN, D. & SAKMANN, B. (1981). Fluctuations in the microsecond time range of the current through single acetylcholine receptor ion channels. *Nature*, **294**, 464-466.

COLQUHOUN, D. SAKMANN, B. (1985). Fast events in single-channel currents activated by acetylcholine and its analogues at the frog muscle end-plate. *Journal of Physiology* **369**, 501-557.

COLQUHOUN, D. & SHERIDAN, R.E. (1981). The modes of action of gallamine. *Proceedings of the Royal Society of London Series* **B211**, 181-203.

COLQUHOUN, D. & SIGWORTH, F.J. (1983). Fitting and statistical analysis of single channel records. In *Single-Channel Recording*, Ed. Sakmann, B. & Neher, E., pp. 191-263. New York: Plenum Press.

CONSTANTI, A. (1978). The "mixed" effect of picrotoxin on the GABA dose/conductance relation recorded from lobster muscle. *Neuropharmacology* **17**, 159-167.

CONSTANTI, A. & NISTRI, A. (1976). A comparative study of the actions of GABA and piperazine on the lobser muscle fibre and the frog spinal cord. *British Journal of Pharmacology* **57**, 347-358.

CONSTANTI, A. & QUILLIAM, J.P. (1974). A comparison of the effects of GABA and imidazoleacetic acid on the membrane conductance of lobster muscle fibres. *Brain Research* **79**, 306-310.

COTTRELL, G.A., LAMBERT, J.J. & PETERS, J.A. (1985). Chloride currents activated by GABA in cultured bovine chromaffin cells. *Journal of Physiology* **365** , 90P.

COURTNEY, K.R. (1975). The mechanism of frequency-dependent inhibition of sodium currents in myelinated nerve by the lidocaine derivative GEA 968. *Journal of Pharmacology and Experimental Therapeutics* **195**, 225-236.

CULL-CANDY, (1984). Inhibitory synaptic currents in voltage-clamped locust muscle fibres desensitized to their excitatory transmitter. *Proceedings of the Royal Society of London Series* **B221**, 375-383.

CULL-CANDY, S.G. (1986). Miniature and evoke inhibitory junctional currents and γ-aminobutyric acid-activated current noise in locust muscle fibres. *Journal of Physiology* **374**, 179-200.

CULL-CANDY, S.G., HOWE, J.R. & OGDEN, D.C. (1988). Noise and single channels activated by excitatory amino acids in rat cerebellar granule neurones. *Journal of Physiology*, **400**, 189-222.

CULL-CANDY, S.G., MAGNUS, C.J. & MATHIE, A. (1986). Freshly dissociated rat sympathetic neurones: a preparation suitable for patch clamp recording. *Journal of Physiology* **377**, 2P.

CULL-CANDY, S.G. & MATHIE, A. (1986). Ion channels activated by acetylcholine and γ-aminobutyric acid in freshly dissociated sympathetic neurones of the rat. *Neuroscience Letters* **66**, 275-280.

CULL-CANDY, S.G., MATHIE, A. & NEWLAND, C.F. (1987). Influence of picrotoxin on ion channels activated by γ-aminobutyric acid in dissociated neurones of the rat. *Journal of Physiology* **398**, 89P.

CULL-CANDY, S.G., MATHIE, A. & POWIS, D.A. (1988). Acetylcholine receptor-channels and their block by clonidine in cultured bovine chromaffin cells. *Journal of Physiology* **402**, 255-278.

CULL-CANDY, S.G. & MILEDI, R. (1981). Junctional and extrajunctional membrane channels activated by GABA in locust muscle fibres. *Proceedings of the Royal Society London* **B211**, 527-535.

CULL-CANDY, S.G. MILEDI, R. & PARKER, I. (1981). Single glutamate-activated channels recorded from locust muscle fibres with perfused patch-clamp electrodes. *Journal of Physiology*, **321**, 195-210.

CULL-CANDY, S.G. & OGDEN, D.C. (1985). Ion channels activated by L-glutamate and GABA in cultured cerebellar neurons of the rat. *Proceedings of the Royal Society of London Series B224*, 367-373.

CULL-CANDY, S.G. & PARKER, I. (1982). Rapid kinetics of single glutamate-receptor channels. *Nature* **295**, 410-412.

CULL-CANDY, S.G. & PARKER, I. (1983). Experimental approaches used to examine single glutamate-receptor ion channels in locust muscle fibres. *In. Single-Channel Recording*: e.d. Sakmann, B. & Neher, E. pp 389-400.

CULL-CANDY, S.G., & USOWICZ, M.M. (1987). Multiple-conductance channels activated by excitaotry amino acids in cerebellar neurons. *Nature*, 325, 525-528.

CULL-CANDY, S.G. & USOWICZ, M.M. (1989a). Whole-cell current noise produced by excitatory and inhibitory amino acids in large cerebellar neurones of the rat. *Journal of Physiology* **415**, 533-554.

CULL-CANDY, S.G. & USOWICZ, M.M. (1989b). On the multiple-conductance single channels activated by excitatory amino acids in large cerebellar neurones of the rat. *Journal of Physiology* **415**, 555-582.

CURTIS, D.R., GAME, C.J.A., JOHNSTON, G.A.R., McCULLOCH, R.M. & MacLACHLAN, R.M. (1972). Convulsive action of penicillin. *Brain Research* **43**, 242-245.

CURTIS, D.R. & JOHNSTON, G.A.R. (1974). Amino acid transmitters in the mammalian central nervous system. *Ergeb. Physiol.* **66**, 97-188.

DE FEUDIS, F.V. (1977). GABA-receptors in the vertebrate nervous system. *Progress in Neurobiology* **9**, 123-145.

DE GROAT, W.C. (1970). The actions of γ-aminobutyric acid on mammalian autonomic ganglia. *Journal of Pharmacology and Experimental Therapeutics* **172**, 384-386.

DEISZ, R.A. & LUX, H.D. (1985). γ-aminobutyric acid-induced depression of calcium currents of chick sensory neurons. *Neuroscience Letters* **56**, 205-210.

DEL CASTILLO, J. & KATZ, B. (1957). Interaction at end-plate receptors between different choline derivatives. *Proceedings of the Royal Society of London* B146, 369-381.

DIONNE, V.E. (1981). The kinetics of slow muscle acetylcholine-operated channels in the garter snake. *Journal of Physiology* **310**, 159-190.

DIONNE, V.E. & LEIBOWITZ, M. (1982). Acetylcholine receptor kinetics: a description from single-channel currents at snake neuromuscular junctions. *Biophysical Journal* **39**, 253-261.

DOLPHIN, A.C., FORDA, S.R. & SCOTT, R.H. (1986). Calcium-dependent currents in cultured rat dorsal root ganglion neurones are inhibited by an adenosine analogue. *Journal of Physiology* **373**, 47-61

DOLPHIN, A.C. & SCOTT, R.H. (1987). Calcium currents and their modulation by (-)-baclofen in rat sensory neurones: modulation by guanine nucleotides. *Journal of physiology* **386**, 1-17.

DOLPHIN, A.C. & SCOTT, R.H. (1989). Interaction between calcium channel ligands and guanine nucleotides in cultured sensory and sympathetic neurones. *Journal of Physiology* **413**, 271-288.

DREYER, F., WALTHER, C. & PEPER, K. (1976). Junctional and extrajunctional acetylcholine receptors in normal and denervated frog muscle fibres. *Pflügers Archives* **366**, 1-9.

DUDEL, J. (1977). Voltage dependence of amplitude and time course of inhibitory synaptic currents in crayfish muscle. *Pflügers Archives* **371**, 167-174.

DUDEL, J., FINGER, W. & STETMEIER, H. (1980). Inhibitory synaptic channels activated by γ-aminobutyric acid (GABA) in crayfish muscle. *Pflügers Archives* **387**, 143-151.

DUGGAN, M.J. & STEPHENSON, F.A. (1988). Benzodiazepine binding site heterogeneity in the purified $GABA_A$ receptor. *European Journal of Pharmacology* **154**, 293-298.

DUNLAP, K. & FISCHBACH, G.D. (1981). Neurotransmitters decrease the calcium conductance activated by depolarization of embryonic chick sensory neurones. *Journal of Physiology*, **317**, 519-535.

EARL, J. & LARGE, W.A. (1974). Electrophysiological investigation of GABA-mediated inhibition at the hermit crab neuromuscular junction. *Journal of Physiology* **236**, 113-127

ENNA, S.J., COLLINS, J.F. & SNYDER, S.H. (1977) Stereospecificity and structure-activity requirements of GABA receptor binding in rat brain. *Brain Research* **124**, 185-190.

EUGÈNE, D. (1987). Fast non-cholinergic depolarizing postsynaptic potentials in neurones of rat superior cervical ganglia. *Neuroscience Letters* **78**, 51-56.

EUGÈNE, D. & TAXI, J. (1988). GABAergic innervation in rat isolated superior cervical ganglia (SCG) studied by combined electrophysiological and immunocytochemical techniques. *Journal of Physiology* **406**, 175P.

FABER, D.S. & KORN, H. (1980). Single-shot channel activation accounts for duration of inhibitory postsynaptic potentials in a central neuron. *Science* **208**, 612-615.

FABER, D.S. & KORN, H. (1982). Transmission at a central inhibitory synapse. I. Magnitude of unitary post synaptic conductance change and kinetics of channel activation. *Journal of Neurophysiology* **48**, 654-678.

FARKAS, Z. KÁSA, P., BALCAR, V.J., JOÓ, F. & WOLFF, J.R. (1986). Type A and B GABA receptors mediate inhibition of acetylcholine release from cholinergic nerve terminals in the superior cervical ganglion of rat. *Neurochemistry International* 8, 565

FARRANT, M. & WEBSTER, R,A. (1988). GABA antagonists: their use and mechanism of action. *In. Neuromethods. Neuropharmacology* II. *Drugs as tools in neurotransmitter research.* ed. Boulton, A.A., Baker, G.B. & Juorio, A.V. Humana Press, New Jersey.

FELTZ, A., DEMENEIX, B., FELTZ, P., TALEB, O., TROUSLARD, J., BOSSU, J-L. & DUPONT, J-L. (1987). Intracellular effectors and modulators of GABA-A and GABA-B receptors: a commentary. *Biochimie* **69**, 395-406.

FELTZ, A. & TRAUTMANN, A. (1982). Desensitization at the frog neuromuscular junction: a biphasic process. *Journal of Physiology* **322**, 257-272.

FENWICK, E.M., MARTY, A. & NEHER, E. (1982). A patch-clamp study of bovine chromaffin cells and their sensitivity to acetylcholine. *Journal of Physiology* **331**, 577-597.

FFRENCH-MULLEN, J.M.H., TOKUTOMI, N. & AKAIKE, N. (1988). The effect of temperature on the GABA-induced chloride current in isolated sensory neurones of the frog. *British Journal of Pharmacology* **95**, 753-762.

FUCHS, K. & SIEGHART, W. (1988). Evidence for the existence of several different α- and β-subunits of the GABA/benzodiazepine receptor complex from rat brain. *Neuroscience Letters* **96**, 329-333.

FUJIMOTO, M. & OKABAYASHI, T. (1981). Effect of picrotoxin on benzodiazepine receptors and GABA receptors with reference to the effect of Cl^- ion. *Life Sciences* **28**, 895-901.

GAGE, P.W. & McKINNON, D. (1985). Effects of pentobarbitone on acetylcholine-activated channels in mammalian muscle. *British Journal of Pharmacology* **85**, 229-235.

GÄHWILER, B.H. & BROWN, D.A. (1985). $GABA_B$-receptor-activated K^+ current in voltage-clamped CA_3 pyramidal cells in hippocampal cultures. *Proceedings of the National Acadamy of Sciences of the USA* **82**, 1558-1562.

GALINDO, A. (1969). GABA-picrotoxin interaction in the mammalian central nervous system. *Brain Research* **14**, 763-767.

GALLAGHER, J.P., HIGASHI, H. & NISHI, S. (1978). Characterization and ionic basis of GABA-induced depolarizations recorded *in vitro* from cat primary afferent neurones. *Journal of Physiology*, **275**, 263-282.

GALLAGHER, J.P., NAKAMURA, J. & SHINNICK-GALLAGHER, P. (1983). The effects of temperature, pH and Cl-pump inhibitors on GABA responses recorded from cat dorsal root ganglia. *Brain Research* **267**, 249-259.

GARDNER, P., OGDEN, D.C. & COLQUHOUN, D. (1984). Conductances of single ion channels opened by nicotinic agonists are indistinguishable. *Nature* **309**, 160-162.

GERSCHENFELD, H.M. (1973). Chemical transmission in invertebrate central nervous systems and neuromuscular junctions. *Physiological Reveiw* **53**, 1-119.

GRAY, R. & JOHNSTON, D. (1985). Rectification of single GABA-gated chloride channels in adult hippocampal neurons. *J. Neurophys.* **54**, 134-142.

GREEN, K.A. & COTTRELL, G.A. (1988). Actions of baclofen on components of the Ca-current in rat and mouse DRG neurones in culture. *British Journal of Pharmacology* **94**, 235-245.

GREENLEE, D.V., VAN NESS, P.C. & OLSEN, R.W. (1978). Gamma-aminobutyric acid binding in mammalian brain: receptor-like specificity of sodium-independent sites. *Journal of Neurochemistry* **31**, 933-938.

GRUNDFEST, H., REUBEN, J.P. & PICKLES, W.H. (1959). The electrophysiology and pharmacology of lobster neuromuscular synapses. *Journal of General Physiology* **42**, 1301-1323.

GURNEY, A.M. & RANG,H.P.(1984). The channel-blocking action of methonium compounds on rat submandibular ganglion cells. *British Journal of Pharmacology* **82**, 623-642.

GYENES, M., FARRANT, M. & FARB, D.H. (1988). "Run-down" of γ-aminobutyric acid$_A$ receptor function during whole-cell recording: a possible role for phosphorylation. *Molecular Pharmacology* **34**, 719-723.

HAMANN, M., DESARMENIEN, M., DESAULLES, E., BADER, M.F. & FELTZ, P. (1988). Quantitative evaluation of the properties of a pyridazinyl GABA derivative (SR 95531) as a GABA$_A$ competitive antagonist. An electrophysiological approach. *Brain Research* **442**, 287-296.

HAMILL, O.P., BORMANN, J. & SAKMANN, B. (1983). Activation of multiple-conductance state chloride channels in spinal neurones by glycine and GABA. *Nature* **305**, 805-808.

HAMILL, O.P., MARTY, A., NEHER, E. SAKMANN, B. & SIGWORTH, F.J. (1981). Improved patch clamp techniques for higher resolution current recording from cells and cell-free membrane patches. *Pflügers Archive* **391**, 85-100.

HESS, P., LANSMAN, J.B. & TSIEN, R.W. (1984). Different modes of Ca channel gating behaviour favoured by dihydropyridine Ca agonists and antagonists. *Nature* **311**, 538-544.

HOLZ, G.G., RANE, S.G. & DUNLAP, K. (1986). GTP binding proteins mediate transmitter inhibition of voltage-dependent calcium channels. *Nature* **319**, 670-672.

HOWE, J.R., COLQUHOUN, D. & CULL-CANDY, S.G. (1988). On the kinetics of large-conductance glutamate-receptor ion channels in rat cerebellar granule neurons. *Proceedings of the Royal Society of London* **B233**, 407-422.

HUCK, S. & LUX, H.D. (1987). Patch-clamp study of ion channels activated by GABA and glycine in cultured cerebellar neurones of the mouse. *Neuroscience Letters* **79**, 103-107.

HUETTNER, J.A. & BEAN, B.P. (1988). Block of NMDA-activated current by the anticonvulsant MK801: Selective binding to open channels. *Proceedings of the National Acadamy of Sciences of the USA* **85**, 1307-1311.

IKEMOTO, Y., AKAIKE, N., KIJIMA, H. (1988). Kinetic and pharmacological properties of the GABA-induced chloride current in *Aplysia* neurones: a 'concentration clamp' study. *British Journal of Pharmacology* **95**, 883-895.

IMOTO, K., BUSCH, C., SAKMANN, B., MISHINA, M., KONNO, T., NAKAI, J., BUJO, H., MORI, Y., FUKUDA, K. & NUMA, S. (1988). Rings of negatively charged amino acids determine the acetylcholine receptor channel conductance. *Nature* **335**, 645-648.

INENAGAH, K. & MASON, W.T. (1987). γ-aminobutyric acid modulates chloride channel activity in cultured bovine lactotrophs. *Neuroscience* **23**, 649-660.

INOUE, M., MATSUO, T. & OGATA, N. (1985). Baclofen activates a voltage-dependent and -aminopyridine sensitive K^+ conductance in guinea-pig hippocampal pyramidal cells maintained in vitro. *British Journal of Pharmacology* **84**, 833-841.

IVERSEN, L.L. & KELLY, J.S. (1975). Uptake and metabolism of γ-aminobutyric acid by neurones and glial cells. *Biochemical Pharmacology* **24**, 933-938.

JACKSON, M.B., LECAR, H., ASKANAS, V. & ENGEL, W.K. (1982a). Single cholinergic receptor channel currents in cultured human muscle. *Journal of Neuroscience* **2**, 1465-1473.

JACKSON, M.B., LECAR, H., MATHERS, D.A. & BARKER, J.L. (1982b). Single channel currents activated by γ-aminobutyric acid, muscimol, and (-)-pentobarbital in cultured mouse spinal neurones. *Journal of Neuroscience* **2**, 889-894.

JACKSON, M.B., WONG, B.S., MORRIS, C.E., LECAR, H. & CHRISTIAN, C.N. (1983). Successive openings of the same acetylcholine receptor channel are correlated in open time. *Biophysical Journal* **42**, 109-114.

JAHR, C.E. & STEVENS, C.F. (1987). Glutamate activates multiple single channel conductances in hippocampal neurons. *Nature* **325**, 522-525.

JARBOE, C.H., PORTER, L.A. & BUCKLER, R.T. (1968). Structural aspects of picrotoxinin action. *Journal of Medical Chemistry* **11**, 729-731.

KANEKO, A. & TACHIBANA, M. (1986). Effects of γ-aminobutyric acid on isolated cone photoreceptors of the turtle retina. *Journal of Physiology* **373**, 443-461.

KATZ, B. & MILEDI, R. (1975). The effect of procaine on the action of acetylcholine at the neuromuscular junction. *Journal of Physiology* **249**, 269-284.

KATZ, B. & MILEDI, R. (1978). A re-examination of curare action at the motor endplate. *Proceedings of the Royal Society of London* **B203**, 119-133.

KATZ, B. & THESLEFF, S. (1957). A study of the 'desensitization' produced by acetylcholine at the motor end-plate. *Journal of Physiology* **138**, 63-80.

KATZ, B. & MILEDI, R. (1972). The statistical nature of the acetylcholine potential and its molecular components. *Journal of Physiology* **224**, 655-699.

KEHL, S.J., HUGHES, D. & MCBURNEY, R.N. (1987). A patch clamp study of β-aminobutyric acid (GABA)-induced macroscopic currents in rat melanotrophs in cell culture. *British Journal of Pharmacology* **92**, 573-585.

KELLY, J.S. & BEART, P.M. (1975). Amino acid receptors in CNS. II. GABA in supraspinal regions. *In Handbook of Psychopharmacology. Volume 4. Amino Acid Neurotransmitters.* e.d. Iversen, L.L., Iversen, S.D. & Snyder, S.H. pp. 129-209. Plenum Press. New York.

KHODOROV, B., SHISHKOVA, L., PEGANOV, E. & REVENKO, S. (1976). Inhibition of sodium currents in frog *Ranvier* node treated with local anaesthetics: role of slow sodium inactivation. *Biochemical Biophysics Act* **433**, 409-435.

KLUNK, W.E., KALMAN, B.L., FERRENDELLI, J.A. & COVEY, D.F. (1983). Computer-assisted modeling of the picrotoxinin and γ-butyrolactone receptor site. *Molecular Pharmacology* **23**, 511-518.

KONNERTH, A., EDWARDS, F. & SAKMANN, B. (1989). GABAergic synaptic and single-channel currents recorded in rat hippocampal slices. *Pflügers Archives Abstracts* R149, 286.

KRNJEVIĆ, K. (1974). Chemical nature of synaptic transmission in vertebrates. *Physiological Reveiw* **54**, 418-540.

KROGSGAARD-LARSEN, P., HJEDS, H., CURTIS, D.R. & LODGE, D. (1979). Dihydromuscimol, thiomuscimol and related heterocyclic compounds as GABA analogues. *Journal of Neurochemistry* **32**, 1717-1724.

KUDO, Y., NIWA, H., TANAKA, A. & YAMADA, K. (1984). Actions of picrotoxinin and related compounds on the frog spinal cord: the role of a hydroxl-group at the 6-position in antagonizing the actions of amino acids and presynaptic inhibition. *British Journal of Pharmacology* **81**, 373-380.

LANDAU, E.M., GAVISH, B., NACHSHEN, D.A. & LOTAN, I. (1981). pH dependence of the acetylcholine receptor channel: a species variation. *Journal of General Physiology* **77**, 647-666.

LEBEDA, F.J., HABLITZ, J.J. & JOHNSTON, D. (1982). Antagonism of GABA-mediated responses by d-tubocurarine in hippocampal neurons. *Journal of Neurophysiology*, **48**, 622-632.

LEEB-LUNDBERG, F. & OLSEN, R.W. (1980). Picrotoxinin binding as a probe of the GABA postsynaptic membrane receptor-ionophore complex. *In. Psychopharmacology and Biochemistry of Neurotransmitter Receptors.* ed. Yamamura, H.I., Olsen, R.W. & Usdin, E. pp 593-606.

LEVITAN, E.S., SCHOFIELD, P.R., BURT, D.R., RHEE, L.M., WISDEN, W., KÖHLER, M., FUJITA, N., RODRIGUEZ, H.F., STEPHENSON, A., DARLISON, M.G., BARNARD, E.A., SEEBURG, P.H. (1988). Structural and functional basis for $GABA_A$ receptor heterogeneity. *Nature* **335**, 76-79.

LIPPA, A.S., GARRETT, K.M., TABAKOFF, B., BEER, B., WENNOGLE, L.P. & MEYERSON, L.R. (1985). Heterogeneity of brain bezodiazepine receptors: effects of physiological conditions. *Brain Research Bulletin* **14**, 189-195.

MACDONALD, R.L. & BARKER, J.L. (1979). Enhancement of GABA-mediated postsynaptic inhibition in cultured mammalian spinal cord neurones: A common mode of anticonvulsant action. *Brain Research* **167**, 323-336.

MACDONALD, J.F., MILJKOVIC, Z. & PENNEFATHER, P (1987). Use-dependent block of excitatory amino acid currents in cultured neurones by ketamine. *Journal of Neurophysiology* **58**, 251-266.

MACDONALD, R.L., ROGERS, C.J. & TWYMAN, R.E. (1989a). Kinetic properties of the $GABA_A$ receptor main conductance state of mouse spinal cord neurones in culture, *Journal of Physiology* **410**, 479-499.

MACDONALD, R.L., ROGERS, C.J. & TWYMAN, R.E. (1989b). Barbiturate regulation of kinetic properties of the $GABA_A$ receptor channel of mouse spinal neurones in culture. *Journal of Physiology* **417**, 483-500.

MAGAZANIK, L.G. & VYSKOCIL, F. (1976). Desensitization at the neuromuscular junction. *In Motor Innervation of Muscle.* ed. Thesleff, S. pp. 151-176. Academic Press. London.

MALEQUE, M.A., SOUCCAR, C., COHEN, J.B. & ALBUQUERQUE, E.X. (1982). Meprodifen reaction with the ion channel of the acetylcholine receptor: potentiation of agonist-induced desensitization at the frog neuromuscular junction. *Molecular Pharmacology* **22**, 636-647.

MAKSAY, G. & TICKU, M.K. (1985). GABA depressants and chloride ions affect the rate of dissociation of ^{35}S-t-butylbicyclophosphorothionate binding. *Life Sciences* **37**, 2173-2180.

MANALIS, R,S. (1977). Voltage-dependent effects of curare at the frog neuromuscular junction. *Nature* **267**, 366-367.

MATHERS, D.A. (1985). Spontaneous and GABA-induced single channel currents in cultured murine spinal cord neurones. *Canadian Journal of Physiology and Pharmacology* **63**, 1228-1233.

MATHERS, D.A. & WANG, Y. (1988). Effect of agonist concentration on the lifetime of GABA-activated membrane channels in spinal cord neurones. *Synapse* **2**, 627-632.

MATHIE, A., CULL-CANDY, S.G. & COLQUHOUN, D. (1988). Single-channel and whole-cell currents evoked by acetylcholine in dissociated sympathetic neurons of the rat. *Proceeding of the Royal Society London* **B232**, 239-248.

MAYER, M.L. & WESTBROOK, G.L. (1985). The action of N-methyl-D-aspartic acid on mouse spinal neurones under voltage clamp. *Journal of Physiology* **361**, 65-90.

MAYER, M.L. & WESTBROOK, G.L. (1987). Permeation and block of N-methyl-D-aspartic acid receptor channels by divalent cations in mouse cultured central neurones. *Journal of Physiology* **394**, 501-527.

MAYER, M.L., WESTBROOK, G.L. & GUTHRIE, P.B. (1984). Voltage-dependent block by Mg^{2+} of NMDA responses in spinal neurones. *Nature* **309**, 261-263.

MAYER, M.L., WESTBROOK, G.L. & VYKLICKY Jr, L. (1988). Sites of antagonist action of N-methyl-D-aspartic acid receptors studied using fluctuation analysis and a rapid perfusion technique. *Journal of Neurophysiology* **60**, 645-663.

MATSUMO, K. & FUKUDA, H. (1982). Anisatin modulation of GABA- and pentobarbital-induced enhancement of diazepam binding in rat brain. *Neuroscience Letters* **32**, 175-179.

MCBURNEY, R.N. & BARKER, J.L. (1978). GABA-induced conductance fluctuations in cultured spinal neurones. *Nature* **274**, 596-597.

MCBURNEY, R.N., SMITH, S.M. & ZOREC, R. (1985). Conductance states of γ-aminobutyric acid and glycine activated chloride channels in rat spinal neurones in cell culture. *Journal of Physiology* **365**, 87P.

MCMANUS, O.B., BLATZ, A.L. & MAGLEBY, K.L. (1987). Sampling, log binning, fitting, and plotting durations of open and shut intervals from single channels and the effects of noise. *Pflügers Archives* **410**, 530-553.

MILEDI, R., PARKER, I, & SUMIKAWA, K. (1983) Recording of single γ-aminobutyrate- and acetylcholine-activated receptor channels translated by exogenous mRNA in *Xenopus* oocytes. *Proceedings of the Royal Society of London* **B218**, 481-484.

MULRINE, N. & OGDEN, D.C. (1989). Activation of ion channels at the rat endplate *in vitro* by acetylcholine at low and physiological temperatures. *Journal of Physiology* **415**, 35P.

NEHER, E. & STEINBACH, J.H. (1978). Local anaesthetics transiently block currents through single acetylcholine-receptor channels. *Journal of Physiology* **277**, 153-176.

NEWBERRY, N.R. & NICOLL, R.A. (1984). Direct hyperpolarizing action of baclofen on hippocampal pyramidal cells. *Nature* **308**, 450-452.

NICOLL, R.A. (1972). The effects of anaesthetics on synaptic excitation and inhibition in the olfactory bulb. *Journal of Physiology* **223**, 803-814.

NICOLL, R.N. & WOJTOWICZ, J.M. (1980). The effects of pentobarbital and related compounds on frog motoneurons. *Brain Research* **191**, 225-237.

NISTRI, A. & CONSTANTI, A. (1979). Pharmacological characterization of different types of GABA and glutamate receptors in vertebrates and invertebrates. *Progress in Neurobiology* **13**, 117-235.

NOWAK, L., BREGETOVSKI, P., ASCHER, P., HERBET, A. & PROCHIANTZ, A. (1984). Magnesium gates glutamate-activated channels in mouse central neurones. *Nature* **307**, 462-465.

OGDEN, D.C. & COLQUHOUN, D. (1985). Ion channel block by acetylcholine, carbachol and suberyldicholine at the frog neuromuscular junction. *Proceedings of the Royal Society of London Series B***225**, 329-355.

OGDEN, D.C., SIEGLEBAUM, S.A. & COLQUHOUN, D. (1981). Block of acetylcholine-activated ion channels by an uncharged local anaesthetic. *Nature* **289**, 596-598.

OLSEN, R.W. (1981). The GABA postsynaptic membrane receptor-ionophore complex. Site of action of convulsant and anticonvulsant drugs. *Molecular and Cellular Biochemistry* **39**, 261-279.

OLSEN, R.W. (1982). Drug interactions at the GABA receptor-ionophore complex. *Annual Reveiw of Pharmacology and Toxicology* **22**, 245-277.

OLSEN, R.W., TICKU, M.K. & MILLER, T. (1978a). Dihydropicrotoxinin binding to crayfish muscle sites possibly related to γ-aminobutyric acid receptor-ionophores. *Molecular Pharmacology* **14**, 381-390.

OLSEN, R.W., TICKU, M.K., VAN NES, P.C. & GREENLEE, D. (1978b). Effects of drugs on GABA receptors, uptake, release and synthesis *in vitro*. *Brain Research* **139**, 277-294.

ONODERA, K. & TAKEUCHI, A. (1976). Inhibitory postsynaptic currents in voltage-clamped crayfish muscle. *Nature* **263**, 153-154.

PATLAK, J.B. (1988). Sodium channel subconductance levels measurted with a new variance-mean analysis. *Journal of General Physiology* **92**, 12-430.

PATLAK, J.B., GRATION, K.A. & USHERWOOD, P.N.R. (1979). Single glutamate activated channels in locust muscle. *Nature*, **278**, 643-645.

PATLAK, J.B., ORTIZ, M. & HORN, R. (1986). Opentime heterogeneity during bursting of sodium channels in frog sekeletal muscle. *Biophysical Journal* **49**, 773-777.

PEPER, K. & McMAHAN, U.J. (1972). Distribution of acetylcholine receptors in the vicinity of nerve terminals on skeletal muscle of the frog. *Proceedings of the Royal Society of London* **B181**, 431-440.

PORTER, L.A. (1967). Picrotoxin and related substances. *Chemical Reveiw* **67**, 441-464.

PRICHETT, D.B., SONTHEIMER, H., SHIVERS, B.D., YMER, S., KETTENMANN, H., SCHOFIELD, P.R., SEEBURG, P.H. (1989). Importance of a novel $GABA_A$ receptor subunit for benzodiazepine pharmacology. *Nature* **338**, 582-585.

QUAST, U. & BRENNER, O. (1983). Modulation of [^{3}H] muscimol binding in rat cerebellar and cerebral cortical membranes by picrotoxin, pentobarbitone, and etomidate. *Journal of Neurochemistry* **41**, 418-425.

QUAYLE, J.M., STANDEN, N.B. & STANFIELD, P.R. (1988). The voltage-dependent block of ATP sensitive potassium channels of frog skeletal muscle by caesium ions. *Journal of Physiology* **405**, 677-697.

RAMANJANEYULU, R. & TICKU, M.K. (1984). Binding characteristics and interactions of depressant drugs with [^{35}S]t-butylbicyclophosphorothionate, a ligand that binds to the picrotoxinin site. *Journal of Neurochemistry* **42**, 221-229.

RANG, H.P. (1982). The action of ganglionic blocking drugs on the synaptic responses of rat submandibular ganglion cells. *British Journal of Pharmacology* **75**, 151-168.

RANSOM, B.R. & BARKER, J.L. (1976). Pentobarbital selectively enhances GABA-mediated post-synaptic inhibition in tissue cultured spinal neurones. *Brain Research.* **114**, 530-535.

ROBBINS, J. & VAN DER KLOOT, W.G. (1958). The effect of picrotoxin on peripheral inhibition in crayfish. *Journal of Physiology* **143**, 541-552.

ROBERTSON, B. (1989). Characteristics of GABA-activated chloride channels in mammalian dorsal root ganglion neurones. *Journal of Physiology* **411**, 285-300.

ROBERTSON, B. & TAYLOR, W.R. (1986). Effects of γ-aminobutyric acid and (-) baclofen on calcium and potassium currents in cat dorsal root ganglion neurones *in vitro*. *British Journal of Pharmacology* **89**, 661-672.

ROLE, L.W. (1984). Substance P modulation of acetylcholine-induced currents in embryonic chicken sympathetic and ciliary ganglion neurones. *Proceedings of the National Acadamy of Sciences of the U.S.A.* **81**, 2924-2928.

RUFF, R.L. (1977). A quantitative analysis of local anaesthetic alteration of miniature end-plate current fluctuations. *Journal of Physiology* **264**, 89-124.

RUFF, R.L. (1982). The kinetics of local anaesthetic blockade of end-plate channels. *Biophysical Journal* **37**, 625-631.

SAKMANN, B., HAMILL, O.P. & BORMANN, J. (1983a). Patch-clamp measurements of elementary chloride currents activated by the putative inhibtory transmitters GABA and glycine in mammalian spinal neurones. *Journal of Neural Transmission Supplementum,* **18**, 83-95.

SAKMANN, B., BORMANN, J. & HAMILL, P.O. (1983b). Ion transport by single receptor channels. *In* Cold Spring Harbor Symposia on Quantiative Biology, Vollume XLVIII. *pp* 247-256.

SAKMANN, B., PATLAK, J. & NEHER, E. (1980). Single acetylcholine-activated channels show burst-kinetics in the presence of desensitizing concentration of agonist. *Nature* **286**, 71-73.

SCHMIDT, R.F. (1963). Pharmacological studies on the primary afferent depolarization of the toad spinal cord. *Pflügers Archives* **277**, 325-346.

SCHOFIELD, P.R., DARLISON, M.G., FUJITA, N., BURT, D.R., STEPHENSON, F.A., RODRIGUEZ, H., RHEE, L.M., RAMACHANDRAN, J., REALE, V., GLENCROSE, T.A., SEEBURG, P.H. & BARNARD, E.A. (1987). Sequence and functional expression of the $GABA_A$ receptor shows a ligand-gated receptor super-family. *Nature* **328**, 221-227.

SCHWARTZ, W., PALADE, P.T. & HILLE, B. (1977). Local anaesthetics: effect of pH on use-dependent block of sodium channels in frog muscle. *Biophysical Journal* **20**, 343-368.

SCOTT, R.H. & DOLPHIN, A.C. (1986). Regulation of calcium currents by a GTP analogue: potentiation of baclofen-mediated inhibition. *Neuroscience Letters* **69**, 59-64.

SCUKA, M. (1977). The effect of pH on the conductance change evoked by iontophoresis at the frog neuromuscular junction. *Pflügers Archives* **369**, 239-244.

SEGAL, M. & BARKER, J.L. (1984). Rat hippocampal neurons in culture: voltage-clamp analysis of inhibitory synaptic connections. *Journal of Neurophysiology* **52**, 469-487.

SERNAGOR, E., KUHN, D., VYKLICKY Jr, L. & MAYER, M.L. (1989). Open channel block of NMDA receptor responses evoked by tricyclic antidepressants. *Neurone* **2**, 1221-1227.

SHANK, R.P., PONG, S.F., FREEMAN, A.R. & GRAHAM, L.T. (1974). Bicuculline and picrotoxin as antagonists of γ-aminobutyrate and neuromuscular inhibition in lobster. *Brain Research* **72**, 71-78.

SIGEL, E. & BAUR, R. (1988). Allosteric modulation by benzodiazepine receptor ligands of the $GABA_A$ receptor channel expressed in *Xenopus* oocytes. *The Journal of Neuroscience* **8**, 289-295.

SIGWORTH, F.J. & SINE, S.M. (1987). Data transformation for improved display and fitting of single-channel dwell time histograms. *Biophysical Journal* **52**, 1047-1054.

SIMMONDS, M.A. (1978). Presynaptic actions of γ-aminobutyric acid and some antagonists in a slice preparation of cuneate neucleus. *British Jorunal of Pharmacology* **63**, 495-502.

SIMMONDS, M.A. (1980). Evidence that bicuculline and picrotoxin act at separate sites to antagonize γ-aminobutyric acid in rat cuneate nucleus. *Neuropharmacology* **19**, 39-45.

SIMMONDS, M.A. (1982). Classification of some GABA antagonists with regard to site of the action and potency in slices of rat cuneate nucleus. *European Journal of Pharmacology*, **80**, 347-358.

SINE, S.M. & STEINBACH, J.H. (1984a). Activation of a nicotinic acetylcholine receptor. *Biophysical Journal* **45**, 175-185.

SINE, S.M. & STEINBACH, J.H. (1984b). Agonists block currents through nicotinic acetylcholine receptor channels. *Biophysical Journal* **46**, 277-283.

SINE, S.M. & STEINBACH, J.H. (1986). Activation of acetylcholine receptors on clonal mammalian BC3H-1 cells by low concentrations of agonist. *Journal of Physiology* **373**, 129-162.

SINE, S.M. & STEINBACH, J.H. (1987). Activation of acetylcholine receptors on clonal mammalian BC3H-1 cells by high concentration of agonist. *Journal of Physiology* **385**, 325-359.

SMART, T.G. (1983). The interaction of some convulsant drugs with the GABA-receptor system of lobster muscle. *Ph.D. Thesis, University of London.*

SMART, T.G. (1989). Excitatory amino acids: The involvement of second messengers in the signal transduction process. *Cellular and Molecular Neurobiology* **9**, 193-206.

SMART, T.G. & CONSTANTI, A. (1981). A re-examination of the GABA-inhibitory action of bicuculline on lobster muscle. *European Journal of Pharmacology* **70**, 25-33.

SMART, T.G. & CONSTANTI, A. (1986). Studies on the mechanism of action of picrotoxinin and other convulsants at the crustacean muscle GABA receptor. *Proceedings of the Royal Society of London Series B*277, 191-216.

SQUIRES, R.F., CASIDA, J.E., RICHARDSON, M. & SAEDERUP, E. (1983). [^{35}S] t-butylbicyclophosphorothionate binds with high affinity to brain specific sites coupled to γ-aminobutyric acid-A and ion recognition sites. *Molecular Pharmacology*, 23, 326-336.

STELZER, A., KAY, A.R., WONG, R.K.S. (1988). $GABA_A$-receptor function in hippocampal cells is maintained by phosphorylation factors. *Science* 241, 339-341.

STELZER, A., SLATER, N.J. & TEN BRUGGENCATE, G. (1987). Activation of NMDA receptors blocks GABAergic inhibition in an *in vitro* model of epilepsy. *Nature* 326, 698-701.

STELZER, A. & WONG, R.K.S. (1989a). $GABA_A$ responses in hippocampal neurons are potentiated by glutamate. *Nature* 337, 170-173.

STELZER, A. & WONG, R.K.S. (1989b). Activation of protein kinase C reduces $GABA_A$ mediated chloride conductance. *Neuroscience Abstract 369.2*

STETTMEIER, H. & FINGER, W. (1983). Excitatory postsynaptic channels operated by quisqualate in crayfish muscle. *Pflügers Archives* 397, 237-242.

STRICHARTZ, G.R. (1973). The inhibition of sodium currents in myelinated nerve by quaternary derivatives of lidocaine. *Journal of General Physiology* 62, 37-57.

STUDY, R.E. & BARKER, J.L. (1981). Diazepam and (-)-pentobarbital: fluctuation analysis reveals different mechanisms for potentiation of γ-aminobutyric acid responses in cultured central neurones. *Proceedings of the National Acadamy of Sciences of the USA.* 78, 7180-7184.

SUPAVILAI, P & KOROBATH, M. (1984). [^{35}S]t-butylbicyclophosphorothionate binding sites are constituents of the γ-aminobutyric acid benzodiazepine receptor complex. *Journal of Neuroscience* **4**, 1193-1200.

SUPAVILAI, P., MANNONEN, A., COLLINS, J.F. & KAROBATH, M. (1982). Anion-dependent modulation of [^{3}H]muscimol binding and of GABA-stimulated [^{3}H]flunitrazepam binding by picrotoxin and related CNS convulsants. *European Journal of Pharmacology* **81**, 687-691.

SWEETNAM, P.M., LLOYD, J., GALLOMBARDO, P., MALISON, R.T., GALLAGER, D.W., TALLMAN, J.F. & NESTLER, E.J. (1988). Phosphorylation of the $BABA_A$/Benzodiazepine receptor α subunit by a receptor-associated protein kinase. *Journal of Neurochemistry* **51**, 1274-1284.

TAKEUCHI, A. & TAKEUCHI, N. (1969). A study of the action of picrotoxin on the inhibitory neuromuscular junction of the crayfish. *Journal of Physiology* **205**, 377-392.

TALEB, O., TROUSLARD, J., DEMENEIX, B.A., FELTZ, P., BOSSU, J-L., DUPONT, J-L., FELTZ, A. (1987). Spontaneous and GABA-evoked chloride channels on pituitary intermediate lobe cells and their internal Ca requirements. *Pflügers Archieve* **409**, 620-631.

TICKU, M.K., BAN, M. & OLSEN, R.W. (1978). Binding of [^{3}H]α-dinydropicrotoxinin, a γ-aminobutyric acid synaptic antagonists, to rat brain membranes. *Molecular Pharmacology*, **14**, 391-402.

TRIFILETTI, R.R., SNOWMAN, A.M. & SNYDER, S.H. (1984). Anxiolytic cyclopyrrolone drugs allosterically modulate the binding of [^{35}S]t-butylbicyclophosphorothionate to the benzodiazepine/γ-aminobutyric acid-a receptor/chloride anionophore complex. *Molecular Pharmacology* **26**, 470-476.

USHERWOOD, P.N.R. & GRUNDFEST, H. (1965). Peripheral inhibition in skeletal muscle of insects. *Journal of Neurophysiology* **28**, 497-518.

VAN DER KLOOT, W.G. & ROBBINS, J. (1959). The effects of γ-aminobutyric acid and picrotoxin on the junctional potential and the contraction of crayfish muscle. *Experientia* **15**, 35-36.

VAN RENTERGHEM, C., BILBE, G., MOSS, S., SMART, T.G., CONSTANTI, A., BROWN, D.A. & BARNARD, E.A. (1987). GABA receptors induced in *Xenopus* oocytes by chick brain mRNA: evaluation of TBPS and use-dependent channel-blocker. *Molecular Brain Research,* **2**, 21-31.

WANKE, E., FERRONI, A., MALAGARAOLI, A., AMBROSINI, A., POZZAN, Y. & MELDOLESI, J. (1987). Activation of muscarinic receptor selectively inhibits a rapidly inactivated Ca^{2+} current in rat sympathetic neurones. *Proceedings of the National Acadamy of Sciences of the U.S.A.* **84**, 4313-4317.

WEISS, D.S. (1988). Membrane potential modulates the activation of GABA-gated channels. *Journal of Neurophysiology* **59**, 514-527.

WEISS, D.S., BARNES, J.R., & HABLITZ, J.J. (1988). Whole-cell and single-channel recordings of GABA-gated currents in cultured chick cerebral neurons. *Journal of Neurophysiology* **59**, 495-513.

WEISS, D.S. & MAGLEBY, K.L. (1989). Gating scheme for single GABA-activated Cl channels determined from stability plots, dwell-time distributions, and adjacent-interval durations. *The Journal of Neuroscience* **9**, 1314-1324.

WICHMANN, B.A. & HILL, I.D. (1985). An efficient and portable pseudo-random number generator. *In Applied Statistics Algorithms.* e.d. Griffiths, P. & Hill, I.D. **283**, 238-242.

WILLOW, M. (1981). A comparison of the action of pentobarbitone and etomidate on [^{3}H]-GABA binding to crude synaptosomal rat brain membranes. *Brain Research* **220**, 427-431.

WILLOW, M. & JOHNSTON, G.A.R. (1980). Enhancement of GABA binding by pentobarbitone. *Neuroscience Letters* **18**, 323-327.

WOLFF, J.R., JOÓ, F., KÁSA, P., STORM-MATHIESEN, J., TOLDI, J. & BALCAR, V.J. (1986). Presence of neurones with GABA-like immunoreactivity in the superior cervical ganglion of the rat. *Neuroscience Letters* **71**, 157-162.

YAKUSHIJI, T., TOKUTOMI, N., AKAIKE, N., CARPENTER, D.O. (1987). Antagonists of GABA responses, studied using internally perfused frog dorsal root ganglion neurons. *Neuroscience* **22**, 1123-1133.

YANG, J. & ZORUMSKI, C.F. (1989). Trifluoperazine blocks GABA-gated chloride currents in cultured chick spinal cord neurones. *Journal of Neurophysiology* **61**, 363-373.

YASUI, S., ISHIZUKA, S. & AKAIKE, N. (1985). GABA activates different types of chloride conducting receptor-ionophores complexes in a dose-dependent manner. *Brain Research* **344**, 176-180.

YELLEN, G. (1984). Ionic permeation and blockade in Ca^{2+}-activated K^{+} channels of bovine chromaffin cells. *Journal of General Physiology* **84**, 157-186.